Cadherin Function in Bronchial Epithelial Wound Healing.

by

Sarah L. Williams

A Thesis Submitted to the University of Southampton for the Degree of Doctor of Philosophy.

Faculty of Medicine
Southampton General Hospital
Tremona Rd
Southampton
Hants SO16 6YD

GlaxoSmithKline Plc
Medicines Research Centre
Gunnelswood Rd
Stevenage
Herts SG1 2NY

September 2001

UNIVERSITY OF SOUTHAMPTON

ABSTRACT

FACULTY OF MEDICINE

RESPIRATORY CELL & MOLECULAR BIOLOGY

Doctor of Philosophy

Cadherin Function In Bronchial Epithelial Wound Healing.

by Sarah L. Williams

The bronchial epithelial lining is often impaired in asthma with observed epithelial denudation. Normal epithelium is scaffolded by various adhesion molecules which interact and co-exist in such a fashion that together they support an epithelium that functions to line the airway lumen forming a selectively permeable barrier, protecting the underlying tissue from harmful noxious agents in the exterior environment.

The process of epithelial shedding is not fully understood. Putative restitution stages have been observed where the remaining epithelia undergo flattening, migration, proliferation and differentiation stages to restore an intact epithelial barrier.

The detailed examination of bronchial epithelial morphology of non-asthmatic, asthmatic and chronic asthmatic patients in this study revealed characteristic cell phenotypes for each patient grouping. Non-asthmatics in general had an intact uniform epithelium, asthmatics tended to have suprabasal denudation, with 'flattened' basal cells remaining, whereas chronic asthmatics tended to have a predominantly denuded basement membrane with complete cell loss.

Using models of epithelial development and repair, this study has demonstrated molecular modifications that are characteristic of these epithelial cell phenotypes. The adherens junction associated cell adhesion molecules E- and P-cadherin were shown to have contrasting expression patterns in epithelial development *in vitro*. Elevated P-cadherin immunoreactivity was seen at pre-confluence in parallel with a reduction in E-cadherin immunoreactivity. Similar observations in the early stages of repair suggest a disruption of the rigid permanent E-cadherin contacts on epithelial damage, allowing migration and more dynamic

adhesion, accompanied by seemingly elevated P-cadherin levels promoting proliferation and differentiation to occur.

Epithelial cells transfected with sense and antisense E-cadherin genes demonstrated a co-dependence between the expression of E- and P-cadherin expression. Preliminary work was undertaken to establish cells with altered P-cadherin expression levels. These clones, in conjunction with the epithelial models established in this study will prove essential tools in the investigation of cadherin involvement in epithelial cell adhesion and wound repair.

Acknowledgements.

I would like to acknowledge the help and encouragement of my supervisors, Peter Lackie and Mike West who were always on hand for advice and reassurance. I received invaluable research assistance from the labs at GlaxoSmithKline and Southampton General Hospital.

Thanks to Will, Angus and Matt in Southampton for unlimited advice and supportive cups of tea and Steve Evans at Stevenage for listening and taking me for chicken!! Thanks also to everyone in Wessex Lane for the light relief and 'being in the same boat', especially head girl Ray Charles and Aussie Anna for always being at hand for distraction! Thanks to Kate and Reggie who kept me sane through the latter part of this project, -heres to lots more S.I. at London Welsh!

Finally I'd like to thank my family who have given me great support over the past four years, down the phone, down the M4 and down the bank!! Hopefully I'll see a bit more of you now.

Contents

Chapter One

1. Introduction.

Chapter Two

2. General Methods

PAGE

Chapter Three

3. Morphometric Characteristics of Bronchial Epithelium in Normal and Asthmatic Human Subjects.

Chapter Four

4. Adhesion Molecule Expression During Development and Repair of Bronchial Epithelial Layers *in vitro.*

Chapter Five

5. Examination of Cadherin Function by Manipulation of Cadherin Levels in Bronchial Epithelial Cells.

Chapter Six

Chapter One

Introduction.

1 Introduction.

1.1 Epithelia.

Epithelia cover the surfaces and line the cavities of the body as a sheet-like organisation of cells held together by intercellular junctions and supported on an underlying basement membrane. Differentiated epithelium is polarised with respect to the localisation of the cellular junctions, proteins, membrane channels and intracellular organelles. This property assists in directional vectorial transport of molecules across the epithelial barrier (Rodriguez-Boulan et al, 1989).

Epithelia can be characterised by the number of layers (simple, stratified or pseudostratified), cell shape (squamous, cuboidal, columnar) and whether they are ciliated or non-ciliated. In airway epithelium the non-ciliated cells can be secretory or non-secretory (reviewed by Jeffery et al, 1983). Epithelia differentiate into combinations of these characteristics depending on the circumstances and tissue requirements.

The underlying basement membrane (lamina lucida) acts as both an epithelial scaffold and as a structural barrier to the passage of cells and macromolecules. The layer is less than 150nm thick and is comprised of type IV collagen, laminin, fibronectin, proteoglycans, entactin and nidogen (Jeffery et al, 1989). Below this lies the 'reticular lamina' consisting primarily of fibronectin and collagen types III and V.

1.1.1 Bronchial Epithelium.

Human bronchial epithelium consists of two distinct cell layers. A 'basal' cell layer of non-ciliated, non-secretory cuboidal cells, lies immediately upon the basement membrane (Plopper et al, 1983). Between the basal cells and the airway lumen lies a second layer of morphologically distinct cells. This layer consists of

ciliated columnar epithelial cells interspersed with non-ciliated cells and goblet cells, the latter contributing to the lumenal mucous secretions.

Together the cell bilayer forms a barrier separating the airway lumen from the underlying tissue. This is an important function of the lung epithelium as it limits exposure of the airway to allergens, pathogens and potential noxious agents.

The cells of the columnar layer secrete various molecules and substances such as water, salts and mucins contributing to the lumenal mucous layer which functions to trap foreign particles which are then cleared by mucociliary clearance (Jeffery et al, 1983).

Given the distinct differences between the two layers there is dispute over the identity of the stem cells. The basal, columnar and secretory cells have all previously been implicated as the progenitor cells (McDowell et al, 1985, Evans et al, 1990, Erjefält et al, 1995). Pulse-chase [^{3}H] thymidine-labelling experiments indicated the basal cells to be the true epithelial stem cells (Donnelly et al, 1982), although experiments by McDowell where the basal cell was shown to be non-essential in epithelial repair cannot be ignored (McDowell et al, 1985). It may be that columnar epithelial cells have potential stem cell capabilities, which come into play in the absence of basal cell proliferation. Boers and coworkers (1998), found there to be a high proportion of basal cells contributing to the proliferation compartment of normal human airway epithelium, supporting the theory that the basal cells are the predominant progenitor cells.

Despite the putative stem cell role, the main function of the basal cell is thought to be the anchorage of the columnar epithelial layer to the basement membrane. Columnar cells make desmosomal attachments to adjacent columnar epithelial cells and basal cells but make no direct junctional contact with the basement membrane. Basal cells also form desmosomal contacts with adjacent cells but form hemidesmosomes with the extracellular matrix (Evans et al, 1989). There is no evidence that columnar cells form hemidesmosomal contacts at any time.

The basal-basement membrane attachment is thought to be much stronger than that of the basal-columnar cell, demonstrated in a study by Motojima and coworkers (1989), where an increased concentration of MBP (major basic protein -a toxic

cationic protein found in eosinophils) was required to dislodge the basal cells as compared with the columnar.

Epithelial height varies with species, demonstrated in a study by Evans (1989), where epithelia from a wide range of species was examined for epithelial height and cell coverage. In this study, hamster epithelium was found to have a height of ~8.6μm, whereas sheep epithelium had a height over six times taller at ~56.8μm.

The number of hemidesmosomes per basal cell was found to be the same for a given tissue whereas the number of desmosomes increases with epithelial height. However given that the number of basal cells is positively correlated to epithelial height (as is keratin filaments), strength of attachment per given area of epithelia is likely to remain the same (Garrod et al, 1986, Wiseman et al, 1981, Evans et al, 1988, 1990).

1.1.2 Epithelial Cell Adhesion.

1.1.2.1 Cell-Extracellular Matrix interactions.

The extracellular matrix is made up of two layers, the 'lamina lucida' (basement membrane) on which the epithelia rests, and the underlying 'reticula lamina' below which are the mesenchymal cells.

The basement membrane consists of type IV collagen, laminin, fibronectin entactin and nidogen (Jeffery et al 1989). In addition the basement membrane contains numerous proteoglycans to which more glycosaminoglycans are covalently attached.

The reticula lamina is comprised primarily of fibronectin, elastin and collagen types III and V. The collagens and elastin are the most abundant proteins in the lung and their ordered distribution is vital to maintain the structural integrity of the tissue. Increased collagen deposition in the asthmatic airways leads to airway wall thickening and increased bronchial hyperresponsiveness.

In addition to a structural role, the attachment of cells to the extracellular matrix and to each other is an important means of cellular communication. Adhesion plaque formation with the matrix allows potential for direct signalling between fibroblasts of the mesenchymal trophic layer and the epithelium (Hanks et al, 1997), this would be of particular importance in inflammation (Evans et al, 2001)

1.1.2.1.1 Hemidesmosomes

Hemidesmosomes are junctional structures that mediate adhesion of epithelial cells to the underlying basement membrane (reviewed by Nievers et al, 1999). These structures are highly important in maintaining tissue integrity, demonstrated by the tissue fragility and skin blistering associated with hemidesmosomal abnormalities.

The hemidesmosomes, though originally described as 'half' desmosomes, contain a distinct set of proteins that differ from those seen at desmosomal attachments between adjacent epithelial cells. Like desmosomes the hemidesmosomes attach to intermediate filaments but via a plaque structure consisting of proteins BP230, HD1 and plectin (the latter two are possibly identical) (Smith et al, 1996). The inner plaque is linked to an outer plaque which contains the transmembranous proteins BP180 and integrin $\alpha_6\beta_4$ (Sonnenberg et al, 1990). The $\alpha_6\beta_4$ integrin mediates binding of the basal cell to the basement membrane and collagen IV via laminin 5.

It has also been suggested that the hemidesmosomes not only give firm epithelial adhesion but also are involved in signal transduction via the integrins (Giancotti et al, 1996).

1.1.2.2 Cell-Cell Interactions.

Bronchial epithelia are polar structures with their apical and basolateral surfaces differing in protein and phospholipid composition. The junctional structures of the epithelia play an essential role in the maintenance of this polarity. Basal and

columnar epithelial cells form desmosomal junctions. Columnar cells in addition form tight junctions and intermediate junctions at their apical regions and gap junctions and desmosomes along the lateral surfaces (figure 1.1).

1.1.2.2.1 Tight Junctions.

The tight junctions or zonula occludens are near the apex of epithelial cells at which the plasma membranes of neighbouring cells are so proximal that outer membrane leaflets seem to fuse. In freeze fracture experiments the tight junctions appear as a mesh-like organization of strands between neighbouring cells which is localised to a belt of cytosolic actin forming a perijunctional actin 'belt' (Farquhar et al, 1963).

The primary function of the tight junctions is to seal together the apicolateral surfaces of adjoining cells. This creates a selective barrier to molecular transport that allows transcellular vectorial transport. The tight junctions not only restrict transcellular transport but also intramembranal lipid movement forming definite apical and basolateral domains and establishing cell polarity (Balda et al, 1996).

Paracellular pores are thought to be formed in the strands and function as selective filters for ion, molecules and cells across the epithelium. The level of semipermeability alters from tissue to tissue according to requirements. In the kidney for example, epithelia of the proximal tubules have a high permeability to allow re-absorption of valuable nutrients whereas epithelia of the distal tubules have a low permeability to *prevent* re-absorption of toxins from urine.

A number of putative regulatory systems have been proposed for the tight junctions involving amongst others, the tight junctional proteins 'occludin' and 'claudins' as well as a signal cascade involving myosin light chain kinase.

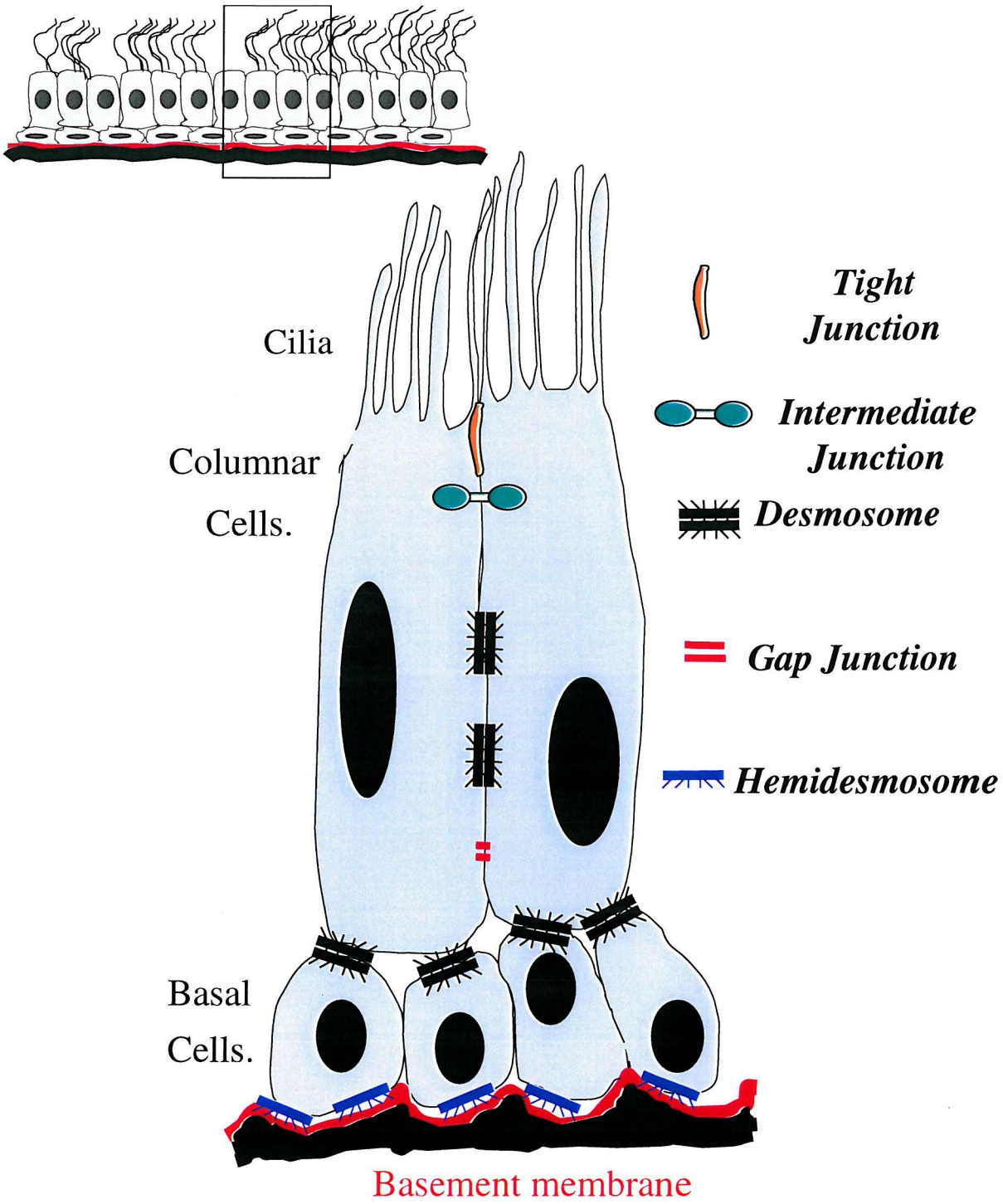

Figure 1.1. Cell-cell Interactions in Bronchial Epithelia.

There are two distinct sheets of cells which make up airway epithelia, a basal layer immediately above the basement membrane, and below a columnar cell layer.
The tight junctions are loacated near the apex of the columnar cells, sealing the gap between adjacent cells, just below this are the intermediate junctions. The desmosomes scattered along the lateral surface provide further adhesion whereas the gap junctions form hydrophilic channels beween the cells.
The desmosomes not only adhere neighbouring columnar cells but also bind columnar cells to the basal cells layer. The basal cell is then attached to the basement membrane via hemidesmosomal attachment.

1.1.2.2.1.1 Structure Of The Tight Junction.

The tight junction consists of 3 integral membrane proteins and 9 peripheral membrane proteins.

1.1.2.2.1.1.1 Tight Junction Integral membrane proteins.

1.1.2.2.1.1.1.1 Occludin.

Occludin is a 65kD transmembrane protein expressed in epithelia, endothelia, neurons and astrocytes (Furuse et al, 1993, Bauer et al, 1999). It has been shown to be directly involved in the formation of tight junctions. Structural studies have shown 4 membrane spanning regions with cytosolic N- & C-terminals.

Antibodies to occludin stain the characteristic tight junction strands (Furuse et al, 1993) therefore occludin was originally assumed to be the main component of tight junctions. However when occludin expression was blocked, the intermembranous strands still formed (Saitou et al, 1998), therefore occludin is localised at these strands but is not essential for their formation (Balda et al, 1996). Since the discovery of the claudins (Furuse et al, 1998a&b), a more regulatory role has been attributed to occludin at the tight junction.

The C-terminal of occludin interacts with various peripheral membrane molecules and has been shown to be important in the selective permeability of the paracellular pores (Balda et al, 1998 & 2000). The N-terminal has been studied in less detail and a function has not been attributed to this region as yet, however an occludin isoform has been identified called 'occludin 1B' which differs from occludin at the N-terminal (Muresan et al, 2000). Despite suggestions of a possible structural role, the significance of this isoform is yet to be established.

1.1.2.2.1.1.1.2 Claudins.

There have been 18 types of claudin identified to date ranging from 22-24 kDa. These proteins are localised exclusively to the tight junction at the intermembrane strands with occludin although there seems to be no sequence similarity between the two protein types. Structurally they are the same however with 4 transmembrane regions and again, cytosolic N- and C-terminals (Morita et al, 1999, Furuse et al, 1998a).

Expression of different types of claudins differs from tissue to tissue relating to distinct paracellular permeability properties. It is thought that the claudins make up most of the structural aspect of the transmembrane region of the tight junctions (Furuse et al, 1998b, Gow et al, 1999, Inai et al, 1999).

1.1.2.2.1.1.1.3 JAM (Junctional Adhesion Molecule).

JAM is a single span transmembrane protein belonging to the immunoglobin superfamily (Martin-Padura et al, 1998). It was originally identified in endothelia but has also been found at the tight junctions in epithelia as well as on the surface of human leukocytes (Ozaki et a, 2000, Williams et al, 1999). Despite having been shown to induce cell adhesion under certain circumstances, unlike the other integral proteins JAM is thought to be less involved in adhesion and more involved in interaction with cells crossing the tight junction barrier (Martin-Padura et al, 1998, Del Maschio et al, 1999)

1.1.2.2.1.1.2 Tight Junction Peripheral membrane proteins.

1.1.2.2.1.1.2.1 MAGUK Proteins

Members of the Membrane Associated GUanylate Kinase family of proteins, all have PDZ, SH3 and GK domains which are important for protein binding and signal transduction (reviewed by Gonzalez-Mariscal, 2000).

PDZ domains are protein-binding modules. Of which there are two types, class I recognise protesins containing a specific COOH-terminal motif whereas class II recognise COOH-terminals with hydrophobic amino acids at the –2 position. PDZ domains can form dimers, ZO-1 associates through its second PDZ to the second PDZ in ZO-2 and ZO-3(Itoh et al. 1999)

SH3 (Src homology 3) modules mediate protein-protein interactions. In ZO-1, the SH3 domain binds to a serine protein kinase that phosphorylates a C-terminal region to the SH3 domain, although the significance of this phosphorylation is as yet unknown (Balda et al. 1996)

The Guanylate Kinase (GK domain) is homologouse to the enzyme that catalyses the concersion of GMP to GDP at the expense of ATP. The tight junction MAGUK proteins are not known to bind neither GMP or ATP however and are predicted to be enzymatically inactive (Haskins et al, 1998). GK has been found to interact with SH3 in PSD –95 (post-synaptic density protein) (McGee et al 1999).

ZO-1, ZO-2 and ZO-3 are three tight junction associated proteins that belong to the MAGUK family (ZO –zonula occludens). These proteins have a adapter role, linking functionally dissimilar proteins into specific membrane subdomains.

The ZO proteins appear to be able to readily adapt to different circumstances. Normally localising exclusively to the tight junction, they relocate to the nucleus of immature or wounded cells (Gottardi et al, 1996). When tight junction formation is inhibited by low calcium conditions, ZO-1 localises to the adherens junction complexed to α,β and γ -catenins that are not complexed to E-cadherin (Itoh et al, 1997). Upon polarisation, no such complexes are seen.

ZO-1 has a species dependent mass of 210-225 kDa (Anderson et al, 1995, Stevenson et al, 1986), whereas ZO-2 and ZO-3 have masses of 160 and 130 kDa respectively (Gumbiner et al, 1991, Balda et al, 1993).

The C-terminal of ZO-1 has an actin binding site as well as 3 alternatively spliced domains α, β and γ. Most epithelia have ZO-1α^+ and α^- isoforms but more of ZO-1α^+. ZO-1α^- on the other hand, is the predominate form in endothelia. In embryonic assembly, α^- is present prior to tight junction assembly whereas α^+ is involved later (Balda et al, 1993, Sheth et al, 1997). The other identified isoforms of ZO-1 are β_1, β_2, and γ.

1.1.2.2.1.1.2.2 Other Tight Junction Proteins.

Cingulin (140 kDa) (Citi et al, 1993), 7H6 (175 kDa) (Zhong et al, 1993), Rab3B (25 kDa) (Weber et al. 1994), Symplekin (110-150 kDa) (Keon, et al, 1996) and ASIP (100-180 kDa) (Izumi et al, 1998) are also found associated to the tight junction. Cingulin is known to interact directly with the ZO proteins and myosin whereas the roles of the other proteins are yet to be firmly established.

1.1.2.2.1.1.3 Tight Junction Protein Interactions.

The integral and peripheral membrane proteins interact in such a way to create a selective semipermeable barrier with a firm anchor to the perijunctional actin belt. Balda (2000) proposed a model of tight junction structure where the intermembrane strands formed by polymers of one or more different types of claudin (depending on tissue). In addition, the polymers contain occludin which changes functional but not physical properties. The tight junctional strands represent the paracellular barrier with tissue dependent claudin composition in order to vary specificity. The 'gate' action is regulated by a 'junctional lock system' where only one strand is open for any given

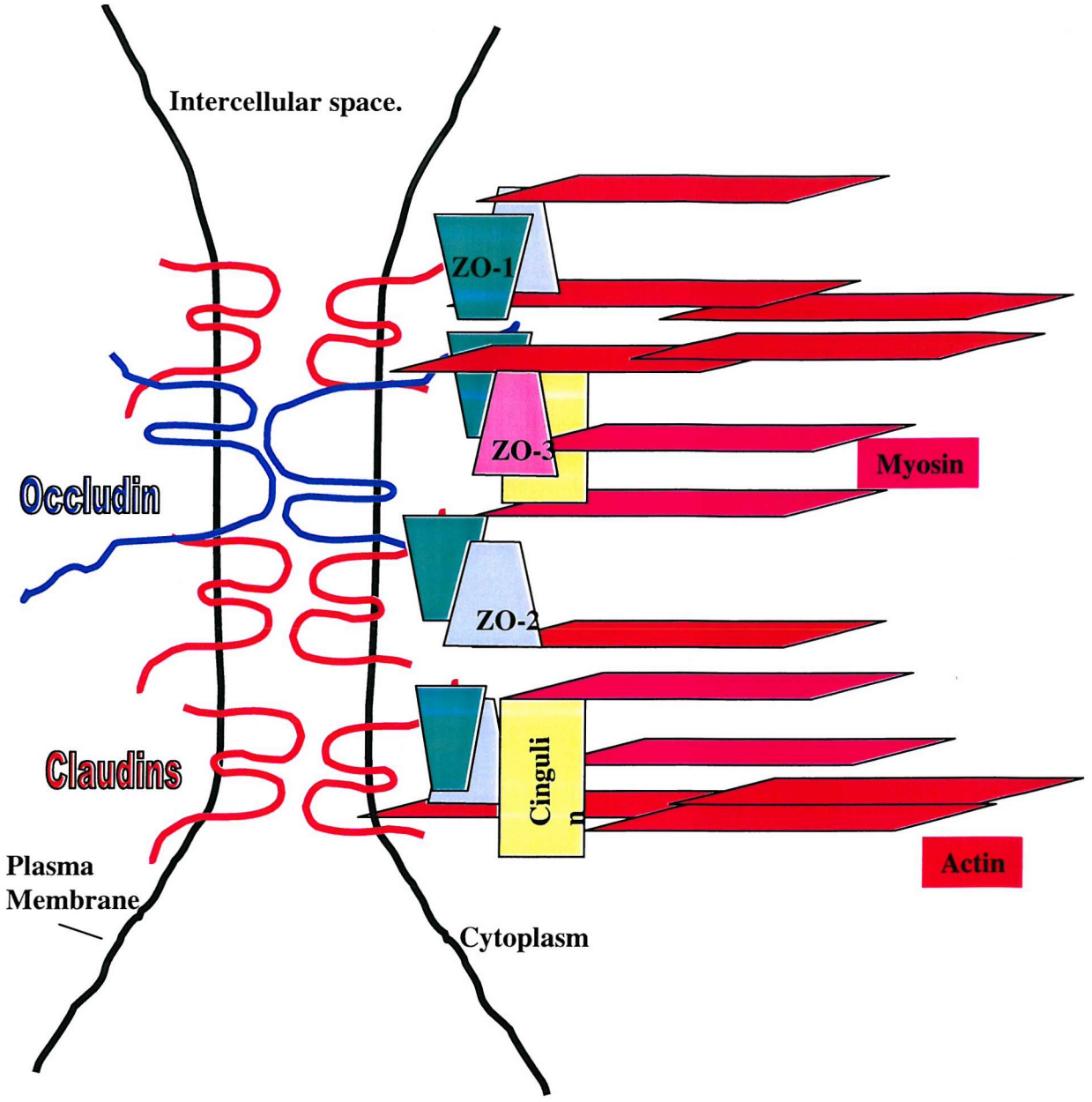

Figure 1.2. Structure of the Tight Junction.

Intramembrane strands are formed by extracellular domains of the Claudins and Occludin. This
system is anchored to the submembranous plaque by interaction of the MAGUK family ZO proteins
with cingulin, actin and myosin.

channel thus avoiding barrier breakdown. The pores within strands are opened in regulated fashion and allow selective diffusion along a concentration gradient

This system is anchored to the submembranous plaque via occludin (which has been shown to bind to ZO-1) and the claudins (which bind with all three ZOs (Itoh et al, 1999)) (see figure 1.2). The ZOs in turn bind to actin (as does occludin) which ZO-1 crosslinks. The ZO proteins interact as dimers of either ZO-1/ZO-2 or ZO-1/ZO-3 which interact with cingulin which also bridges to myosin (Wittchen et al, 1999, Fanning et al, 1998, Haskins et al, 1998).

1.1.2.2.2 The Adherens Junction.

The intermediate junctions or 'zonula adherens' form a ring below the apical tight junctions of epithelial cells. The intercellular space is not obliterated as in tight junctions but is a consistent 25-35 nm in width. This space contains filamentous material where the calcium-dependent cell adhesion molecule E-Cadherin is localised (Gumbiner et al, 1988). E-cadherin constitutes a 'zipper-like' dimer attachment between adjacent epithelial cells and forms complexes with cytoplasmic plaque proteins (the catenins) creating a link to the subapical 'terminal web' rich in actin and myosin (Rodriguez-Boulan 1989).

Nectin complexed with 1-Afadin is also found localised at the adherens junction. Nectin is a member of the immunoglobin superfamily and is a homophilic calcium independent adhesion molecule that dimerises at the cell surface in a similar fashion to E-cadherin (Miyahara et al, 2000). 1-Afadin is an F-actin binding protein, linking the cytoplasmic region of nectin to the actin cytoskeleton. A model for adherens junction formation put forward by Tachibana K (2000), proposed that nectin forms the first transcellular interactions at the epithelial cell surface. E-cadherin is then recruited by 1-afadin and subsequently transinteracts with E-cadherin at nectin based cell-cell adhesion sites on opposing cell surfaces leading to the formation of the adherens junction. Evidence supporting this theory is given by 1-afadin gene

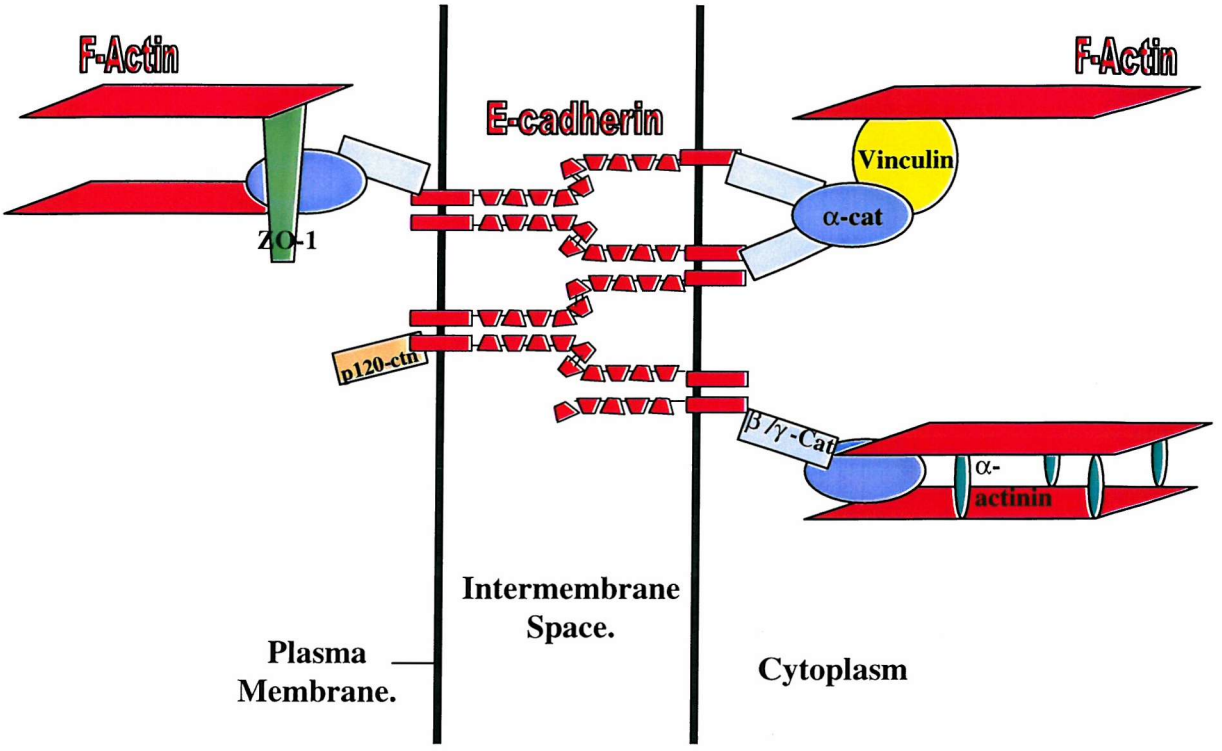

Figure 1.3 Structure of the Adherens Junction.

The intermediate junction although not as constricting as the tight junction is nonetheless a firm bond between adjacent cells. The major adhesion receptors here are calcium dependent homophilic adhesion molecules called cadherins. The cadherins bind with either β or γ catenin which then link to the cytoskeleton via α-catenin.

knockouts where both the adherens junctions and the tight junctions are impaired (Ikeda et al, 1999). Adherens junction assembly has previously been implicated as a prerequisite for tight junction formation (Gumbiner et al, 1988).

1.1.2.2.2.1 Catenins

The catenins are a family of molecules functioning to assist cadherin adhesion, found localised at the cytoskeletal cadherin terminal.

E-cadherin is linked to the underlying cytoskeleton by the α–, β– and γ–catenins. Another catenin called p120ctn also binds to E-cadherin at a site near the transmembrane domain, and has been implicated in intercellular adhesion and cell migration (Anastasiadis et al, 2000) by the recruitment of small GTPases (Noren et al, 2000).

β– and γ-catenin compete for a binding site at a central region of the cytoplasmic domain of E-cadherin (Gumbiner et al, 1993, Kemler et al, 1989). Both of these can then form a bridging link between E-cadherin and the actin cytoskeleton via α–catenin (Rimm et al, 1995). Work by Nagafuchi and coworkers (1994) however, suggests that β– and γ-catenin are dispensable for cell adhesion as long as α–catenin is fused directly to the cadherin cytoplasmic tail.

In addition to a role in cell adhesion, β-catenin is also a transcriptional coactivator in the Wnt growth factor signaling pathway that controls cell fate determination (Polakis, 2000, Ben-Ze'ev et al, 2000). Outside adherens junctions, a multiprotein complex regulates β-catenin stability. In the absence of secreted Wnt glycoproteins, β-catenin is targeted for degradation via phosphorylation by GSK-3β, catalysed by a complex including axin, APC and GSK binding protein (Orford et al, 1997, Huber et al, 2000). In the presence of Wnt signalling, GSK-3β function is inhibited, disrupting the axin-APC-β-catenin complex leading to reduced degradation and hence elevated levels of β–catenin. Excess β–catenin undergoes nuclear translocation and forms complexes with transcription factors activating transcription.

Elevated cadherin levels lead to sequestering of β–catenin away from the nucleus and therefore inhibition of the signaling function.

1.1.2.2.2.2Cadherins

The cadherins are a family of transmembrane glycoproteins characterised by a distinctive sequence motif that is tandemly repeated in their extracellular segments (Hatta et al, 1991).

The classical cadherins are calcium ion dependent homophilic adhesion receptors, well known to play important roles in cell recognition and cell sorting during development (Takeichi, 1991). Cadherins are the major adhesion receptors of the zonula adherens junctions of epithelia. There are many examples of diffusely distributed cadherins mediating cell-cell adhesion but it is generally assumed that junctional localisation represents stronger points of intercellular attachment.

1.1.2.2.2.2.1 E- and P-Cadherin.

To exhibit functional adhesion activity, cadherins must form complexes with catenins and the actin cytoskeleton (Gumbiner, 1993, Kemler et al, 1989).
Johnson and coworkers (1993), used monoclonal antibodies against both alpha and beta catenin and showed that in cells simultaneously expressing E- and P-cadherin, each cadherin appears to be present in a separate cadherin/catenin complex.

E- and P-cadherin have been identified previously as immunologically distinct cadherins, although they and the other cadherins share common characteristics, i.e. being calcium ion dependent and having similar structures and molecular masses. Nose (1987,) also deduced a 58% amino acid homology between E- and P-cadherin and they are almost the same lengths (723 amino acids for P-cadherin and 728 amino acids for E-cadherin). Nose's investigation revealed that homology between these two

cadherin is highest in the N-terminal region and gradually decreases as it approaches the transmembrane region. In addition the two cadherins appear to have different glycosylation properties.

1.1.2.2.2.2.2 Cadherin localisation and structure.

Wu and colleagues (1993), looked at the localisation of E and P-cadherin in the epithelial MDCK cell line. They found a similar distribution for the two cadherins, but found P-cadherin to be extracted with greater ease than E-cadherin. This suggests a weaker anchorage to the actin cytoskeleton and therefore possibly less permanent cell-cell interactions than those of E-cadherin.

Different cadherins have different tissue distributions, E-cadherin mediating a Ca^{2+} dependent adhesion between epithelial cells is most concentrated at the adherens junction (Nagafuchi et al, 1987). Many epithelial cells express only E-cadherin (Yoshida-Noro et al, 1984), and the uterine decidua express only P-cadherin (Nose et al, 1986).

The extracellular domains of the classic cadherins are divided into five repeated sub-domains EC1 to EC5. Binding specificity appears to reside in the first (N terminal) cadherin domain (Blaschuk et al, 1990). X-ray crystallographic studies of the N-cadherin EC1 domain show that it forms a dimer, called the strand dimer, in which the monomers are orientated in parallel with their adhesive binding surfaces directed outward from the plasma membrane (Shapiro et al, 1995). A zipper-like supermolecular ribbon is formed with cadherins on an opposing cell. This is believed to be the fundamental unit of cadherin adhesion.

A Ca^{2+} binding site is located away at the interface between successive cadherin domains (Shapiro et al, 1995), the extracellular domain becomes a stiff rod in the presence of Ca^{2+} (10^{-4}-10^{-3} M [Ca]) and collapses in its absence. Ca^{2+} therefore appears to be acting to stabilise interactions between successive cadherin domains (Pokutta et al, 1994).

1.1.2.2.2.2.3 Cadherin Function.

E-cadherin gene knockouts in mice are embryo lethal (Larue et al, 1994), this giving us some indication of the level of importance of E-cadherin in cellular integrity.

In the absence of E-cadherin expression, epithelial cell junctional proteins fail to maintain intercellular adhesion (Takeichi, 1991). Adhesion maintained by E-cadherin is thought to act as a suppressor of epithelial tumor cell invasiveness and metastasis. E-cadherin deficiencies or mutations correlate with the invasiveness of certain human tumours.

Despite the homophilic nature of constitutive cadherin binding, E-cadherin has been shown to participate in heterotypic adhesive interactions between epithelial cells and intraepithelial lymphocytes *in vitro* by acting as a ligand for the $\alpha_E\beta_7$ integrin on the surface of translocating cells (Cepek et al, 1994).

E-cadherin is also thought to play a role in 'outside-in' signal transduction via the MAPK pathway (mitogen-activated protein kinases) (Pece et al, 2000). MAPKs integrate signals from a range of cell membrane receptors involved in cell fate determination (Zhu et al, 1999). Pece and colleagues (2000), found that adherens junction assembly leads to a significant increase in MAPK activation mediated by cadherins (via activation of epithelial growth factor activation).

1.1.2.2.2.2.3.1 Differential Cadherin Expression.

P-cadherin in many studies appears to be closely associated with the actively proliferating cells with E-cadherin having a more rigid permanent cell-cell attachment role. Tooth cells of the enamel knot (thought to control tooth morphogenesis) strongly express P-cadherin at the cap stage (Obara et al, 1999). Also the expression of P-cadherin was prominent in the inner enamel epithelium during the early to mid bell stage. When the cells of the inner enamel began to polarise and differentiate at the

late bell stage, the cells lost P-cadherin and strongly expressed E-cadherin, however this E-cadherin was lost at later stages.

In the mammary ducts, there are two layers of ectodermally derived epithelium. Immunostaining by Daniel and coworkers (1995), showed abundant E-cadherin on the lateral membranes of end bud body cells but no P-cadherin. However the basally located cap cells and the ductal myoepithelial cells displayed only P-cadherin. Antibodies to both cadherins used separately resulted in disruptions of their associated cell layers, indicating that compartmental expression of E- and P-cadherin is required for mammary tissue integrity and normal rates of DNA synthesis.

Hair follicle morphogenesis studies by Muller-Rover and colleagues (1999), showed P-cadherin to be restricted to the neonatal epidermis basal layer whereas E-cadherin is seen in all epidermal layers. Later stages show a strong E-cadherin expression in the outermost portion of the root sheath while the innermost portion exhibited isolated P-cadherin, indicating segregation of hair follicle keratinocytes into functionally distinct sub-populations.

P-cadherin expression has been observed in a similar localisation to E-cadherin in the epithelial cells of the seminal vesicles and ejaculatory ducts. In the prostate however it was limited to the basal cells of the prostatic acini. E and P-cadherin are expressed in distinct regions of the epidermis, E-cadherin is expressed on all epidermal layers and P-cadherin only in the basal layer (Shirahama et al, 1996).

An adhesive role for P-cadherin is observed in the postnatal development of the testis (Lin et al, 1996a). P-cadherin is initially expressed by Sertoli cells during postnatal development then in the peritubular cells, and correlated with β-catenin expression and the development of a mature network of actin filaments. The same group (Lin et al, 1996b) also suggest a role for P-cadherin in testicular cord formation.

Each of these examples demonstrates the adhesive function of cadherins but also an apparent differential cadherin specific adhesive function, indicated by the need for spatial and temporal expression differences between E- and P-cadherin.

1.1.2.2.2.2.3.2 Cadherin crosstalk.

All epithelial cells of the lung express both E- and P-Cadherin at the early developmental stage. P-Cadherin, however, gradually disappears during development, initially from the main bronchi and eventually from all epithelial cells (Hirai et al 1989a). When a monoclonal antibody to E-Cadherin (ECCD-1) was added to monolayer cultures of mouse lung epithelial cells, it induced a partial disruption of their cell-cell adhesion, while a monoclonal antibody to P-Cadherin (PCD-1) showed a more subtle disruption. A mixture of the two antibodies, however, displayed a synergistic effect (Hirai et al, 1989a). The effect of antibodies on the morphogenesis of lung primordia using an organ culture system showed that in the control media, explants formed typical bronchial trees. In the presence of ECCD-1, the explants grew up at the same rate as the control, but their morphogenesis was affected. The control explants formed round epithelial lobules with an open lumenal space at the tips of the bronchial trees, whereas the lobules of explants incubated with ECCD-1 tended to be flat and devoid of the lumenal space. PCD-1 showed a similar but very small disruption. A mixture of the two antibodies, however, showed a stronger effect: the branching of epithelia was partially suppressed and the arrangement of epithelial cells was distorted in many places. These results suggest that E- and P-Cadherin have a synergistic role in the organisation of epithelial cells in lung morphogenesis.

1.1.2.2.2.2.3.3 Cadherins in Neoplasia.

The expression of E- and P-Cadherin is altered in malignant carcinoma. An inverse relationship between E-cadherin expression and malignancy has been detected in different types of carcinoma (reviewed by Birchmeier and Behrens, 1994). Loss of expression or function in tumours has been linked to the invasive and metastatic phenotype.

Altered E- and P-cadherin expression has been demonstrated in pre-malignant and malignant skin tumours, such as the aberrant suprabasal localisation of P-cadherin and the focal loss of E-cadherin at cell junctions in murine p53-null

papillomas (Cano et al, 1996), reduced E-cadherin and aberrant P-cadherin expression in human SCC (squamous cell carcinoma) (Shirahama et al, 1996, Wakita et al, 1998), and reduced expression of one or both cadherins in nodular basal-cell carcinomas (Pizarro et al, 1995).

E-cadherin and β-catenin were regulated in advanced stages of nasopharyngeal cancer and expression was linked with short survival (Zheng et al, 1999). Both E- and P-cadherin are expressed in normal breast tissue. E-cadherin in the lumenal and myoepithelial cells, whereas P-cadherin is confined to the myoepithelium. Antibodies to E-cadherin and the catenins in grade III ductal carcinoma of the breast showed that reduced E-cadherin-catenin complex expression was associated with a decrease in contact inhibition of motility but not growth (Gillet et al, 2001). E-cadherin was present in invasive and in situ ductal carcinoma whereas nearly all lobular carcinomas had complete loss of E-cadherin. P-cadherin on the other hand was absent from all benign breast lumenal epithelium and some ductal and lobular. Droufakou and colleagues (2001), showed that most invasive lobular carcinomas of the breast show genetic or epigenetic changes affecting the E-cadherin gene leading to decreased E-cadherin expression.

In the lung, reduced E-cadherin expression is associated with tumour dedifferentiation, lymph node metastasis and poor prognosis in non-small cell lung cancer. A study by Liu (2001) implicated decreased tyrosine phosphorylation of E-cadherin as a causative factor in the redistribution and consequent loss of function of the E-cadherin/β-catenin complex.

Cadherin transfection into Lewis lung carcinoma cells decreased invasiveness (*in vitro*). This was true for both E- and P-cadherin although invasion suppression was evident only in cells with other contact (Foty et al, 1997).

Reduced E-cadherin expression has also been associated with the invasiveness of tumours of the GI tract (Shimoyama et al, 2000), the bladder (Shariat et al, 2001) amongst others. In glandular tumours of the cervix however, in all cases, E-cadherin expression is similar in both normal and malignant glands. P-cadherin on the other

hand, although not observed in benign glands was aberrantly expressed in 96% of invasive cancer studied (Han et al, 2000).

Each of the above examples displays invasiveness related to altered cadherin expression. This further demonstrates the need for strong regulation of cadherin expression, given that divergent levels are associated with and perhaps influence phenotypic cell changes.

1.1.2.2.3 Desmosomes.

The desmosomes form part of a lateral transcellular network, serving as cell surface attachment sites (0.1-1.5μm in diameter) for intermediate filaments giving the epithelia high tensile strength (Garrod et al, 1993).

Desmosomal assembly is calcium dependent and requires contact from two neighbouring cells (Mattey et al, 1986a). Adjacent epithelial cells have desmosomal mirror image cytoplasmic 'plaques', which serve as membrane anchorage sites for the keratin filaments. The two major glycoproteins which comprise the desmosomal plaque are the desmosomal cadherins 'desmoglein' and 'desmocollin', for which there are a variety of isoforms with distinct tissue specific patterns of expression (Kreis and Vale (eds) 1994, Garrod et al, 1993). These are structurally related to the classical cadherins, with major differences seen in their cytoplasmic domains, the desmosomal cadherins being much longer in this region. This difference allows the interactions with the intermediate filaments (Suzuki et al, 1996).

The desmosomal cadherins probably mediate desmosomal adhesion via heterophilic interactions between them (Chitaev et al, 1998). The plaque is then linked to keratin filaments via two cytoplasmic armadillo proteins, plakoglobin and plakophilin (Bierkamp et al, 1996)

Plakoglobin is identical to the adherens junctional associated protein γ-catenin, which has also been implicated in signal transduction (Kanai et al, 1995, Fuchs et al, 1996). Plakoglobin is sometimes found at the adherens junction associated with classical cadherins, probably in place of γ-catenin (Troyanovski et al, 1993, Peifer et al 1992, Korman et al 1989).

Desmosomes of epithelial cells have been shown to differ in adhesive properties according to the level of cell confluence. Pre-confluent cell cultures are calcium dependent, with an increase in calcium concentration from low (<0.1mM) to physiological levels (1.8-2mM) resulting in an increased level of desmosomal assembly (as would be expected as members of the cadherin family). However, confluent cultures of epithelial cells are seemingly calcium independent and become resistant to the desmosomal disruption seen in sub-confluent cultures on removal of calcium (Mattey et al, 1986a&b).

1.1.2.2.4 Gap Junctions.

The gap junction or 'macula communicans', is a discrete focal structure that in cross section appears as an area in which the two opposing plasma membranes come in close proximity. The gap between them is approximately 2-4nm in width (Revel et al, 1967).

Gap junctions are hydrophilic arrays of intercellular membrane channels which allow passage of inorganic ions, second messenger substances and small metabolites up to 2000 Da from cell to cell (reviewed by Bruzzone,1998).

The 'unit' of the gap junction is the connexon. This is a cylindrical structure which forms a channel in the membrane. End to end docking of connexons from two adjacent cells creates the intercellular channel. Each connexon comprises 6 connexin subunits (Unger et al, 1999). Connexins are a family of >15 members ranging from 26-57kDa (Bruzzone et al 1998). All have 4 transmembrane domains with cytosolic N- and C-terminals.

The diversity of gap junctions stems not only from the variation of connexins in homotypic junctions but also the existence of heterotypic junctions of different connexons *and* connexins .

1.1.3 Epithelia in Asthma.

Asthma is a condition of reversible obstruction of the conducting airways accompanied by damage to the bronchial epithelium. Susceptible individuals, have recurrent episodes of wheezing, breathlessness, chest tightness and cough, usually associated with variable airflow limitation often accompanying inflammation.

Although asthma can occur in patients with no demonstrable allergy (intrinsic asthma), most asthma occurs in association with allergy (atopic asthma), particularly from house dust mites, pets and pollens. Allergens cause sensitisation of the airways by interaction with antigen-presenting cells. In order to achieve this, allergens must first cross the epithelial barrier, the mechanisms involved is yet to be established.

The cysteine proteinase allergen Dermatophagoides pteronyssinus 1 (Der p 1) from the faecal pellets of house dust mite, was found to induce cleavage at the tight junction after inhalation (Wan et al. 1999). Putative Der p 1 cleavage sites were found in the extracellular domain of occludin and claudin-1, resulting in tight junction breakdown, increased barrier permeability and passage of Der p 1 through the paracellular pathway. Cleavage may on the otherhand, be indirectly induced by an external cleavage signal cascade triggered by Der p 1 and resulting in degradation of occludin. Wan and coworkers reported no inhibition of this process by protease inhibitors and therefore concluded the most probable mechanism to be direct cleavage of occludin by Der p 1.

Similarly Goto et al (2000) found adherens junction disruption in guinea pig airways following ovalbumin sensitisation. Here E-cadherin was found to detach from the lateral surface of the epithelia cells before release into the lumen.

Studies with Aspergillus fumigatus (A. fumigatus), also showed cellular disruption (Tomee et al, 1999). Culture filtrates from A. fumigatus induced production of proinflammatory cytokines and caused cell detachment in pulmonary epithelial cell lines. These actions were inhibited by inhibition of fungal serine protease activity, indicating that the release of serine proteases from A. fumigatus initiates these effects. Tomee and coworkers suggest that the cell detachment exposes

subepithelial structures and facilitates fungal access to lung parenchuma resulting in infection.

Each of these investigations indicate a mechanism of transepithelial allergen delivery, it is still unknown however why some individuals are more susceptible to allergy than others. It may be that the inflammatory response of the epithelium may be impaired in some individuals. These defence mechanisms are important in chemoattraction and activation of monocytes, lymphocytes and neutrophils, downregulation would leave the airway epithelium vulnerable to allergen challenge.

Epithelial biopsies in asthmatics show abnormal histology (Laitinen et al. 1985, Jeffery et al 1989), with epithelial shedding, inflammation, goblet cell hyperplasia and exposure of the basal cells and nerve endings. In addition 'airway remodelling' is seen in airways of all sizes in fatal asthma regardless of the underlying cause of asthma.

Remodelling involves the thickening of the wall and smooth muscle of the airway. The airway is irreversibly narrowed by smooth muscle shortening thus heightening the predisposition of asthmatics to asthma exacerbation and even death from airway obstruction caused by smooth muscle contraction, airway edema and mucus plugging (Fahy et al, 2000).

The apparent thickening of the subepithelial basement membrane in asthma is misleading however. Deposition of collagens I, III and IV as well as fibronectin to the lamina reticularis layer gives the impression of a thickened basement membrane whereas the actual fibrosis occurs immediately below with the basement membrane remaining at a relatively constant thickness in asthmatics and controls (Homer et al, 2000). The lamina reticularis on the other hand can range from 4-5μm in normals. To 7-23μm in asthmatics

Changes to subepithelial vascularity are also seen in asthma, in that there is increased blood flow to the airways post-antigen exposure. This coincides with increased airway resistance and is thought to be the major contributor to exercise induced asthma (Kuwano et al, 1993,) .

Abnormal airway mucus production is associated with the loss of lung function in asthma (Aikawa et al, 1992). The mucus of the respiratory system is formed mainly from the secretion of the submucosal glands, goblet cells and tissue fluid (Reid et al, 1965). Mucus content in asthma is quantitatively and qualitatively different from normal with increased levels of mucin, albumin and DNA (Fahy et al, 1993), and increased concentrations of plasma derived proteins, cytokines and chemokines (Smith et al, 1993). Airway secretions also contain an increased level of eosinophils leading to the presence of the eosinophilic breakdown products 'Charcot-Leydon' crystals (crystals of eosinophil lysophospholipase) (Sakula, 1986).

Another feature of asthmatic mucus is the presence of clumps of fully functional shed columnar epithelial cells. These 'Creola bodies' are characteristically seen in the sputum of asthmatics (Naylor et al, 1962) and contribute to the mucus plugging associated with diseased airways.

Epithelial shedding further contributes to airway obstruction by the inevitable reduction of mucociliary clearance which further increases the 'clogging' of the airways with cellular debris. Normal clearance involves the coordinated beating of cilia on the surface of the columnar cells creating a wave effect, propagating the mucus and debris for subsequent expectoration (Sleigh, 1966).

1.1.3.1 Inflammatory Response.

Asthma as an inflammatory disorder involves mediator release from activated mast cells and eosinophils as well as the recruitment of infiltrating neutrophils into the region of damage. Concentrated regions of both eosinophils and neutrophils are found within area of epithelial denudation, as well as clusters of free eosinophil granules.

The epithelial cell itself is suspected to be playing an active role in initiating or at least amplifying airway inflammation (Jacoby et al, 1997). It is an important source of inflammatory mediators including endothelin-1, nitric oxide and cytokines which,

along with altered adhesion molecule expression, participate directly in inflammatory cell recruitment and activation.

Exposure of the asthmatic airway to inhaled allergens results in the uptake and processing by antigen-presenting cells (e.g. dendritic cells and macrophages). Effector cell-associated cytokines are subsequently released, stimulating transendothelial migration of recruited leukocytes.

Leukocytes must adhere to endothelial cells before they can migrate into the extravascular tissue. Their surface adhesion molecules interact with those of the endothelial cell, these surface adhesion molecules are upregulated during inflammation leading to positive feedback and an enhanced recruitment of infiltrating cells (Raeburn et al, 1994).

The eosinophil is an end stage cell with acid staining granules of two types, the larger of which being mainly comprised of major basic protein (MBP). Other constituents include eosinophil cationic protein (ECP) and eosinophil peroxidase (EPO), all of which may contribute to damage of the airway epithelium (Middleton et al, 1981, Yukawa et al, 1990).

Eosinophil number and activation is increased in asthmatic airways (Roisman et al, 1995), this is thought to damage the epithelium leading to a release of viable cells probably due to a targeted attack on the intercellular junctions. The fact that the shed cells observed in the bronchoalveolar lavage have preserved ciliary function (Montefort et al, 1993) suggests sloughing of intact, functional cells and therefore a possible defect of their adherence and not primarily a cytotoxic effect.

In vitro studies by Persson and coworkers (1996), showed that on epithelial removal, neutrophil number promptly increased under the denuded area and appeared activated. The mediators and cytokines produced and released and the adhesion molecules expressed, encourage the migration, activation and survival of inflammatory cells (especially eosinophils) in asthmatic airways. Although neutrophils and eosinophils are considered to be one of the main culprits of airway damage, in the absence of an intact epithelium, these leukocytes may play a role in mucosal defence. Several studies have indicated a proinflammatory role for the epithelium with a role for the leukocytes in the protection of the naked basement

membrane from the allergens and pathogens of the bronchial lumen from which it would normally be separated (Roisman et al, 1995, Raeburn et al, 1994).

Recent findings indicate that asthma is more than an inflammatory response (Holgate et al. 2000a). Results suggest that the asthmatic state results from an interaction between susceptible epithelium and TH-2 (T-helper-2 lymphocyte) mediated inflammation that alters communication between the epithelium and the mesenchymal cells causing disease persistance, airway remodelling and decreased responsiveness to corticosteroid treatment.

There is evidence that the asthmatic epithelium has increased suceptibility to injury and an impaired ability to repair itself resulting from and imbalance in signalling by members of the EGF (epidermal growth factor) and TGF-β (transforming growth factor-β) growth factor families. EGF promotes proliferation and the production of MMP (matrix metalloproteases) which degrade the ECM. TGF-β on the other hand inhibits proliferation and promotes ECM synthesis. These growth factors therefore would be expected to act in opposition, this may provide an explanation for why there an inadequate proliferative response is seen in asthma (reviewed by Holgate, 2000b).

Normal bronchial epithelium has elevated EGF expression solely in areas of structural damage (Davies et al, 1999) whereas in asthma EGF is overexpressed both in damaged and morphologically intact epithelium, the extent of which correlates with the collagen thickness of the reticula lamina (Puddicombe et al, 2001).

1.1.3.2 Epithelial Shedding.

A feature of asthma attacks is the presence of clusters of cells in the sputum of sufferers. These clusters of cells, known as 'creola bodies', consist of ciliated columnar cells, sloughed off from the airway epithelial lining (Naylor et al, 1962). Sections of human asthmatic trachea show areas of epithelium from which these functional cells have been shed as denuded patches resulting in exposure of basal

cells and nerve endings (Jacoby et al, 1997), consequently the epithelial barrier function is impaired and there is increased contact with irritants. Loss of the ciliated columnar cells would also result in an inability to clear airway secretions and hence an accumulation of fluid.

Damage in vivo, results in both short-lived denuded areas of naked basement membrane and areas of loss of clusters of columnar epithelial cells, in the latter case, non-ciliated, low height basal cells remain (Persson et al, 1996). Biopsy studies such as those by Soderberg and colleagues (1990) have shown airways with up to 50% denudation. When columnar cells are shed in this manner, the damage appears to be localised along the basal-columnar cell junctions. Montefort (1993) suggested that either this was a result of increased inflammatory cell infiltrate or a weakness of adhesive mechanisms along this plane in asthmatics. As these regions are particularly dense with desmosomal attachments, their presence was either a compensatory strengthening mechanism or that they were already there but are vulnerable to damage exerted on this plane in asthma (Montefort et al, 1993).

The exposure of submucosal nerve endings to the inhaled noxious agents of the lumen is thought to initiate a signal resulting in vasodilation of submucosal microvessels and an increased plasma protein leakage (Montefort et al, 1993). However, the expected increase in permeability is not routinely observed (Elwood et al, 1993).

Erjefält and coworkers (1997), looked at the barrier function of airway epithelial basal cells after loss of columnar epithelial cells in human and guinea pig airways. By selective removal of the columnar cells using a tissue adhesive glue, the guinea pig airway was found to have patchy denudation, focal inflammation and instantaneous repair. The remaining cells took less than 20 minutes *in vivo* to become extensively flattened and cover the denuded basement membrane. A poorly differentiated layer of cells covering the denuded area was established, with overlapping cytoplasmic protrusions between the flattened cells at the borders. This study suggests that this may be an important epithelial defence mechanism, in that the

new poorly differentiated layer of cells has less cells and therefore less junctions for permeation of molecules from the airway lumen to the tissue. Erjefält (1997), also suggested that increased permeability is transient and rapidly reversed, this may be due to the high speed of airway epithelial restitution processes.

1.1.3.2.1 Epithelial Restitution.

1.1.3.2.1.1 Supramembranal Gel.

Immediately after the initial damage, there is an extravasation of plasma from the microcirculation beneath the denuded area. The exudate passes through the epithelial basement membrane and up between epithelial cells without any long term disturbance structurally or functionally to the intercellular junctions (Erjefält et al, 1995). Not even the barrier forming tight junctions of an intact epithelial lining appear to be significant obstacles to further flux of exudate into the airway lumen (Persson et al, 1993). Putative paracellular pores are formed which allow the relatively un-sieved transepithelial passage of bulk plasma.

The damaged area of airway is promptly covered in a gel rich in extracellular matrix fibres, adhesive proteins such as fibrinogen and fibronectin as well as growth factors and cytokine binding proteins. The plasma derived gel is also rich in eosinophils, these are normally located in the basal epithelial cell layer (guinea-pig airways, Persson et al, 1996). However, less than 10mins after damage has occurred the eosinophils have migrated into the lumen and the supramembranal gel.

Meanwhile, beneath the basement membrane, neutrophils are recruited and within minutes become distributed along the area just under the area of denuded basement membrane. These leukocytes are capable of releasing chemoattractant and proliferative factors, and therefore may assist in the re-epithelialisation process, as well as a putative role protecting the naked basement membrane from invading

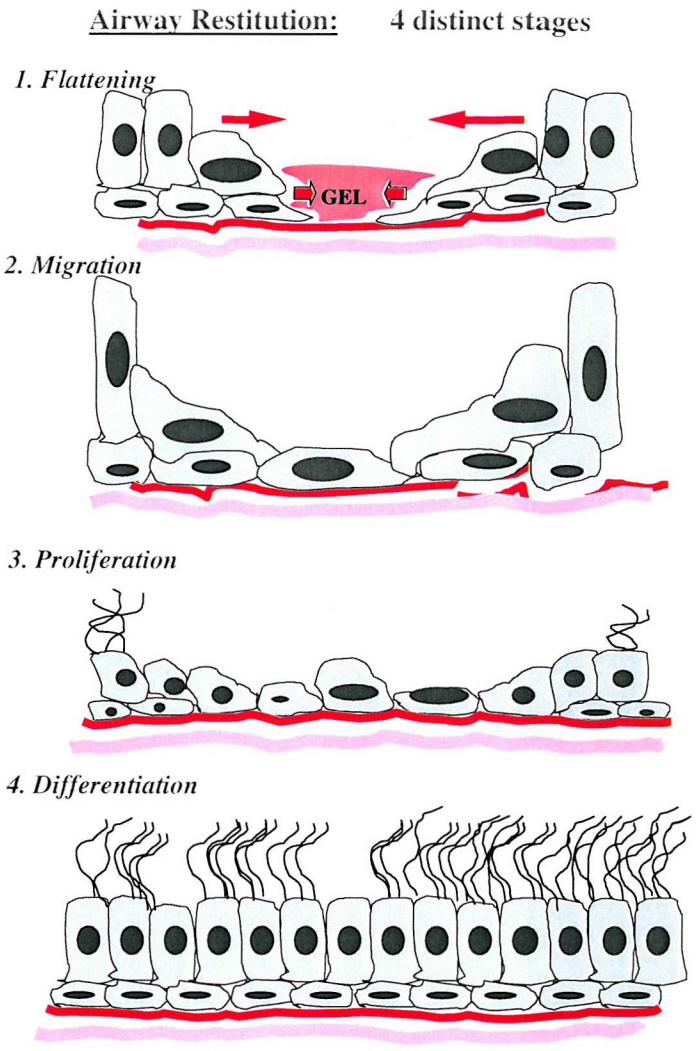

Fig 1.4 Epithelial Damage and Subsequent Restitution Stages.

Immediately after the appearance of a damaged region there is rapid extravasation of plasma from the microcirculation beneath the denuded area, resulting in the presence of a supramembranal gel which is continuously renewed until a new sheet of cells is established. Cells bordering the denuded region flatten and migrate to cover the naked basement membrane.
A layer of poorly differentiated restitution cells is established, proliferation is markedly increased in these cells which later undergo a differentiation stage resulting in a once again intact functional epithelium.

allergens and pathogens. During the course of restitution, a gradual decrease in the number of these cells present is observed (Persson et al, 1996).

The basement membrane of the damaged region is reformed as the epithelium heals (Furutani et al, 1998). The basement membrane component Laminin-1 was shown to appear under migrating epithelial cells 24hr post injury during corneal wound healing (Suzuki et al, 2000). Laminin-2 has also been shown to be expressed in the basement membrane of asthmatic airways (Altraja et al, 1996). The bronchial epithelial cells use integrin receptors to adhere and migrate over laminins-1 and -2 and collagen post-injury (White et al, 1999). The supramembranal gel prevents the basement membrane from being exposed during the healing process, as well as protecting the migrating epithelial cells on its surface. It vanishes only when new epithelial cover has been established.

1.1.3.2.1.2Migration.

Basal cells respond to loss of neighbouring columnar cells by prompt flattening, spreading out laterally to cover the denuded area. The flattened cells change their phenotype and migrate into the wounded area. The restitution cells of the repairing epithelium may also originate from secretory and ciliary cells that have dedifferentiated and migrated on the appearance of the denuded area (Persson et al, 1996). This migration probably requires cycles of junctional assembly and disassembly to allow such dynamic movement.

The cell spreading and migration depend on cell-matrix interactions, mediated by fibronectin and one of its cellular receptors, the $\alpha_5\beta_1$ integrin (Herard et al, 1996), both of which are upregulated in repair. Throughout this migration phase the supramembranal gel is constantly renewed with extravasations of bulk plasma, and remains until the denuded area is completely covered with a sheet of tightly bound although poorly differentiated epithelial cells, providing an interim cover .

Epithelial migration during repair has been proposed to occur by two distinct methods. Firstly via lamellipodia advancement of leading edge cells (Legrande et al, 2001). These protrusions are anchored to the basement membrane onto collagen IV via primordial contacts. MMP-9 was found to accumulate just behind these contacts and has been suggested to be involved in the specific degradation of collagen IV. Subsequently more stable fibronectin-containing contacts are formed in the central part of the cell, while new primordial contacts with collagen IV are made on the forefront, thus powering cell advancement.

In repairing corneal epithelium, wound healing probably via lamellipodia occurs at a steady rate for approx. 6 hours at which time healing accelerates dramatically (Buck et al, 1979). The second putative migratory mechanism which would account for this change involves the actin filament network which is found localised to the leading edge of migratory epithelium (Bement et al 1993). Danjo and co-workers (1998) propose a model of migration where the actin cable, seemingly running cell to cell, contracts as a 'purse-string' drawing in the wound edge across the damaged region. This model allows for the coordinated sheet-like migratory movement observed in repairing epithelium. Although given that as the wound area decreases the number of cells at the leading edge would also decrease, the actin anchoring adherens junctions must be less stable and have different characteristics to those of non-motile cells.

In vivo experiments carried out by Erjefält (1996) demonstrated an extremely fast migration of flattened epithelial cells at a few μm/min, much faster than had been witnessed *in vitro* by Zahm and coworkers (1991). The *in vitro* study involved the chemical wounding of an epithelial sheet at confluence creating a circular wound. Migratory speed in this experiment was highest in cells at the wound edge but only reaching 0.75μm/min. An earlier experiment by this group using smaller mechanically induced wounds had an even slower migratory speeds of under. 0.43 μm/hr (Zahm et al, 1992).

Erjefält (1996) suggest that plasma-derived factors and also leukocyte derived factors such as chemoattractants and proliferative factors contribute to this distinction.

1.1.3.2.1.3Proliferation.

When the migration phase is complete, mitosis is markedly increased accompanied by a slight proliferation activity increase in the old epithelium as well as in the underlying subepithelial fibroblasts and smooth muscle cells , possibly contributing to the observed basement membrane thickening in asthma.

Zahm and colleagues (1997), quantified this epithelial cell proliferation using a Ki67 antigen which is a marker of cycling cells. Mitosis in the repairing area peaked at 48 hours post damage in cells 160-400μm from the wound edge.

Increased mitotic activity has been shown to occur predominantly in the wound area and to halt upon wound closure (Zahm et al, 1997, Shimizu et al, 1994). It has also been suggested that migration has an inverse relationship to proliferation, speeds slowing as the number of cells increases (Abercrombie et al, 1953).

1.1.3.2.1.4Differentiation.

A differentiation stage to a normal phenotype occurs (Raeburn et al, 1994). A study by Barrow (1993) showed that growth factors stimulated such cell proliferation and differentiation after epithelial injury. Around four to eight days after denudation, the number of cells returned to normal as does the height and morphology.

Due to the speedy *in vivo* restitution process (Erjefält et al, 1995), extensive shedding may occur or may have occurred recently also in airways where denuded areas are not found, but only a single layer of undifferentiated cells is seen.

1.2 Aims and Objectives.

This thesis aims to identify morphological and molecular correlates of airway epithelial repair. In order to understand the importance of epithelial disruption in disease, we need to understand the processes involved in repair and regeneration of the epithelium.

Firstly the aim of the work presented in chapter 3 is to gain further knowledge of the morphology of the airway epithelium, distinguishing 'normal' from repairing epithelium and identifying features characteristic of restitution. A detailed morphological investigation using bronchial biopsies and image analysis will help toward characterisation of the cell phenotype associated with repair.

As the repairing bronchial epithelial cells adhere, proliferate and migrate to form a confluent cell layer, cell adhesion molecule expression and function must accompany these restitution processes in such a way that the epithelial sheet forms a barrier but still enables intercellular reorganisation.

In order to examine influences and interactions between the component molecules of the epithelial junction, chapter 4 will focus on looking at the coordination of adhesion molecule expression in models of developing epithelium and comparing these with wounded, with the ultimate aim of modeling key aspects of 'normal' and 'asthmatic' cell phenotypes.

This work will give a clearer picture of how adhesion molecule expression levels alter in response to epithelial damage. Barrier function experiments in parallel will also establish the efficiency of the repair response and indicate the speed with which an intact functioning epithelium can successfully reform.

E-cadherin is known to have a major role in the formation of cell contacts, it forms the adherens junction and is a prerequisite for tight junction assembly, therefore it must undergo intensive regulation in order to instigate these activities. For this reason the focus in chapter 5 is on E- and P-cadherins, the extent of their influence in repair and epithelial integrity.

Bronchial epithelial cell clones of varying E-cadherin expression will be used to examine the relevance of E-cadherin expression and the consequences of E-cadherin manipulation. This study will look at whether the level of E-cadherin expression affects the expression levels of the other prominent cadherin of the adherens junction, P-cadherin. This system will also be used to determine the effect of E-cadherin expression on barrier integrity.

The mechanisms and triggers of junctional adhesion are not fully understood, particularly in the case of P-cadherin mediated junctional attachment. This cadherin in particular is believed to be associated with actively proliferating cells and so its expression patterns may differ to those of E-cadherin. It may be that P-cadherin should be the focus of attempts to increase the rate of epithelial repair given that a higher proportion of proliferating cells would be required during this process.

The generation of a range of over-expressing P-cadherin clones of varying levels would give a means of assessing the relevance of P-cadherin expression. These clones will be used in conjunction with the E-cadherin clones to look at the relationship between the two cadherins and the importance of this relationship in ongoing repair. By establishing expression patterns we can speculate on the roles of these molecules and look further into their functions using blocking and migration experiments.

Consideration of the data from each of these studies together will help towards the characterisation of the bronchial epithelial restitution process and the integral molecular interactions, furthering our understanding of the regulation of cellular junctions and the potential enhancement of cell adhesion. A more efficient repair process would be of utmost importance reducing periods of epithelial denudation and therefore tissue exposure seen to extreme degrees in asthmatic patients.

Chapter Two

General Methods.

2 General Methods.

2.1 Cell Culture

2.1.1 Routine Cell Maintenance.

16HBE14o- cells were maintained at 37°C and 5% CO_2, in MEM supplemented with 5% FCS with medium changes every 3-4 days and subculture when necessary.

For subculture, cells were exposed to cell dissociation solution (Sigma) and trypsin for 5-15 minutes depending on the resilience of the cell layer, until cells had rounded up and detached from the flask and each other. Media including FCS is added to the cell suspension and the mixture transferred to a universal bottle for cell counting. Appropriate dilutions were made by adding the appropriate volume of cells to medium in a culture flask.

16HBE14o- E-cadherin transfected clones were maintained in the same way as the untransfected cells, with additional supplements to the media (see solutions section 2.1)

2.1.2 Freezing cells.

Cells were routinely frozen in liquid nitrogen for long term storage. Approximately 10^6 exponentially growing cells were resuspended in 1ml of a 1:1 mixture of growth media and freezing media (MEM with 35% FCS and 20% Glycerol). Aliquots were frozen slowly by storage at -70°C in an insulating container for 24hrs before transfer to liquid nitrogen.

When required, cells were thawed quickly at 37°C, washed free of the freezing medium by centrifugation in 5ml fresh medium (900rpm, 5mins at r.t.), resuspended in 5ml medium and cultured as normal in a $25cm^2$ flask.

2.1.3 Transepithelial Electrical Resistance (TER).

Cells were harvested as normal and seeded onto transwell membranes (Costar) at a density of $3x10^4$ cells/membrane. Coating medium (50µl) was added to the apical surface of the transwell and these were incubated at 37°C for a minimum of 30 minutes pre-seeding. Growth medium (200µl) was added to the apical membrane compartment and 500µl to the basal compartment.

TER was measured using a Millipore®-ERS resistance meter by insertion of electrodes simultaneously into the basal and apical transwell compartments.

2.1.4 Permeability Assay.

Cells were plated in 200µl medium/transwell as detailed above and TER was monitored as described above. Permeability was assessed on the 14^{th} day post-passage at which point resistances were well developed (400-1000Ωcm^2).

110µl of culture medium was removed from the apical membrane compartment. Fluoresceinated dextran (10µl, 4.4kD, 5mg/ml in H_2O, Sigma.) was added to each apical compartment. Plates were incubated at 37°C for 30 mins to allow equilibration. After this time transwells were transferred to a fresh plate with 700µl media (pre-warmed to 37°C). These plates were incubated for a further 2 hrs and then the transwells transferred back to the original plate which can then be used in a resumed TER experiment..

Solutions for a fluoresceinated dextran standard curve were made up (0.01-3.0µg/ml) 200µl/well in a 96 well plate. Absorbencies were measured using a

Wallace plate reader. Samples were taken from the 700µl remaining in the flux assay 24 well plate and assayed alongside the standards.

2.1.5 Cell Counting

Cell number was assessed using a Coulter Counter® ZM (model no. 0901). Samples of cells were diluted in electrolyte and counted by drawing sample through the counter. As each cell passes through the detector, it changes the resistance to the current flowing through by an amount proportional to the volume of the cell. This generates a pulse which is amplified and counted.

2.2 Cell Adhesion Molecule Analysis.

2.2.1 Immunoblotting of Cell Adhesion Molecules.

Immunoblotting enables the detection of cellular antigens immobilised on a membrane matrix using antibody probes. Cellular protein extracts are separated by polyacrylamide gel electrophoresis (PAGE) and electrotransferred to the membrane matrix where they are readily accessible to detection by antibodies.

2.2.1.1 Whole Cell Lysis to Produce Soluble Extract of Proteins.

Cells and tissues must be lysed to release the antigen protein for analysis by immunoblotting.16HBE14o- cells were grown as normal in 6 well plates from an initial plating density of 10^5/well. At the required time-point, medium was removed and the cells washed briefly in PBS. 250µl of boiling 2% SDS was added directly to the cell surface. Cells were collected using a cell scraper and a positive displacement pippette. Each sample was heated for 4mins at 100°C then stored overnight at -70°C or longer term in liquid nitrogen.

2.2.1.2 Protein Assay.

A Bio Rad DC Protein assay was used and is a colorimetric assay for protein concentration following detergent solubilisation. This is a modified version of the Lowry assay (Lowry OH., et al., 1951).

The reaction is between protein and copper in an alkaline medium which subsequently reduces the Folin agent (reagent B).

Samples were prepared according to kit instructions, in each experiment loaded alongside a set of BSA standards (0-0.4 mg/ml). A characteristic blue colour developed the absorbance of which was read at 750_{nm}.

2.2.1.3 SDS-PAGE.

SDS extraction as described above, coats polypeptides with a uniform negative charge in a constant charge to mass ratio. Polypeptides were resolved on the basis of size due to the sieving effects of the polyacrylamide matrix.

Gradient gels of the NuPAGE bis-tris system(Novex) were used with an acrylamide concentration of 4-12%. Prior to loading the amount of protein in the cell lysates was normalised by protein assay and subsequent concentration adjustment. Sample buffer (4x NuPAGE LDS 1:4) and reducing agent (NuPAGE 1:10) were added directly to the lysate. The final sample solution was heated for 10mins at 70°C.

Samples were loaded in consecutive wells on the gel alongside a set of pre-stained molecular weight standards (Bio-Rad) to allow molecular weight estimation by comparison.

Gels were placed within the gel tank and the outer chamber was filled with running buffer (20x NuPage MOPS (3- (N-morpholino)propane sulfonic acid) diluted appropriately). Reducing conditions were used therefore NuPAGE antioxidant was

added to the running buffer of the upper chamber of the gel tank (500µl in 200ml 1x running buffer).Gels were run at 150V until the dye front reached the base of the gel (approx. 1hr)

2.2.1.4 Western Blotting.

Proteins were transferred from the polyacrylamide matrix to a nitrocellulose membrane by generation of an electric field.

Gels from SDS-PAGE were placed on nitrocellulose membranes (NuPAGE, pore size -0.2µm) which had been soaked briefly in transfer buffer (1L transfer buffer –NOVEX NuPAGE transfer buffer (20x) 50ml; NuPAGE sample antioxidant 1ml; methanol 100ml and ultrapure water 849ml).

Sponge pads (also soaked in transfer buffer) were used to ensure tight compression in the transfer cassette. The 'sandwich' was orientated in the cassette such that the membrane is closest to the anode to allow transfer of proteins in the right direction. The transfer cassette was filled with buffer until the gel/membrane sandwich was covered. The entire cassette was then submerged in a tank of de-ionised water. Transfer conditions were 30V constant for approx. 1.5hrs.

Ponceau S was used to stain the membrane post transfer to obtain a total protein pattern. This step is completely reversible and compatible with subsequent immunoblotting.

2.2.1.5 Immunodetection of Blotted Proteins.

Prior to incubation with antibody, the non-specific protein binding sites on the membrane blot were blocked by incubation overnight at 4°C with blocking buffer (5% skimmed milk powder and 1% sheep serum in TBST). Blotted membranes were

then transferred to 50ml falcon tubes such that the blotted surface faced inwards. This facilitated the subsequent washing of the blots and their incubation with antibodies, these steps were performed whilst rolling the tubes on their sides at room temperature.

Membranes were probed with primary antibodies (2hrs) diluted as required with blocking solution then washed 3x 5mins with TBST. Blotted membranes were then incubated with horseradish peroxidase (HRP) conjugated secondary antibodies diluted in blocking solution (2 hrs) then washed as above.

HRP-conjugated secondary antibodies were detected by enhanced chemiluminescence (ECL), here oxidation of luminol by HRP in the presence of chemical enhancers leads to the producation of luminol radicals which emit light as they decay.

Blotted membranes were incubated for 5 mins with a 1:1 mixture of ECL detection reagents (luminol/enhancer solution and a stable peroxide solution – Pierce 'West Pico' chemiluminescent substrate).

The blot was removed from the ECL substrate and wrapped in Saran wrap. Immuno-detected blotted proteins were detected on autoradiography film sensitive to the blue light produced by ECL (Hyperfilm-ECL, Amersham). Exposure time typically ranged from 15 seconds to 5 minutes. ECL signal bands were then quantified from the film using 'Quanitity-One' densitometry software.

2.2.1.6 Densitometry.

Autoradiographic ECL images were scanned directly into densitometry software 'QuantityOne'. 'Regions of interest' (R.O.I) were established for each band as 'boxes' surrounding the band. For an individual membrane, one box size was determined to accomodate the largest band then replicated for the other bands. For

each R.O.I, density/mm^2 was measured following subtraction of the background signal.

2.2.2 Quantification of Cadherin Expression.

Cell based ELISAs (Enzyme linked immunosorbant assays) were used to determine the relative amounts of cadherin expressed in bronchial epithelial cells in culture. There were two experimental steps needed for the calculation, firstly cadherin detection and secondly total protein quantification to create a ratio comparable between the samples.

2.2.2.1 Cell Based Cadherin ELISA.

Cells were grown for 7 days in 96 well plates from an initial plating density of 10^4cells/well. Cells were washed briefly in PBS, fixed in 1:1 methanol/acetone then rehydrated in PBS.

Cells were incubated overnight at 4°C with primary antibody (alongside the appropriate control IgG) diluted as required in blocking solution then washed 3x5mins in TBST. Cells were then incubated with HRP-conjugated secondary antibody for 2hrs and washed as above.

HRP-conjugated secondary antibodies were detected using TMB-liquid substrate system (Sigma, 3,3',5,5'-tetramethylbenzidine) (100µl/well, 0.5hrs). 'Stop' solution (1M H_2SO_4) (25µl/well) was added at the end of the relevant incubation period and the cadherin signal read at OD_{450nm}

2.2.2.2 Crystal Violet Staining for Total Protein.

TMB and stop solution were removed from the cell surface and the cells were washed 3x5mins in PBS. Cells were stained with 100µl/well 0.1% crystal violet in H_2O (30mins). Crystal violet was removed by extensive H_2O washing (including overnight shaking).

Stained cells were solubilised in 200µl/well 4M Guanidine HCL for 2hrs. 100µl aliquots of the resulting solution were then read at OD_{595nm}.

2.2.2.3 NaOH Solubilisation for Protein Assay.

TMB and stop solution were removed from the cell surface and the cells were washed 3x5mins in PBS. Cells were solubilised with 0.2M NaOH (100µl/well shaking for 1-2hrs at 50°C). Aliquots of the resulting solution were measured for total protein by the method described in section 2.1.2.1.2.

2.3 P-Cadherin Transfection of 16HBE14o- cells.

2.3.1 Transformation of E.Coli Cells

Subcloned vectors were used to transform E.Coli Solopack Gold cells (Stratagene. Genotype $Tet^R\Delta$ (mcrA) 183Δ (mcrCB-hsdSMR-mrr) 173endA1 supE44 thi-1 recA1 gyrA96 relA1 Hte [F'proAB $lacI^q$ ZΔM15Tn10 (Tet^R) Amy Cam^R]. 1µl of XL10-Gold β-mercaptoethanol mix (provided with competent cells) was added to the tube of solopack cells which were then incubated on ice for 10 minutes. 0.01-50ng of DNA was then added to the cells on ice and the resulting mixture was heat-shocked for 1 minute at 54 C before snap cooling on ice for 2 minutes. The cells were then resuspended in 500µl L-Broth (1% typtone, 0.5% yeast extract, 1% NaCl) and incubated, with shaking, for 1 hr at 37 C.

Fractions of the experimental transformation reaction were plated onto L-AMP plates (L-agar supplemented with 100μg/ml ampicillin) and incubated overnight at 37 C. Colonies were picked and allowed to replicate in 5ml of L-broth containing 100μg/ml ampicillin.

2.3.2 Preparation of Plasmid DNA from Transformed Cells.

DNA was prepared from cell pellets using modified versions of the alkaline lysis method (Sambrook et al. 1988). Here alkaline lysis of bacterial cells is followed by adsorption of DNA onto silica in the presence of high salt.

'Mini-preps' of plasmid DNA (up to 10μg) were used in restriction digests to identify recombinant transformants. Larger scale plasmid preparations or 'maxi-preps' were used when sufficient DNA (up to 100μg) for a number of preparative digests was required.

2.3.3 Mini-Preps.

Qiagen's QIAprep mini-prep kit was used to purify and isolate plasmid DNA. Ampicillin resistant colonies were cultured in 2ml of L-broth (100μg/ml ampicillin) overnight at 37 C. 1ml of each overnight culture was pelleted by centrifugation at 6000rpm for 1 minute in a microfuge. The supernatant was discarded and the cells washed by resuspending and vortexing in 250μl of RnaseA containing buffer P1 (Qiagen). Cells were lysed by adding 250μl of buffer P2(Qiagen) which contains NaOH and SDS. Tubes were mixed by inversion then stood for 5minutes allowing maximum release of plasmid DNA without release of chromosomal DNA. Lysis was stopped by addition of buffer N3 (Qiagen), this solution is of high salt concentration which causes denatured proteins, chromosomal DNA, cellular debris and SDS to precipitate while the smaller plasmid DNA renatures correctly and stays in solution. Particulate matter was pelleted by centrifugation at 15,000rpm for 5 minutes. The DNA containing supernatant was removed to a fresh tube and washed with buffer PE

(Qiagen). DNA was eluted by centifugation into a fresh 1.5ml microfuge tube with 50µl H_2O.

2.3.4 Maxi-Preps.

Plasmid containing bacterial cell suspensions were prepared from 100-500ml of overnight culture using the Promega Wizard Plus Maxipreps DNA Purification System.

The entire culture was pelleted by centrifugation at 5,000g for 10minutes. The cell pellet was resuspended in 15ml cell resuspension solution (Promega –50mM Tris-HCL (pH7.5), 10mM EDTA, 100µg/ml RnaseA).

Cells were lysed by adding 15ml of cell lysis solution (Promega, 0.2M NaOH, 1% SDS) and were left to stand for 20 minutes. Lysis was stopped by addition of 15ml of neutralisation solution (Promega, 1.32M potassium acetate (pH4.8)).

Cells were centrifuged at 14,000g for 15 minutes then the supernatant was filtered and transferred to a fresh tube. Plasmid DNA was precipitated with 0.5 volume of isopropanol followed by centrifugation at 14000g for 15 minutes. The supernatant was discarded and the DNA pellet was resuspended in 2ml of TE buffer (10mM Tris-HCL pH 7.5, 1mM EDTA).

For plasmid purification, 10ml of DNA purification resin (Promega) was added to the TE buffer/DNA solution. 'Maxicolumns' were supplied with the maxiprep kit and were fitted onto vacuum manifold ports. The resin/DNA mix was transferred to the maxicolumn and pulled into the column by vacuum.

The resin was washed with wash solution (Promega, 55% ethanol, 80mM potassium acetate, 8.3mM Tris-HCL (pH7.5) and 40µM EDTA), followed by 80% ethanol. 1.5ml of pre-heated (70 C) H_2O was then added to the resin and subsequently eluted by centrifugation. The final DNA containing eluate was filtered and stored at –20 C.

2.3.5 Restriction Digests.

Purified DNA was digested with restriction enzymes to determine plasmid identity and insert orientation.

For each digest, 1μg of DNA was added to 2μl buffer, 2 units of restriction enzyme and 8μl H_2O. The mixture was incubated at 37 C for 2hrs.

Loading buffer (2μl) was added to cleaved fragments which were subsequently separated by electrophoresis alongside a 1kb DNA ladder marker for size comparison. Electrophoresis was on an agarose gel (0.8mg agarose in 100ml tris-EDTA acetate running buffer containing 0.01μl/ml ethidium bromide (Promega)). Gels were run in running buffer at 100V for approx. 1hr.

2.3.6 Band Purification.

Seperated fragments were visualised under UV light and excised from the gel using a scalpel blade. Each DNA fragment was extracted from the gel using the QIAquick gel extraction kit (Qiagen). The binding buffers in the extraction kit provide the correct salt concentration and pH for adsorption of DNA to the QIAquick membrane..

For each volume of gel, 3 volumes of buffer QG (Qiagen) were added. The mixture was incubated at 50 C for 10 minutes then 1 volume of isopropanol was added. The sample was added to the QIAquick spin column (provided with kit) and centrifuged for 1 minute to bind the DNA. The column was washed with Buffer PE (Qiagen) then eluted in 50μl of H_2O.

2.3.7 Transfection.

Cells for transfection were grown to 80-90% confluence in a 100mm dish. Working with a 1μg/ml DNA concentration, 7.5μg plasmid DNA was added to 67.5μl

OPTIMEM (Sigma). In a second tube, 45µl DOTAP (Sigma) was added to 95µl of OPTIMEM. The two solutions were gently mixed and stood on a vibration free surface at r.t. for 15 minutes before addition of a further 10ml OPTIMEM.

Medium was removed from cells and then rinsed with OPTIMEM, the entire DNA/DOTAP OPTIMEM mixture was then added to the dish of cells.

Cultures were incubated overnight then the medium was replaced with normal growth medium. 3 days after transfection, cells from 2x100mm dishes were harvested and suspended in 10ml growth media supplemented with G418 (300µg/ml) and the entire cell suspension plated on a single 100mm dish.

Resistant colonies emerged after approx. 1 week. These colonies when large enough were inoculated into different wells of a 96 well plate.

2.3.8 Ring Cloning of Transfected Cells.

Colonies were selected on the basis of their isolation and the location of the selected clone was marked on the underside of the dish. The medium was removed by suction and the dish washed in PBS. Sterile plastic cloning rings were coated in sterile vacuum grease and placed over the marked clones. Trypsin/EDTA was added into the cloning ring and the dish returned to a 37°C incubator for 2-3 minutes. Once cells were observed to be 'rounding-up', using phase-contrast microscopy, the contents of the cloning ring were transferred to a 35mm dish containing normal growth medium.

Chapter Three.

Morphometric Characterisation of Bronchial Epithelium in Normal and Asthmatic Human Subjects.

3 Morphometric Characteristics of Bronchial Epithelium in Normal and Asthmatic Human Subjects.

3.1 Introduction.

The normal bronchial epithelium may be considered to be organised layers of cells involving two distinct sheets. Immediately above the basement membrane lies a sheet of basal cells firmly attached via hemidesmosomes (Evans et al, 1991, Jeffery et al 1983), above this is a second layer consisting of ciliated columnar epithelial cells. Together the two layers function to form a physical barrier separating the underlying tissues from the airway lumen.

The bronchial epithelial lining is often impaired in asthma, with clusters of epithelial cells seen in the sputum of sufferers (creola bodies) (Naylor et al., 1962). Sections of human bronchus show denuded patches where the underlying tissue is exposed to the lumen, resulting in increased contact with irritants.

The apparent resilience of the basal cell is thought to be due to a much stronger attachment than that of the columnar cell, demonstrated in a study by Motojima (1989), in which an increased concentration of Major Basic Protein (MBP) was required to dislodge the basal cells compared with columnar. Sections of human asthmatic trachea show areas of epithelium from which these functional cells have been shed as denuded patches resulting in exposure of basal cells and nerve endings, consequently the epithelial barrier is impaired and there is increased contact with irritants (Jacoby et al, 1997, Montefort et al., 1993).

On appearance of such a denuded patch there is an immediate extravasation of plasma from the underlying microcirculation (Persson et al, 1996). This supramembranal gel is rich in eosinophils. The gel decreases the contact of exposed airway tissue to noxious agents. Basal cells either side of the damaged area flatten and migrate inwards to cover the denuded area, a new layer of poorly differentiated cells is established, then mitosis and proliferation is markedly increased followed by a differentiation stage to a normal phenotype (Erjefält et al, 1997).

A study by Erjefält (1997) investigated the barrier function of airway epithelial basal cells following loss of columnar epithelial cells. After selective removal of the columnar cells using tissue adhesive glue, an observed flattening of the basal cells was shown, forming a poorly differentiated layer of cells covering the denuded area and the presence of overlapping cytoplasmic protrusions between the flattened cells at the borders. Erjefält suggests that increased permeability is transient and rapidly reversed due to the high speed of airway epithelial restitution processes. The undifferentiated new layer of cells has less cells and therefore less junctions allowing less permeation of molecules from airway lumen to tissue.

After migration, mitosis is markedly increased accompanied by a slight proliferation activity increase in the old epithelium as well as in the underlying subepithelial cells (Zahm et al, 1997), the latter a possible cause for the observed membrane thickening in asthma. Zahm and coworkers (1997), quantified this epithelial cell proliferation by immunostaining for the Ki62 antigen which is a marker of cycling cells, mitosis in a repairing area peaked 48 hrs after damage. A differentiation stage to a normal phenotype occurs, around 4 to 8 days after denudation, the number of cells returns to normal as does the height and morphology (Barrow et al, 1993).

This study aims to characterise the repair stages using computer aided image analysis to perform detailed morphometry on sections of bronchial biopsies from both asthmatic and normal subjects. The biopsies were examined using several different criteria to investigate the morphological differences between the epithelium of the two groups.

In order to understand the relevance and extent of these repair processes we set about characterising factors of cell height and cell denudation in asthmatic and non-asthmatic patients.

3.2 Results.

3.2.1 Bronchial Biopsy Images

3.2.1.1 Biopsy collection.

Dr Peter Howarth (Consultant respiratory physician, Southampton University/ Southampton General Hospital) provided ready mounted samples which had been prepared from biopsies taken from subjects clinically characterised for another study. Samples from 10 healthy control volunteers; 10 subjects with mild asthma receiving treatment with inhaled beta 2-agonists as required; and 10 chronic asthmatic subjects treated with inhaled corticosteroids as required. Details of patient characteristics are given in appendix 4.

Both atopic and non-atopic asthmatic patients were included in this study whereas the control subjects were required to be non-atopic. Atopic status was determined by skin prick test reactivity to the following aeroallergens: Dermatophagoides pteronyssinus, mixed grasses, cat fur, and dog hair. A skin wheal response was scored as positive if larger than 3 mm in diameter in the presence of negative and positive control reactions. Subjects with a positive skin prick test response and clinical history of atopy, were regarded to be atopic.

Patient's asthmatic status was determined according to the following criteria: normal healthy control subjects (normals) had a resting forced expiratory volume in 1 sec ($FEV_{1)}$ of >90% predicted value and no history of asthma or atopy, asthmatic subjects had a resting FEV_1 of <90% predicted, and a clinical history of asthma. The asthmatic group was further categorised according to therapy. Mild asthmatics (asthmatics) had received solely beta-agonist therapy whereas severe asthmatics (chronic asthmatics) had received regular steroid therapy, often multiple therapy and experienced persistent symptoms despite treatment.

Lung function was determined by measurement of FEV1 with a dry wedge spirometer, with the highest of 3 values recorded. The FEV1 was expressed as a percentage of predicted value adjusted for sex, height, and age. All subjects gave

informed consent, and the study was approved by the Southampton Combined University and Hospital Ethics Committee.

The biopsies provided from this study had previously been fixed in acetone containing protease inhibitors before embedding in glycomethylate resin. Sections had been cut from the resin blocks at a thickness of 0.5 microns before immunostaining with monoclonal antibodies EG2 (against eosinophil cationic protein) or AA1 (against mast cells). Samples were referred to me at this point as slide numbers from which morphological measurements could be taken. Asthma diagnosis was withheld until all measurements were complete.

3.2.1.2 Image Analysis and Epithelial Morphology.

For each patient, sections were imaged using a high resolution cooled CCD camera (Digital Pixel Ltd, Brighton, UK). Images were taken such that successive frames running the length of the epithelial basement membrane were taken with little or no overlap between images. The digitised images were collected, stored and analysed using a PC-based system.

Starting at the first image, every fourth image was selected and measured using a "Scion Image" image analysis system on a PC. This approach provides unbiased random selection of areas to be measured. Three to six images from each sample were then measured, until the last image of the series was reached.

From the original set of 30 patients, one slide per patient was examined and in all cases tissue cross sections were seen, bordered in places by epithelium. These were used to identify areas of basement membrane and underlying connective tissue. Along these cross sections a continuous set of images was collected and from these each 4^{th} digital image was selected, irrespective of the quality of the sample. Samples from these sets were excluded if the plane of sectioning was clearly not perpendicular or if the section was folded or if the section was too small (<16 images). On this basis, 11 of the 30 biopsy samples were excluded, reducing the sample group to 19 patients. The asthmatic status of the patients was unknown at the time of experimentation, but of the 19, 8 were later identified as normal, 5 as asthmatic and 6 as chronic asthmatic.

Each image contained a stretch of basement membrane which could be clearly distinguished on the basis of its sub-epithelial location, morphology and continuity with other areas of basement membrane along the length of the airway (fig. 3.1).

For each image, the total length of the basement membrane, the length of basement membrane which was not covered by cells together with the number of basal and columnar cells and the height of their nuclei and spacing between nuclei of adjacent cells was measured. From these measurements, cell frequency, nuclear height and the percentage of the basement membrane covered by epithelial cells was calculated (fig. 3.2).

All sample averages were calculated as the mean ± SEM. Statistical significance was assessed with a non-paired two-group t test, and the ANOVA test using SPSS analysis software. The T-test for equality of means according to the independent samples test was carried out to compare results between patient groups. In all cases, p values of <0.05 were deemed significant (see table 3.1)

3.2.2 Epithelial Morphology.

The epithelial areas were categorised into 3 clear types, areas with 'intact bronchial epithelium', areas of 'supra-basal denudation' and areas of 'denuded basement membrane'.

3.2.2.1 Intact Bronchial Epithelium

In many cases, the epithelium was intact with continuous layers of both basal and columnar cells (fig 3.1 –area 'A'). In these areas, basal cells were found immediately above the basement membrane and formed a continuous layer, with no gaps between the cells. A continuous layer of supra-basal cells was also seen comprising ciliated and secretory epithelial cells again with no discernible gaps between the cells. Infiltrating cells were frequently seen in the sub-mucosa in all samples

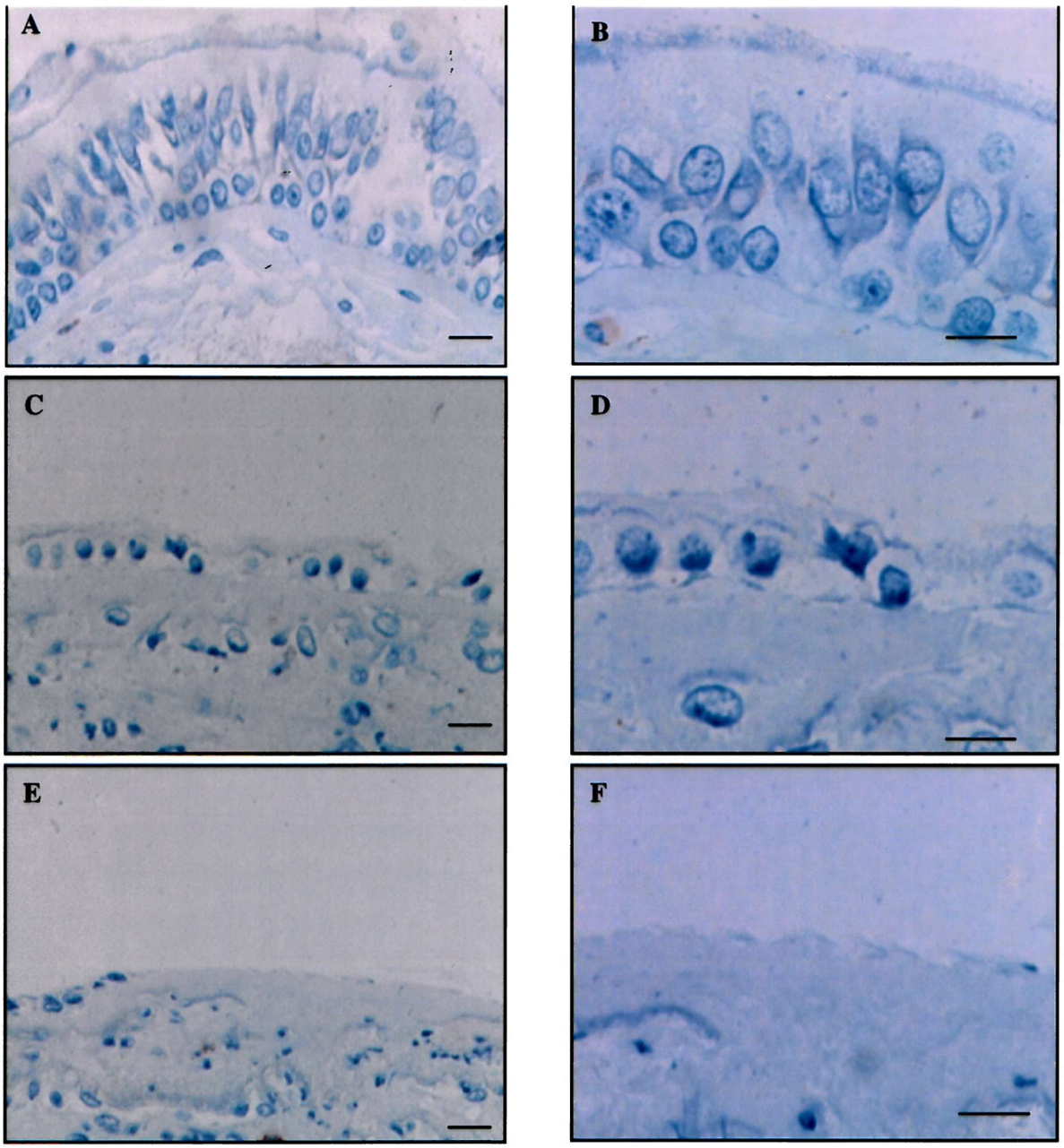

Figure 3.1 Example Bronchial Epithelial Digitised Images.

Consecutive epithelial images were collected and analysed using a PC based system. Each image had a stretch of subepithelial basement membrane but there differences were observed between samples.
A & B are examples of a region of epithelium with continuous layers of both basal and columnar cells.
C & D are examples of areas of cell denudation, this particular stretch of epithelium has extensive columnar cell loss but an almost intact basal cell layer.
E & F show a third type of epithelium where the basal cell layer also suffers extensive denudation.

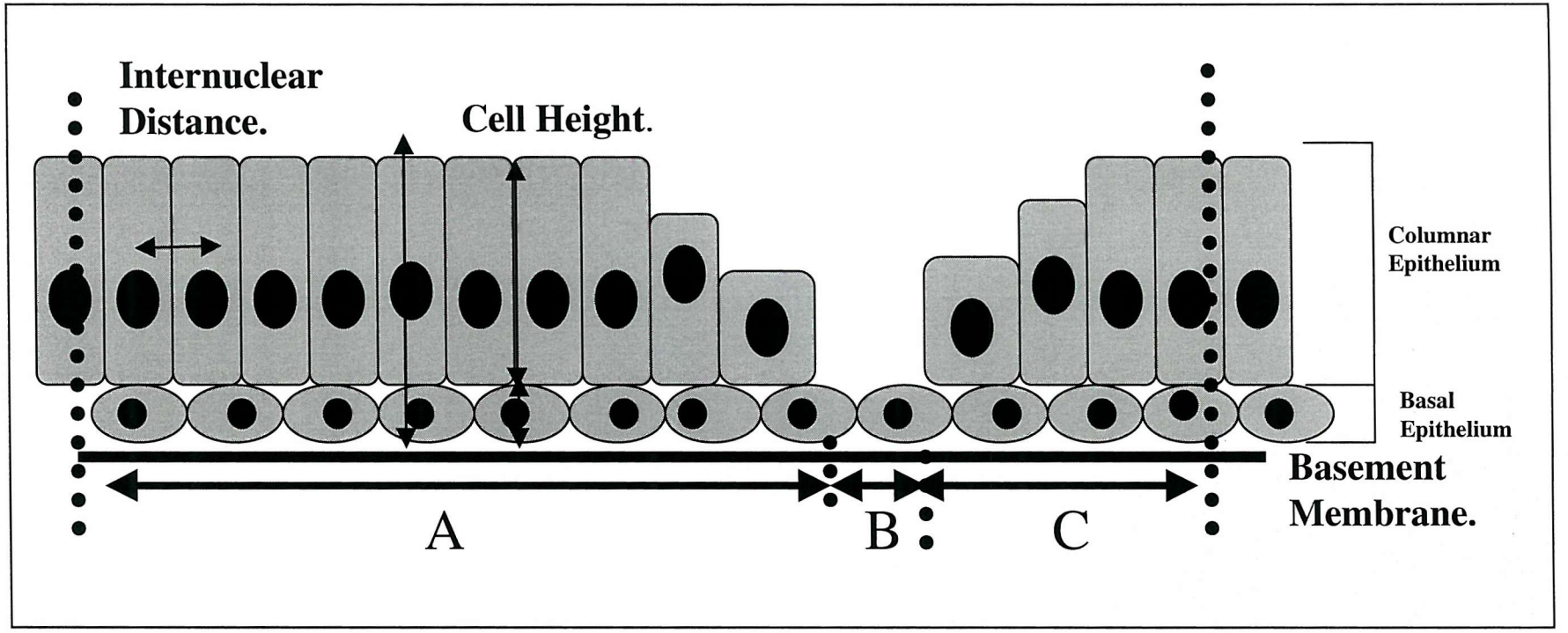

Figure. 3.2 Diagram of Epithelial Morphological Measurements.

Internuclear distances and cell heights of both columnar basal epithelial cells are recorded, internuclear distance is taken as the distance between centre points of neighbouring cell nuclei, cell height is the distance to the top of the cell (excluding cilia) from the base of the cell using the nuclei centre as a reference point.
A,B and C are distances measured along the basement membrane. B is the length of the gap in the columnar epithelial cell layer. This information as a whole is used to give detailed morphological information including cell frequency, cell height, % basement membrane coverage and cell spacing.

3.2.2.2 Areas of Supra-Basal Cell Denudation.

In some areas, columnar cells were missing from the bronchial epithelium leaving cells of a 'basal' morphology on top of the basement membrane (fig. 3.1 – area 'B'). In these areas, there were generally few gaps between the basal cells. Occasional isolated columnar cells were seen attached to the basal cells, often appearing to be damaged, these areas were frequently adjacent to areas of intact epithelium. The basement membrane appeared morphologically indistinguishable from that underlying areas of intact epithelium.

3.2.2.3 Areas of Denuded Basement Membrane.

Areas of basement membrane were less frequently seen without any epithelial cells overlying the basement membrane. These areas were often adjacent to areas of basal cells without supra-basal cells. The basement membrane appeared morphologically indistinguishable from those underlying areas of intact epithelium.

3.2.3 Epithelial Morphological Measurements.

3.2.3.1 Basal Cell Layer.

'Percent cell coverage' was defined as the length of denuded epithelia along the basement membrane compared with the 'total' length measured.

Some images showed areas lacking a continuous basal cell layer, these regions represented only a small proportion of the total area (4% ±1.74 SEM in normals, 6% ±2.47 SEM in asthmatics and 15% ± 4.25 in chronic asthmatics see figures 3.3 and 3.7). The few basal epithelial cells present occurred as solitary cells never forming an intact epithelial sheet.

Other areas, (accounting for the majority of the airway surface) had only small gaps between regions of intact epithelial coverage. In these areas, gaps in the basal cell layer never exposed the basement membrane for greater than 6μm.

Both normal and asthmatic groups had small basal gaps with mean values of 0.87 ±0.303μm SEM in normals, 1.81 ±0.78μm in asthmatics and 4.71 ±1.61μm in chronic asthmatics.

Cell Frequency was defined as the number of cells per 100 μm of basement membrane. Basal cell frequencies were measured in normal asthmatic and chronic asthmatic patient groups, with the number of basal cells 27.37 ±1.38 cells/100μm SEM, 20.4±1.72and 26.3 ±1.64 respectively (figures 3.4 and 3.7).

Distances between neighbouring basal epithelial cell nuclei were also measured to gain internuclear distances (figure 3.5 and 3.7). Normal, asthmatic and chronic asthmatic distances were 3.33 ±0.24μm SEM, 2.78 ±0.87μm SEM and 2.89 ±0.26μm SEM respectively for basal cells.

Cell height was defined as the distance from the top of the cell (excluding cilia) to the base of that cell, using individual cell nuclei as a reference. Basal epithelial cell height was approximately 5 to 7 μm, with a mean value of 5.58 ±0.23μm SEM in normals , 5.73 ±0.17μm SEM in asthmatics and 6.94 ±0.42μm SEM in chronic asthmatics (figure 3.6 and 3.7).

3.2.3.2 Columnar Cell Layer

This study showed the non-asthmatic basement membrane to have 50.2% ±9.13 SEM columnar cell coverage, asthmatics 41.8% ±9.38 SEM and chronic asthmatics 21.7%± 8.79 SEM (figure 3.3 and 3.7). In the chronic asthmatic group however, four of the total of six chronic asthmatic patients had complete loss of their columnar cell layer.

Columnar cells frequencies measured as the number of cells per 100 micrometres were 18.30 ±4.38 SEM in the normal group and 8.07 and 7.76 in the asthmatic and chronic asthmatic respectively. (figure. 3.4 and 3.7).

Columnar epithelial internuclear distances for the normal group was 2.93 ±0.31μm SEM, 3.74 ±0.52μm SEM for the asthmatic group and 2.29 ±0.48 for the chronic asthmatic (figure 3.5 and 3.7).

Columnar cell height varied far more than basal cell, with the mean columnar cell height at 14.33 ±0.94μm SEM in normals, 8.42 ±1.12μm SEM in asthmatics and 17.47 ±1.04μm SEM in chronic asthmatic patients (figure. 3.6 and 3.7).

As shown in the cell height scattergrams, variation of columnar epithelial cell height was seen within patient group. Looking at the results on the whole, there is high variation in all three categories. In all three categories, a definite patient/cell height correlation was seen, with heights recorded for one patient having far less variation than that observed between patients of the same category.

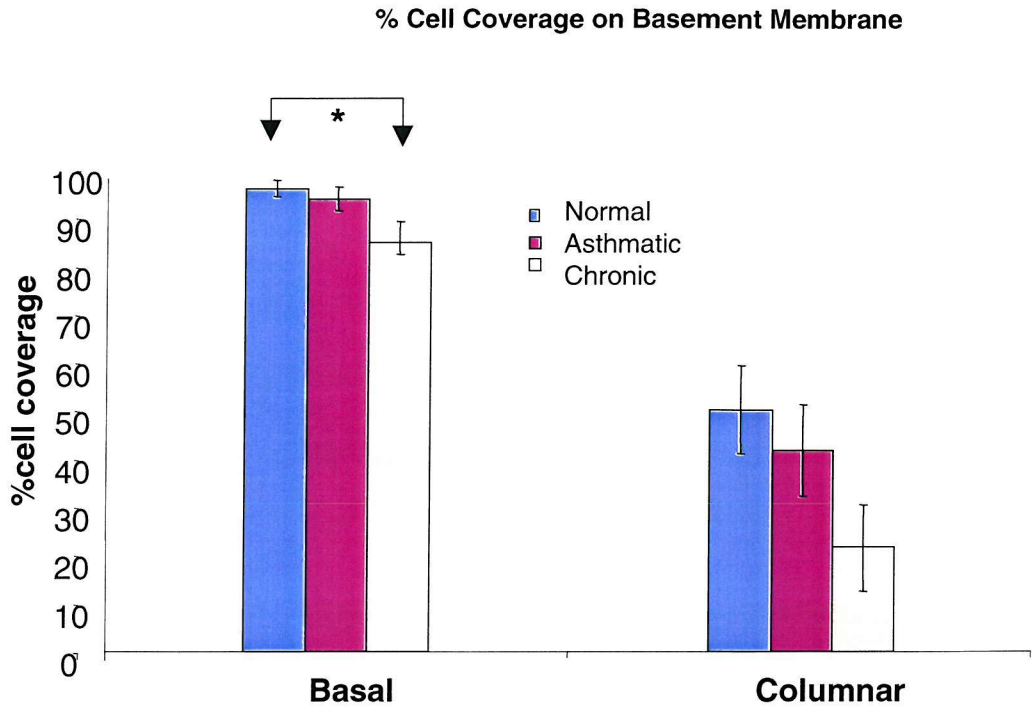

Figure 3.3 Percentage Epithelial Cell Coverage on the Basement Membrane.

Percent cell coverage was determined as the length of denuded epithelium along the basement membrane compared with the 'total' length measured and expressed as percentage cell coverage.
In all three patient types, basal cell coverage was high remaining above 80% in all cases.
Columnar epithelial cell loss however was much higher, normal patients lost on average half of their columnar cells and chronic asthmatics only retaining on average 22% of their columnar cells.
Significant differences in mean cell coverage between patient groups are indicated by '*'.

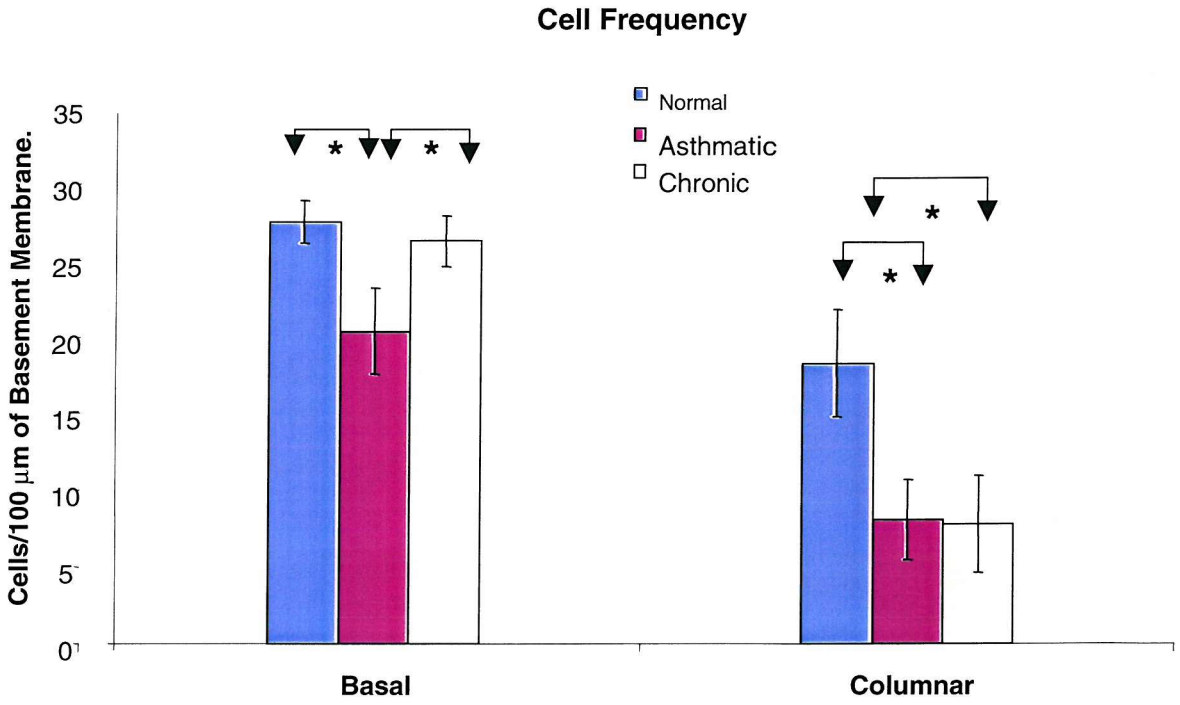

Figure 3.4 Epithelial Cell Frequency.

Cell frequency was measured as the number of cells per hundred microns of basement membrane. Basal cell frequency (20 cells/100µm) was significantly lower in asthmatic patients compared with both normal and chronic asthmatic patients (27 and 26 µm respectively). Columnar epithelial cell frequency is significantly higher in normals than asthmatics and chronic asthmatics as expected given the higher rate of columnar cell loss.
Significant differences in mean cell frequency between patient groups are indicated by '*'.

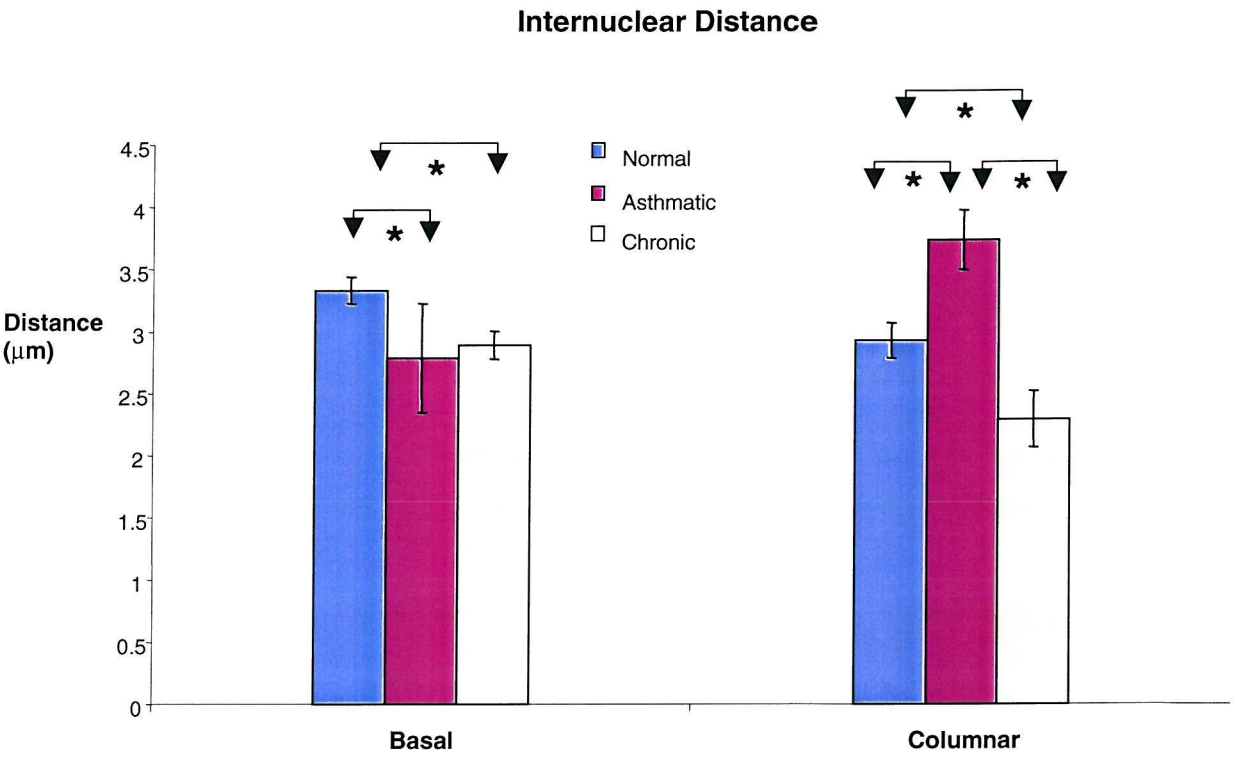

Figure 3.5 Epithelial Internuclear Distance.

Internuclear distance was measured from the images as the distance from the centre of the cell nuclei to the centre of the nuclei of its neighbouring cell. Distances between basal epithelial cell nuclei in normals were slightly higher and more uniform at 3.33 ±0.24μmSEM than in asthmatics and chronic asthmatics (2.78 ±0.87μmSEM and 2.89 ±0.26μmSEM).Internuclear distances in the columnar cell layer were significantly different in all three patient groups at 2.93 ±0.31μmSEM in normals, 3.74 ±0.52μmSEM in asthmatics and 2.29 ±0.24μmSEM in chronic asthmatics.
Significant differences in mean internuclear distances between patient groups are indicated by '*'.

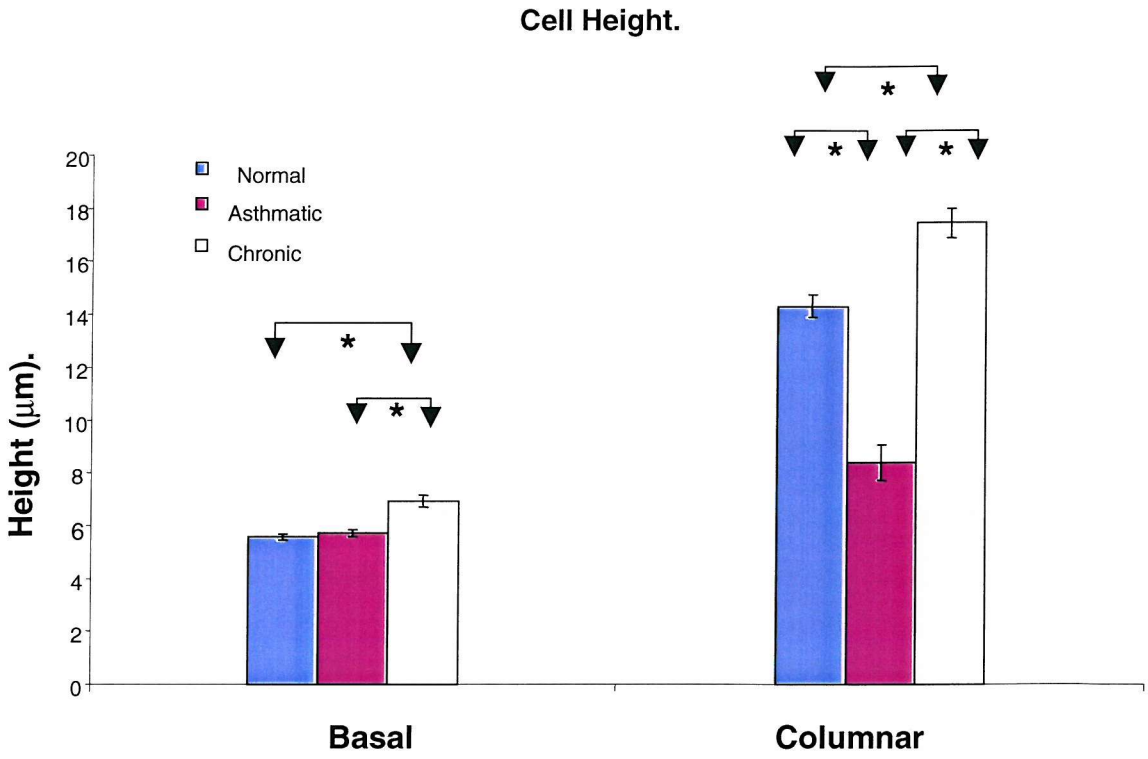

Figure 3.6 Epithelial Cell Height.

Cell Height was defined as the distance from the top of individual epithelial cells (excluding cilia), to the bottom of that cell, using the centrepoint of the cell nucleus as a reference.
Basal epithelial cell height was on average between 5-7µm with slightly taller epithelium in the chronic asthmatic patients. Columnar epithelial height was far more variable with chronic asthmatic columnar cells surprisingly on average nearly double the height of columnar cells in asthmatics.
Significant differences in mean cell height between patient groups are indicated by '*'.

Measurement	Cell Type		Normal			Asthmatic			Chronic Asthmatic		Independent Samples Test.
		n	Mean	SEM	n	Mean	SEM	n	Mean	SEM	T-test for equality of Means.
Basement Membrane Coverage (%).	Basal	31	96	1.74	20	94	2.47	23	84.969	4.25	N/A p= 0.658
											N/C 0.032
											A/C 0.085
	Columnar	31	50.2	9.13	20	41.8	9.38	20	21.7	8.79	N/A 0.683
											N/C 0.136
											A/C 0.921
Cell Frequency (cells/100um of Basement Membrane.)	Basal	32	27.37	1.38	28	20.4	1,72	30	26.3	1.69	N/A 0.032
											N/C 0.194
											A/C 0.048
	Columnar	32	18.3	4.38	28	8.07	2.61	24	7.77	3.16	N/A 0.027
											N/C 0.037
											A/C 0.941
Cell Height (um)	Basal	314	5.58	0.23	315	5.73	0.17	237	6.94	0.42	N/A 0.409
											N/C 0.000
											A/C 0.000
	Columnar	214	14.33	0.94	84	8.42	1.12	50	17.47	1.04	N/A 0.000
											N/C 0.000
											A/C 0.000
Internuclear Distance (um).	Basal	276	3.33	0.24	253	2.78	0.87	190	2.89	0.26	N/A 0.000
											N/C 0.006
											A/C 0.469
	Columnar	131	2.93	0.31	74	3.74	0.52	44	2.29	0.48	N/A 0.002
											N/C 0.024
											A/C 0.000

Figure 3.7 Epithelial Cell Morphology Data.

Table showing morphological measurements of bronchial epithelial cells (basal and columnar) in patients categorised as 'normal' (N), 'asthmatic' (A), and 'chronic asthmatic' (C).
Measurements were expressed as the mean value and the standard error of the mean (S.E.M). Sample size is denoted as 'n'.
In order to compare results between patient category, the independent samples test was carried out on the data using the T-test for equality of means (e.g N/A refers to normal compared with asthmatic). Under this criteria, p values of <0.05 were deemed significant.

3.3 Discussion.

The morphology study revealed three characteristic epithelium categories. Those with 'intact bronchial epithelium', those with areas of 'supra-basal cell denudation' and those with areas of 'denuded basement membrane'.

The three morphological types were seen in all patient groups and often within different epithelial regions of an individual patient. Areas of complete denudation however were most common in the chronic asthmatic patient group as shown by the cell coverage data where there is approximately 10% more basal cell loss than the other two groups. This greater level of tissue exposure would mean increased potential for direct tissue contact with irritants in chronic asthmatics. It is not clear however whether the greater cell loss is a result of some factor stemming from the patient's chronic asthmatic condition, weakening the cell-cell interaction or alternatively if the cell loss is itself a contributing factor to the disease.

It is obvious from the cell coverage data that there is extensive columnar cell loss, even in normals with only 50% columnar epithelial coverage. Columnar epithelial cell coverage was further reduced in asthmatics compared with normals, particularly in chronic asthmatics where there is nearly 80% columnar cell loss. However in most cases, the basal layer remains intact providing a lesser barrier between the tissue and the airway lumen. For some reason the basal cell layer is far more resilient to damage. This may be that the neighbouring columnar cell interactions are more readily cleaved or dismantled than the hemidesmosomal contacts found associated with the basal cells at their interface with the basement membrane.

The 50% columnar epithelial coverage seen in the normal group is probably due in part to artefactual damage during the sampling process. In which case, this indicates once again a greater resilience of the basal cell layer as opposed the columnar, given that with 96% coverage in normals, few basal cells are lost. Columnar cell loss is seen to a much greater extent in the asthmatic groups as opposed to the normals and there is therefore, either an increase in cell shedding in these groups or at least much weaker intercellular contacts to allow the greater level of artefactual damage.

Amin and coworkers (2000) in a similar study also saw columnar epithelial cell denudation in asthmatics, they observed ~30% denudation in non-asthmatics compared with ~75% in asthmatics.

A study by Ordonez (2000) also found there to be a ~50% columnar epithelial cell denudation in non-asthmatics but this was a similar levels to the observed level of denudation in asthmatics in that study. Ordonez and co-workers concluded that epithelial desquamation is a consequence of the biopsy procedure. However the current study and several previous studies have shown significant differences in epithelial desquamation or epithelial coverage between normal and asthmatic subjects (Dunhill et al, 1960, Naylor et al, 1962, Beasley et al, 1989, Jeffery et al, 1989, Chanez et al, 1999and Wardlaw et al, 1988).

Considering the possibility that the damage in non-asthmatics may be non-artefactual, this would mean that the epithelium of normals is similar to the asthmatics in that it is in a constant state of remodelling albeit to a lesser extent. This may be feasible given the apparent resilience and maintained barrier function of the basal cell layer. It may be that in the asthmatic airway, this remodelling is hindered resulting in phenotypic cell changes and exposed airways. However, the studies referenced above report cell shedding to occur predominantly within the asthmatic lung. Therefore it is most likely that although there may be a certain level of cell shedding in the airways of normal patients, the level seen here is due to artefactual damage, hence the increased level of damage seen in both asthma patient categories.

An interesting factor of these results is that looking at the cell height results as a whole, each group has a definite patient/cell height correlation with far less variation intra-patient than inter-patient within the same category. This is the case for both basal and columnar epithelial cell height measurements. This observation suggests a characteristic cell phenotype within cells of the same individual. However despite these diversities, there were still significant observed cellular differences between the patient groups as a whole.

Basal epithelial cell height was similar in normal and asthmatic subjects with mean values of 5.5μm and 5.7μm respectively. Chronic asthmatic basal cell

height was significantly higher at 7μm. Even greater variation was seen in the columnar epithelial cell layer. Non-asthmatic columnar cell height was 14μm whereas the asthmatic columnar cells were much lower at 8.4μm. Chronic asthmatic columnar cells however were much higher at 17.5μm indicating a flattening of epithelial cells in the asthmatic patient group not observed in chronic asthmatic epithelia.

Basal epithelial cell frequency in non-asthmatic patients is similar to the number in chronic asthmatics at 27 and 26cells/100μm of basement membrane respectively, but significantly greater than the 20cells/100μm seen in asthmatic patients. Given that the cell frequency data for the chronic asthmatic group shows greater basement membrane exposure, we can conclude that the chronic asthmatic basal cells when present are more densely packed reflected in shorter inter-nuclear distances. This possibly relates to a greater repair efficiency in the asthmatic group, the cells spreading out to cover the denuded area resulting in less cells per unit length. However, internuclear distance data shows similar values for spacing between basal cells of asthmatics and chronic asthmatics at just below 3μm. The errors are much tighter in the latter showing the basal cell spacing in asthmatics to be more variable, again possibly due to the different stages of cell de-differentiation and flattening thought to be involved in repair. The non-asthmatic cells have on average a more uniform slightly greater spacing, despite having a higher cell frequency, this is accounted for by the higher level of epithelial coverage seen in non-asthmatics.

Columnar epithelial cell frequency is significantly higher in non-asthmatics compared with asthmatics and chronic asthmatics, with 18 cells/100μm for the former and approximately 8 cells/100μm for the latter two showing a dramatic difference between normal and asthmatic patients. Observed internuclear distances differ for all three however, with the greatest internuclear distance seen in asthmatics at 3.7μm compared with 2.9μm in normals and 2.3μm in chronic asthmatics. The more dense chronic asthmatic cell spacing is surprising given the similar cell frequency. Results show a reduced cell coverage and an increased cell height and so the remaining cells must be more closely packed than in the normal

and asthmatic groups. Columnar cells in asthmatic group in contrast, appear to have spread out to counteract the damage. This conclusion is supported by the cell height data where the chronic asthmatic columnar cell height is significantly higher than that of asthmatic columnar cells.

It may be that in some individuals the airway epithelial cells cannot deal will cell loss as well as in others and instead of entering a state of repair and spreading out to lessen the denudation, these cells may instead increase junctional attachments and increase in height. The prolonged period of tissue exposure may induce the state of chronic asthma. If this is the case, such patients would benefit from an increased rate of repair in conjunction with enhanced cell adhesion, inhibiting the denudation in the first instance. In any case, optimisation of these processes would be of major importance in the treatment of asthma.

Chapter Four

Adhesion Molecule Expression During Development and Repair of Bronchial Epithelial Layers *in vitro*.

4 Adhesion Molecule Expression During Development and Repair of Bronchial Epithelial layers in vitro.

4.1 Introduction.

As seen in the previous chapter, there is extensive cell loss in the bronchial epithelium, particularly in the airways of asthmatics. In order to design a therapy for this condition it is imperative we gain further understanding of the processes that are involved in initiating and maintaining epithelial cell adhesion.

Cells surrounding an area of damaged epithelium migrate and proliferate to restore a confluent cell layer. Intracellular junctions together form a tight paracellular barrier which is disrupted in wounded epithelia. Changes in junctional cell adhesion molecule expression and function must accompany the restitution process in such a way to accommodate ongoing cellular migration, differentiation and epithelial reorganisation as well as optimising barrier function.

In order to establish the characteristic patterns of cell adhesion molecule expression within the bronchial epithelium, an *in vitro* model of epithelial confluence was established. An epithelial model that mimics changes seen *in vivo* required a cell line that retained bronchial epithelial morphology and function.

16HBE14o- cells were used in this study, these cells have been shown to retain intermediate and tight junctions and directional ion transport after multiple passages in culture (Cozens et al, 1994). Using SDS-PAGE and western blotting, cells were extracted at time-points established by analysis of morphological and quantitative differences in cell density and probed for E- and P-cadherins as well as the tight junction associated proteins Occludin and ZO-1. This model enabled characterisation and analysis of the changes in expression of these adhesion molecules in developing epithelia.

Denuded areas of epithelium in the airway such as those analysed in chapter 3 are thought to be rapidly repaired by a restitution process involving the remaining cells (Erjefält et al, 1995). This action is different to development, as

the cells suddenly experience disruption of normal homeostatic mechanisms. The changes within a repairing epithelium involve a dynamic process of junctional disruption. Migration of cells over the wounded region must involve substrate disruption, but it is not clear whether there is also intracellular junction disruption. It is not known whether cell adhesion molecule expression patterns in a repairing epithelium mimic those of a developing epithelium or whether there is a distinct repairing cell phenotype.

A model of epithelial repair was established to address these issues again using cells of the bronchial epithelial cell line 16HBE14o-. Mechanically wounded cells were extracted for SDS-PAGE at set time-points post-wounding in order to characterise the restitution process in terms of the expression of cell adhesion molecules which are expected to be involved in cell-cell interactions.

The focus here is on E- and P-cadherin expression, investigating the extent and nature of their reciprocal influence and their role in epithelial development and repair. Given P-cadherin's apparent association with actively proliferating cells (Daniel et al, 1995, Obara et al,1999 and Fujita et al, 1992), it may play an important role in bronchial epithelial morphogenesis and restitution.

Ultimate understanding of the regulation of cell adhesion molecules could potentially lead to enhancement of cell adhesion or more efficient epithelial restitution. Either of these processes could be fundamental in reducing periods of epithelial denudation and therefore tissue exposure seen to extreme degrees in asthmatic patients.

4.2 Results

4.2.1 Development of Confluence in Bronchial Epithelial Cells.

4.2.1.1 Basic Characteristics.

16HBE14o- cells when plated as a uniform single cell suspension in minimum essential media (supplemented with Foetal calf serum), adhere to one another and the substrate forming 'islands' of cells here called colonies. These grow and merge with neighbouring colonies to form a confluent cell sheet with a 'cobblestone-like' appearance (figure 4.1).

Tight junctions have previously been visualised within the 16HBE14o- confluent sheet using transmission electron microscopy (Cozens AL et al., 1994). The tight junction *in vivo* is important in separating the apical and basolateral epithelial cell membranes and allowing a barrier to be formed between the airway lumen and the underlying tissues. As a measure of epithelial barrier integrity in 16HBE14o- cells, transepithelial electrical resistances were tracked over consecutive days to indicate the profile of junctional tightness over a period of time.

Cells were plated on triplicate membranes (see section 2.1.1.2) and media changed every 48 hours. Resistance measurements were recorded prior to media changes. For the first 7 days, resistances remained below $200\Omega cm^2$. This gradually increased over the next few days until a maximum of $\sim 1000\Omega cm^2$ was reached (figure 4.2).

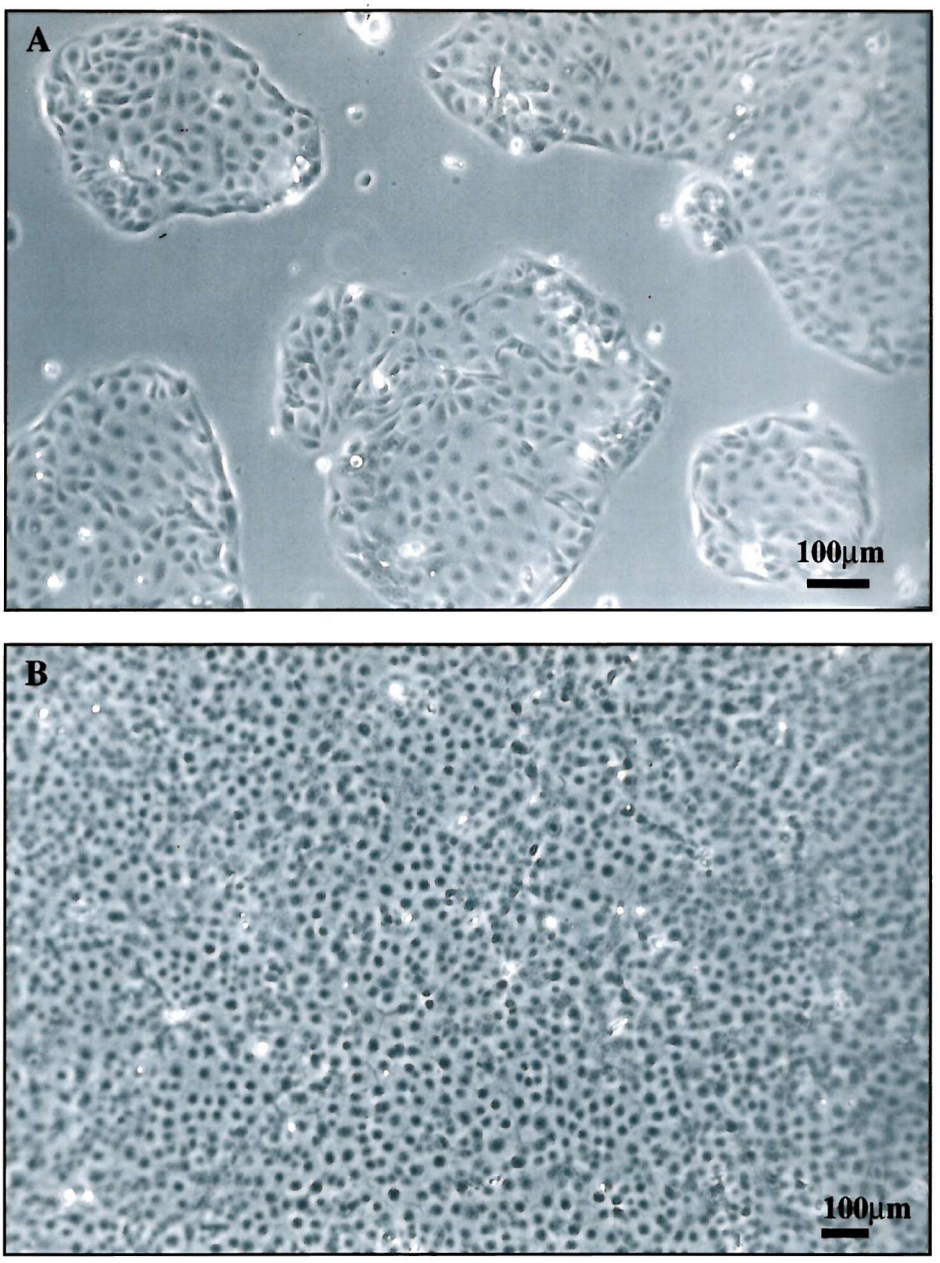

Fig 4.1 16HBE 14o- cells in culture.

16HBE14o- cell line is derived from surface epithelium of mainstream second generation bronchi. These cells retain differentiated epithelial morphology and functions after multiple passages in culture. Recently passaged cells form small colonies (A) which then merge with neighbouring colonies to form a confluent cell sheet (B), where cells have a rounded 'cobblestone-like' appearance.

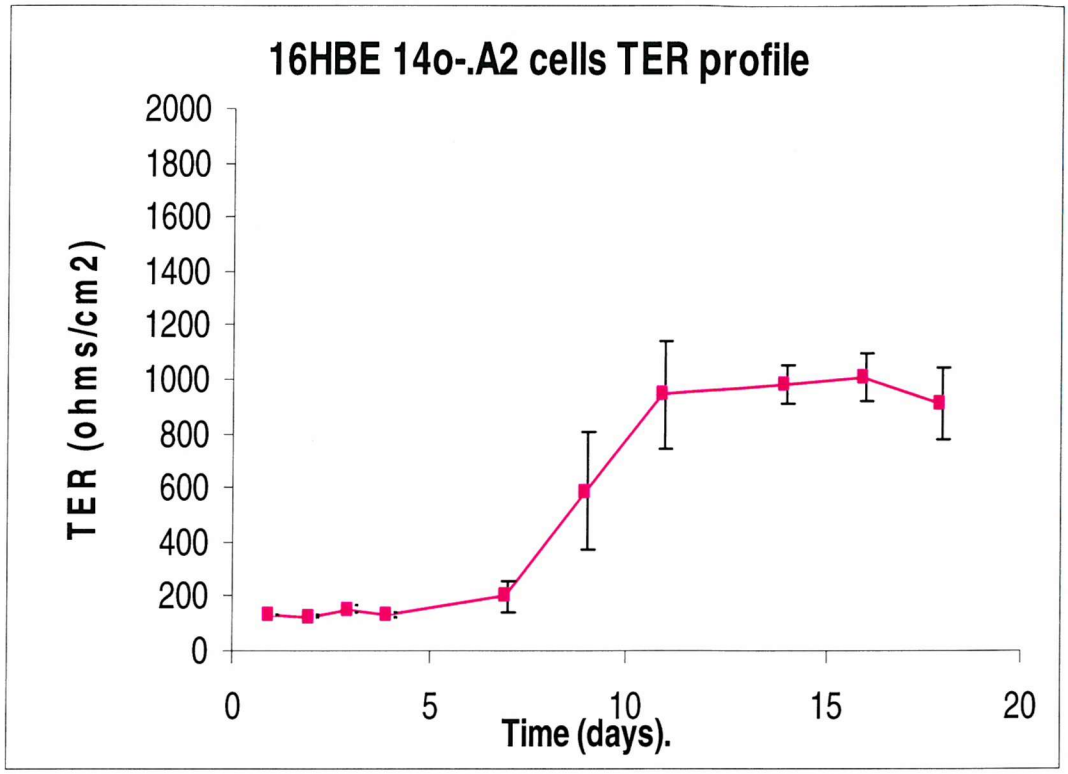

Fig 4.2 TER (transepithelial electrical resistance) profile of 16HBE 14o- cells.

Cultures were plated at day 0 on triplicate membranes with an initial cell density of 3 x10^4 cells/membrane. Resistances were monitored over a period of 18 days. Over the first week while cells were adhering and establishing colonies, resistance remained below 200Ω/cm^2. TER steadily increased over the next 4 days reaching ~1000Ω/cm^2. This profile is indicative of the formation of tight junctions within the epithelial sheet.

4.2.1.2 Stages of Confluence.

Practical and workable standard points for extractions were established on the basis of previous culture experience of 16HBE14o- cells. Time in days was used as extraction points corresponding to distinct stages of confluence in 6 well plates at a density of 10^5 cells/well.

'Pre-confluence' (which I will refer to as 'C1') was defined as 3 days after plating, at this time cells were arranged in discrete separate colonies of 50-100 cells covering approximately 50% of the surface area of the dish (figure 4.3A).

'Confluence' (referred to as 'C2') was defined as 7 days. At this time, colonies have merged to form a continuous cobblestone-like sheet of cells covering 100% of the surface (figure 4.3B).

'Post-confluence' (referred to as 'C3') was defined as 14 days, i.e. 1 week post 'confluence'. Here cells form a more densely packed version of C2 with a greater number of cells (approx. twofold) per unit area. Ridges of cells form within the cell sheet giving a less uniform appearance than that seen at C2 (figure 4.2C).

In two separate experiments, cultures were grown in triplicate and trypsinised at C1, C2 and C3. A 'total cell count' using a Beckman Coulter Counter (Model No. ZM0901) was carried out on each sample (figure 4.3D).

4.2.1.3 Cadherin Expression in Developing Bronchial Epithelium

Changes in cell adhesion molecule expression were examined in order to assess changes accompanying epithelial layer development in 16HBE140- cells.

SDS-PAGE (see section 2.1.2.1.3-4). was used to analyse cell adhesion molecule immunoreactivity of samples extracted at time-points C1, C2 and C3 as defined above. Nitrocellulose membranes were probed for E-cadherin and P-cadherin expression (using mouse anti-E-cadherin (SHE 78.7) 1:4000, mouse anti-P-cadherin (Zymed) 1:100 and visualised using an anti-mouse Ig (immunoglobin) horseradish linked antibody (Amersham lifesciences) 1:20,000 and ECL chemilluminescent system).

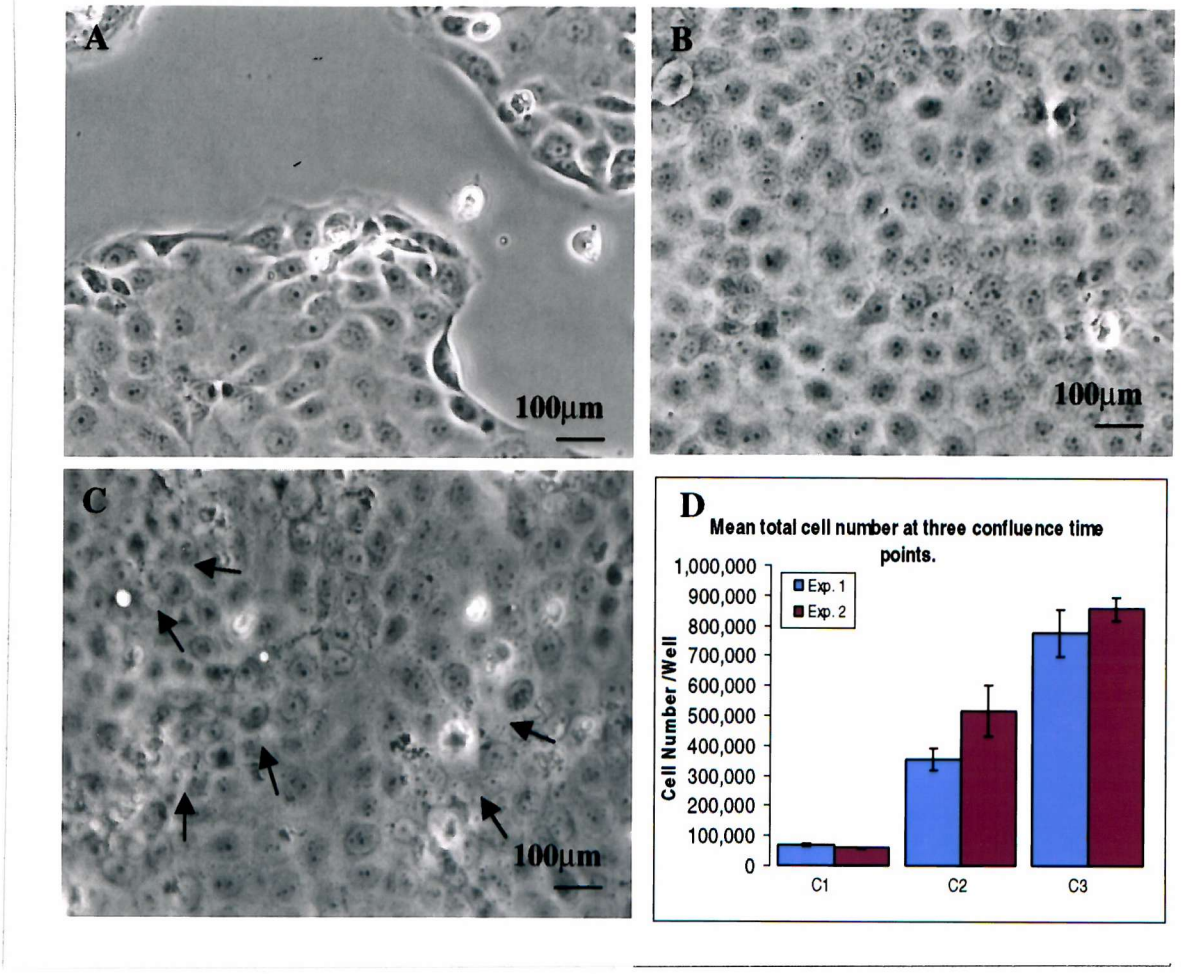

Fig 4.3 16HBE 14o- cells at three time-points during development.

Triplicate wells of 16HBE 14o- cells were grown in 6 well plates. The original plating density in each case was 10^5 cells/well.

At time-point 'C1' (3 days A), colonies do not yet form a continuous cell sheet. At 'C2' (7 days B), cells form a flat continuous cell sheet with a uniform cobblestone-like appearance. By 'C3' (14 days C), cell number has increased and epithelium is more densely packed. Ridges of cells form within the sheet (see arrows) giving a less uniform appearance.

Total cell number (± SD) at each time-point is shown in D. Two separate sets of cultures ('Exp1' and Exp2') were used. Each bar represents mean cell number from 3 wells trypsinised at the relevant time-point. Cell suspensions were analysed using a coulter counter.

Antibodies to E-cadherin showed clear immunoreactive bands at ~120 kD, antibodies to P-cadherin on a second membrane again showed clear immunoreactive bands at ~120kD (figure 4.4). This corresponds with previously reported data for these two cadherins.

In order to determine optimal protein loading levels for band density visualisation, gels were loaded with sample volumes of increasing known protein concentrations (determined by Bio Rad protein assay see section 2.1.2.1.2). Standard curves of various protein loading levels versus immunoreactivity for both cadherins were obtained by probing the resulting blots for E- and P-cadherin (figure 4.4).

Several different blot exposure times were used but for both cadherins, no single exposure time allowed adequate band density differentiation for all levels of loading. A shorter exposure length was therefore used to visualise upper protein levels and a longer exposure blot used for visualisation and analysis of lower protein loading levels. In all cases, densitometry was carried out using 'Quantity One' software. Blots were scanned and band density subsequently measured by image analysis (Section 2.1.2.1.5-6). Whenever possible, comparisons between bands were made on the same blot (see below).

E- and P-cadherin expression with increasing confluence was examined by loading samples extracted at time-points C1,C2 and C3 consecutively on a gel. Gels probed for E-cadherin were loaded with 7.5μg total protein and gels probed for P-cadherin were loaded with 15μg total protein as levels of cellular P-cadherin immunoreactivity are much lower than those of E-cadherin.

In these experiments 27 sets of samples (C1, C2 and C3) i.e. 9 triplicate experiments were analysed for E-cadherin expression (figure 4.5A). Mean E-cadherin expression progressively increased with confluence (figure 4.5B). However the density measurements representing blot immunoreactivity were not directly comparable because band intensity between experiments varies due to different blot exposure times. Figure 4.5C is a dot plot of the crude values between C1 and C3, the trend here was again of an increase in E-cadherin expression from C1 to C3.

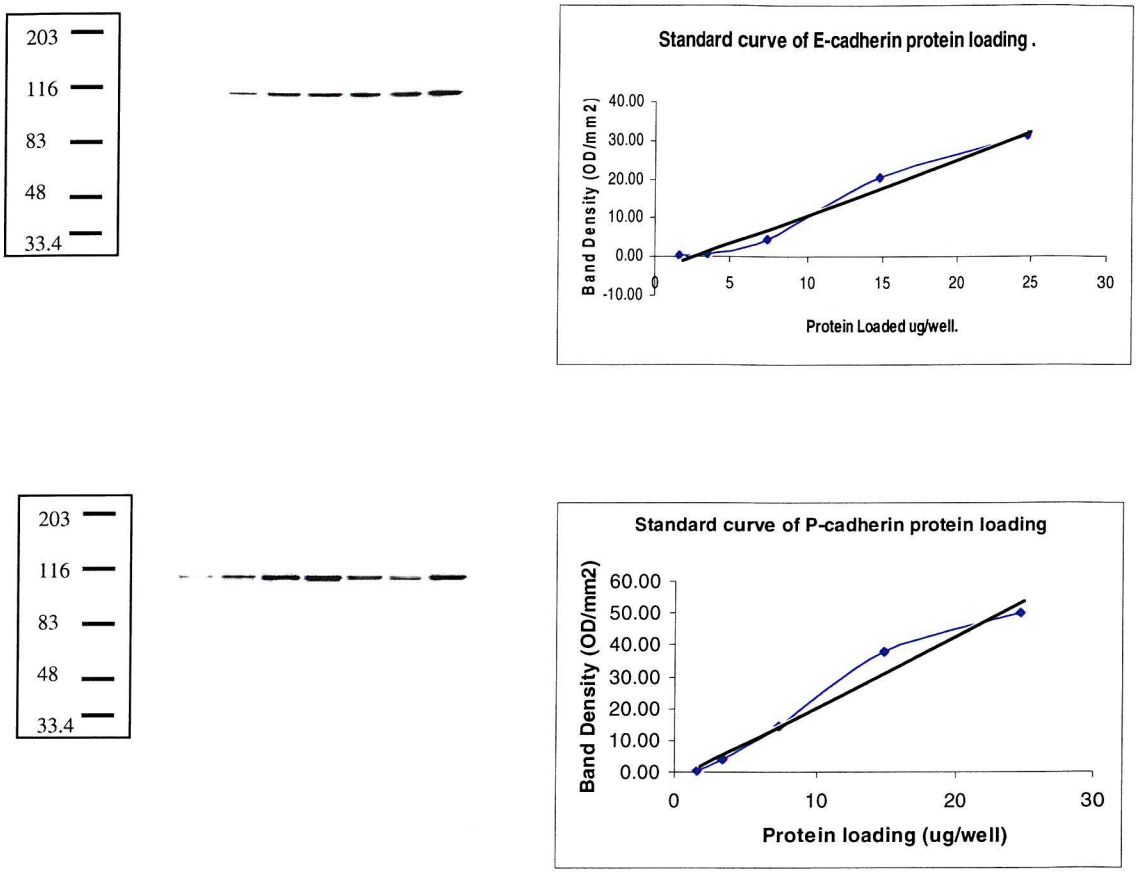

Figure 4.4 Standardisation of cadherin loading.

Gels were loaded with sample volumes of increasing known protein concentrations.
Blots were scanned into densitometry software and band density measured by image analysis Standard curves of protein loading levels versus immunoreactivity for both E- and P-cadherin were obtained..

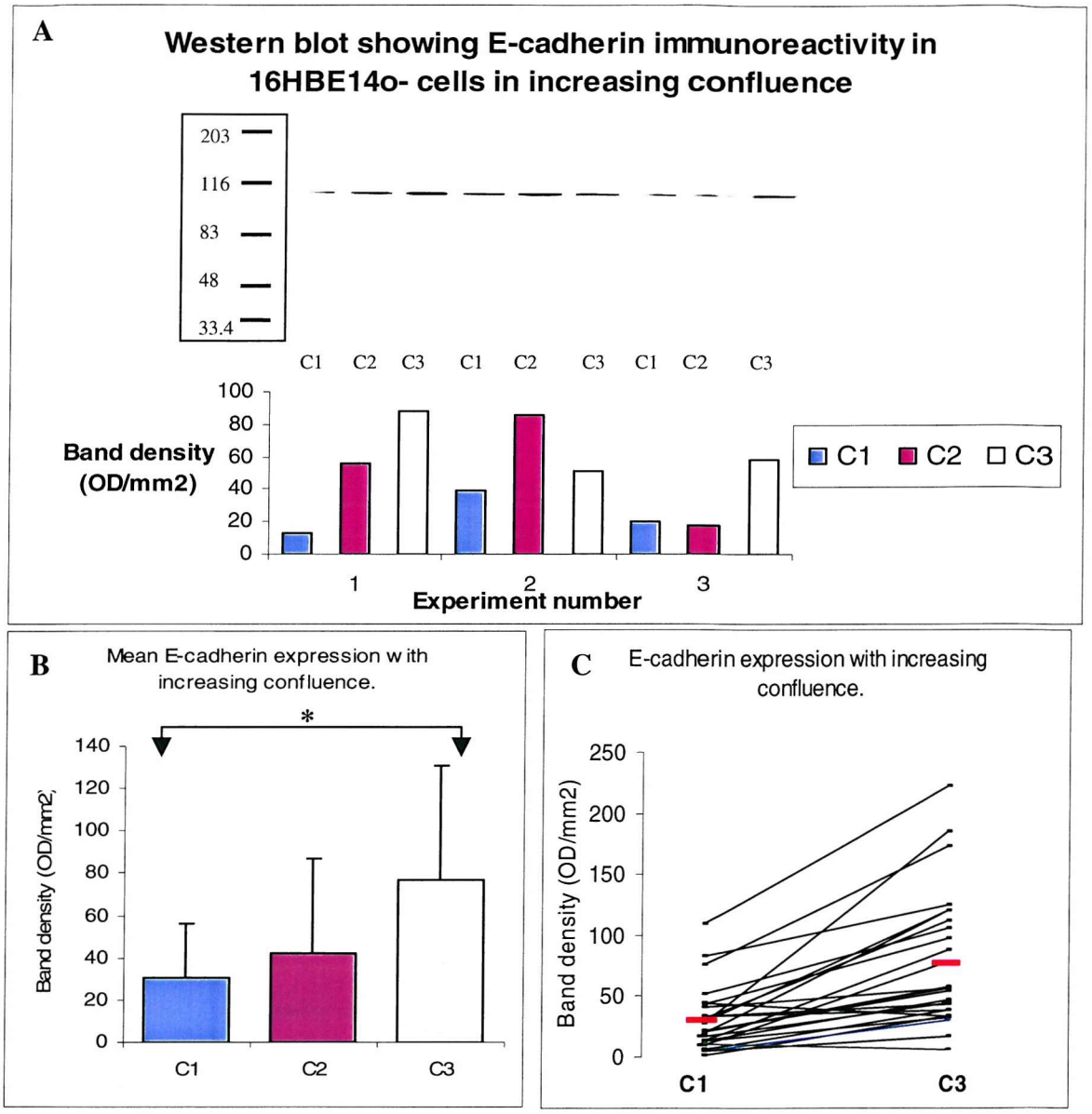

Fig 4.5 E-cadherin expression with increasing confluence.

16HBE 14o- cells were plated in 6 well plates at 10^5 cells/well and extracted in hot SDS at time-points C1, C2 and C3. Extracts were run on SDS-page and western blot then probed for E-cadherin expression (A).

27 separate experiments were run on 9 blots. Mean E-cadherin expressions are shown in (B). Band intensities vary within the time-point groupings as shown by the large standard deviations. This in part is due to different lengths of exposure time used when developing the blots. The dot plot of real values shows a trend for C1 levels to increase at C3 within the same experiment(C). '*' represents a significant increase in expression from C1 to C3 (p=0.004)

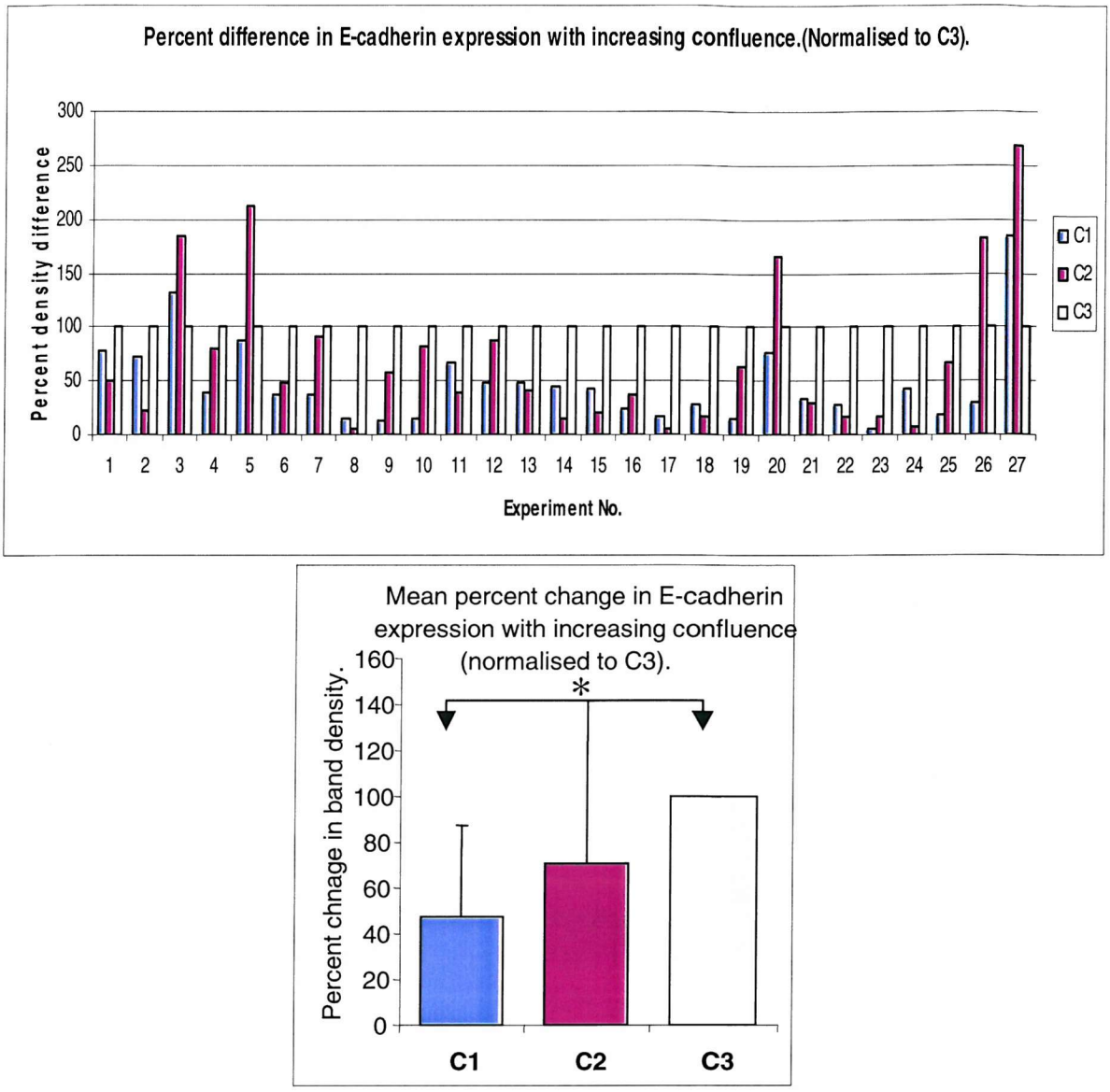

Fig 4.6 **Variation in E-cadherin expression with increasing confluence (normalised to C3).**

C3 was taken as 'normal state' epithelium and for each experiment values are expressed as a percentage of the C3 value (A).

In all but 2 cases (experiments 3 and 27), E-cadherin expression increases between C1 and C3, albeit by varying amounts. E-cadherin expression levels at C2 however, both increase (14/27 cases) and decrease (13/27 cases) from their corresponding C1 level.

Mean normalised band densities (B) show an increase from C1 and C3.

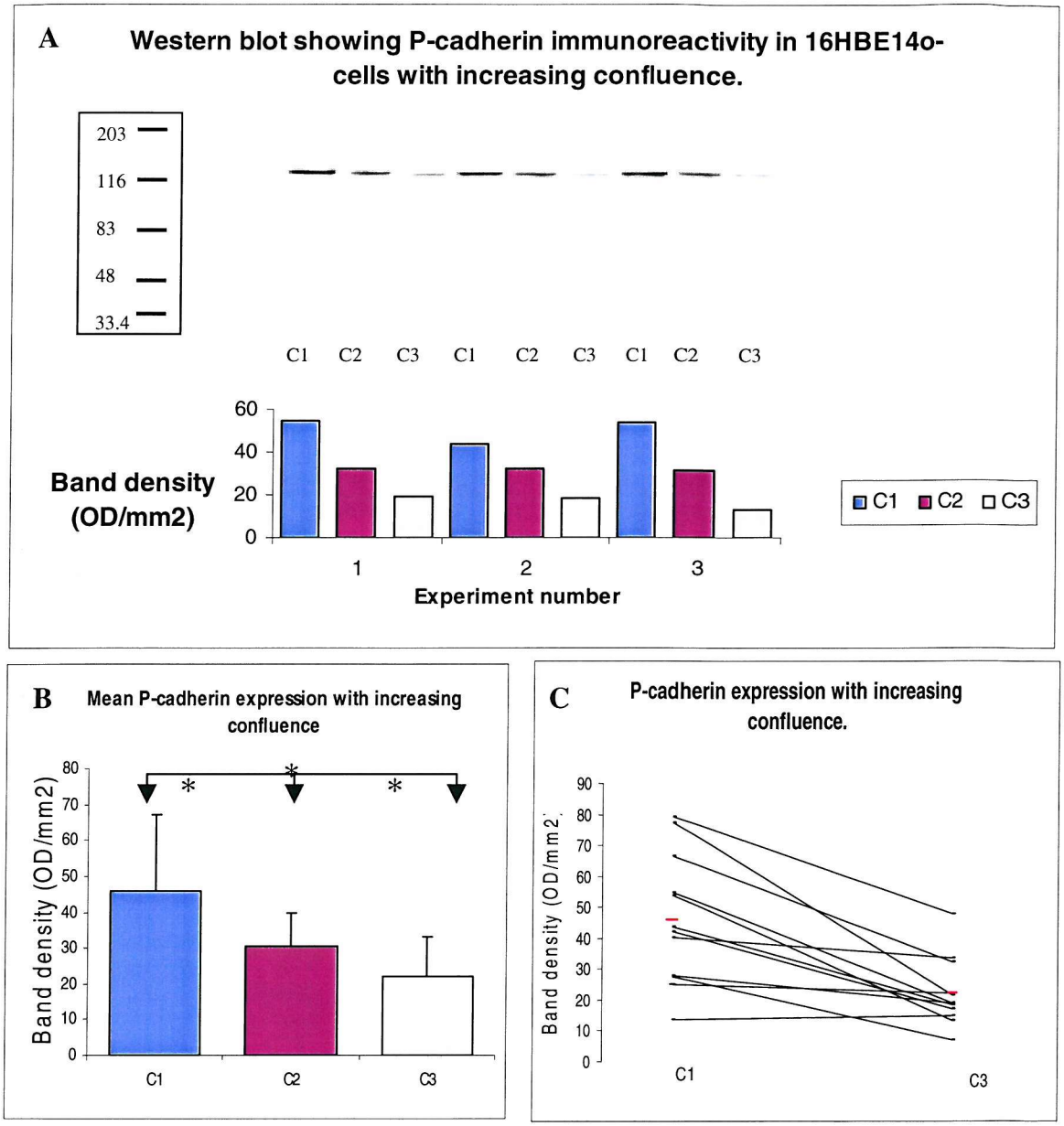

Fig 4.7 P-cadherin expression with increasing confluence.

16HBE14o- cells were plated in 6 well plates at 10^5 cells /well and extracted at time-points C1, C2 and C3. Extracts were run on SDS-Page and western blot then probed for P-cadherin expression (A). 12 separate experiments were run. Mean P-cadherin expression (B) decreases progressively from C1 to C3. Band densities vary between experiments because of different blot exposure times. A dot plot of real band intensities (C) shows a definite trend that band intensity decreases from C1 to C3 samples within the same experiment. '*' represents a significant change in band density between C1/C2, C1/C3 and C2/C3 ($p=0.003$, $p<0.000$, $p=0.003$ respectively).

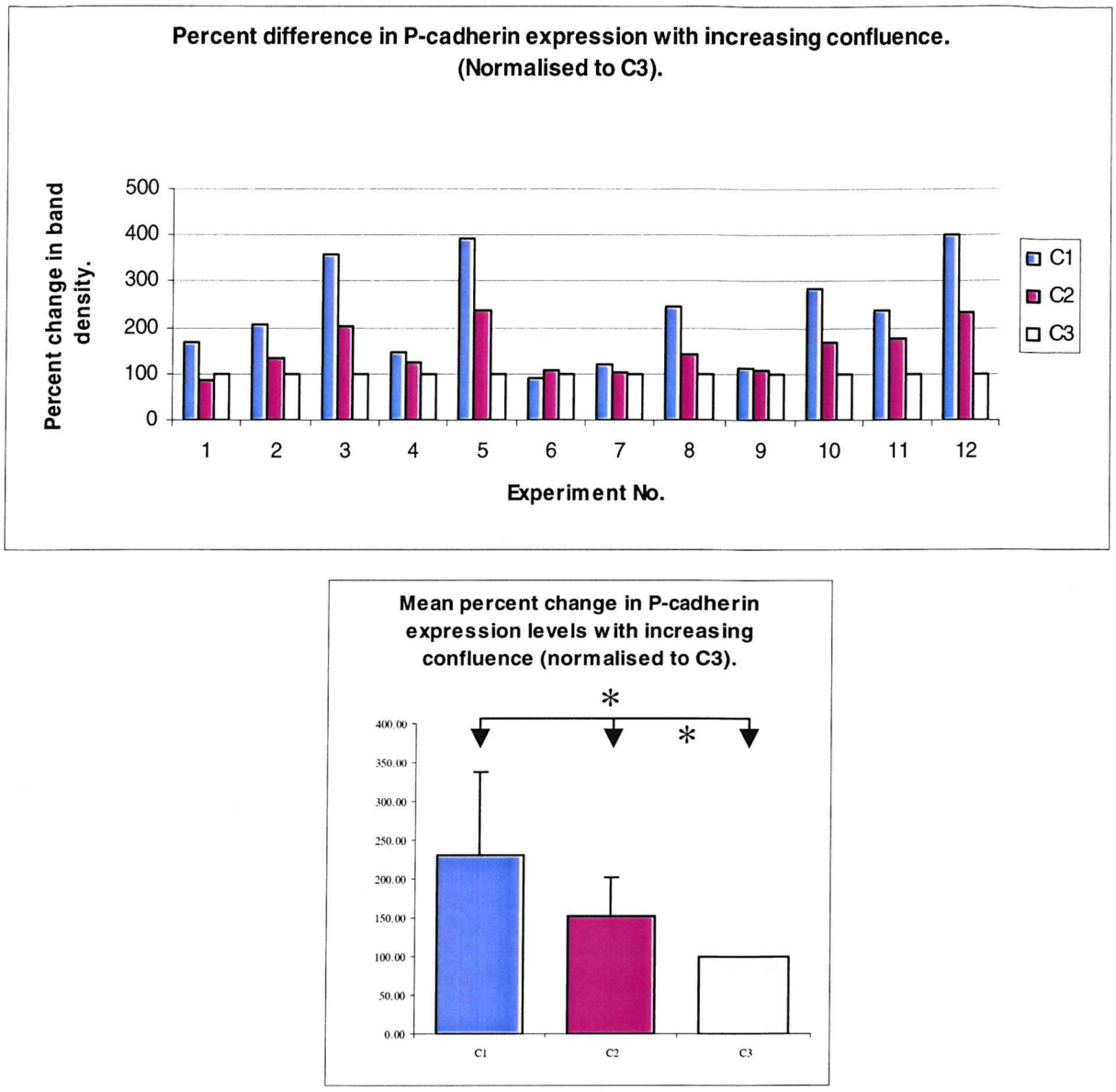

Fig 4.8 Variation in P-cadherin expression with increasing confluence (normalised to C3).

C3 was taken as 'normal state' epithelium and for each experiment values were expressed as a percentage of the C3 value to assess the extent of change in E-cadherin expression despite different blot exposure times (A). In all but one case (6) There was a lower P-cadherin expression at C3 than at C1 and in all but 1 of these cases (1), C3 band intensity is less than C2 which is turn less than C1. Mean normalised values (B) show a clear progressive decrease with confluence.

Comparison of E-cadherin levels from C1 and C3 within an experiment is therefore more valid than between experiments. Changes *within* a group were hence assessed and the *level of change* compared.

Values were normalised to C3 values, regarding this as 100% expression for each experiment. Each sample was calculated as a percentage of the relevant C3 value on the same blot (figure 4.6A). These normalised results show an increase in E-cadherin expression between C1 and C3. 25 out of the 27 sets of samples display a rise in E-cadherin expression pre- to post-confluence, albeit by different extents. Levels at C2 both increased (14/27) and decreased (13/27) from C1 and in some cases (5/27) levels were higher than at C3.

P-cadherin levels were examined in the same way in 12 of the sample sets (fig 4.7A). Mean crude values (figure 4.7B) show a progressive decrease in P-cadherin expression but again are not directly comparable because of differing blot exposure times. A dot plot of real values (figure 4.7C), shows a decrease in P-cadherin levels from C2 to C1 then a further decrease at C3.

Crude values were, as in the E-cadherin analysis, normalised to C3 (figure 4.8A). A progressive decrease in P-cadherin expression is seen from C1 to C2 to C3 in 10 out of the 12 experiments. Again the extent of change varies, the highest variation (as reflected by standard deviations) occurring at C1.

4.2.1.4 Catenin Expression in Developing Bronchial Epithelium

Expression of the cadherin anchoring adherens junction molecules α, β and γ–catenin were also examined in a single triplicate well experiment. Antibodies to these catenin showed immunoreactive bands of ~100, 90 and 80 kDa respectively. In each case band density was highest at C3 (see figure 4.11).

4.2.1.5 Tight Junction Adhesion Molecule Expression in Developing layers of Bronchial Epithelial cells.

The nitrocellulose blotting membranes used for the cadherin analysis above were also probed for the tight junctional proteins occludin and ZO-1 (rabbit anti-occludin (Zymed) 1:3,000, rabbit anti ZO-1 (Zymed) 1:150 and visualised using anti-rabbit horseradish peroxidase linked antibodies (Amersham lifesciences) 1:15,000).

Occludin immunoreactivity (figure 4.9A) was seen as bands running at ~65kD. The band densities were normalised to C3 (in the same way as the cadherins), allowing comparison of change across the whole group. Figure 4.19B is a chart of the mean normalised occludin expression values. A progressive increase in band density is seen from C1 to C2 to C3.

ZO-1 immunoreactivity (figure 4.10A) was seen as several sets of bands; firstly a doublet at ~210kD, a less intense band at ~200kD and a third band of much higher intensity at ~35kD.

Previous studies have reported ZO-1 to be a 210kD protein with no mention of the other two bands visualised in this experiment (Anderson et al, 1985 and Stevenson et al, 1986), therefore for this experiment I have chosen to analyse only the 210kD bands. The doublet at ~210kD represents the two isomers of a protein which have previously been identified as the tight junctional adhesion molecule ZO-1. It is this molecule which this study is interested in and so only this doublet was analysed by densitometry.

Figure 4.10B is a chart showing mean normalised ZO-1 band densities. Here decrease in immunoreactivity is seen with increasing confluence with the mean value at C1 ~2000 times that at C3.

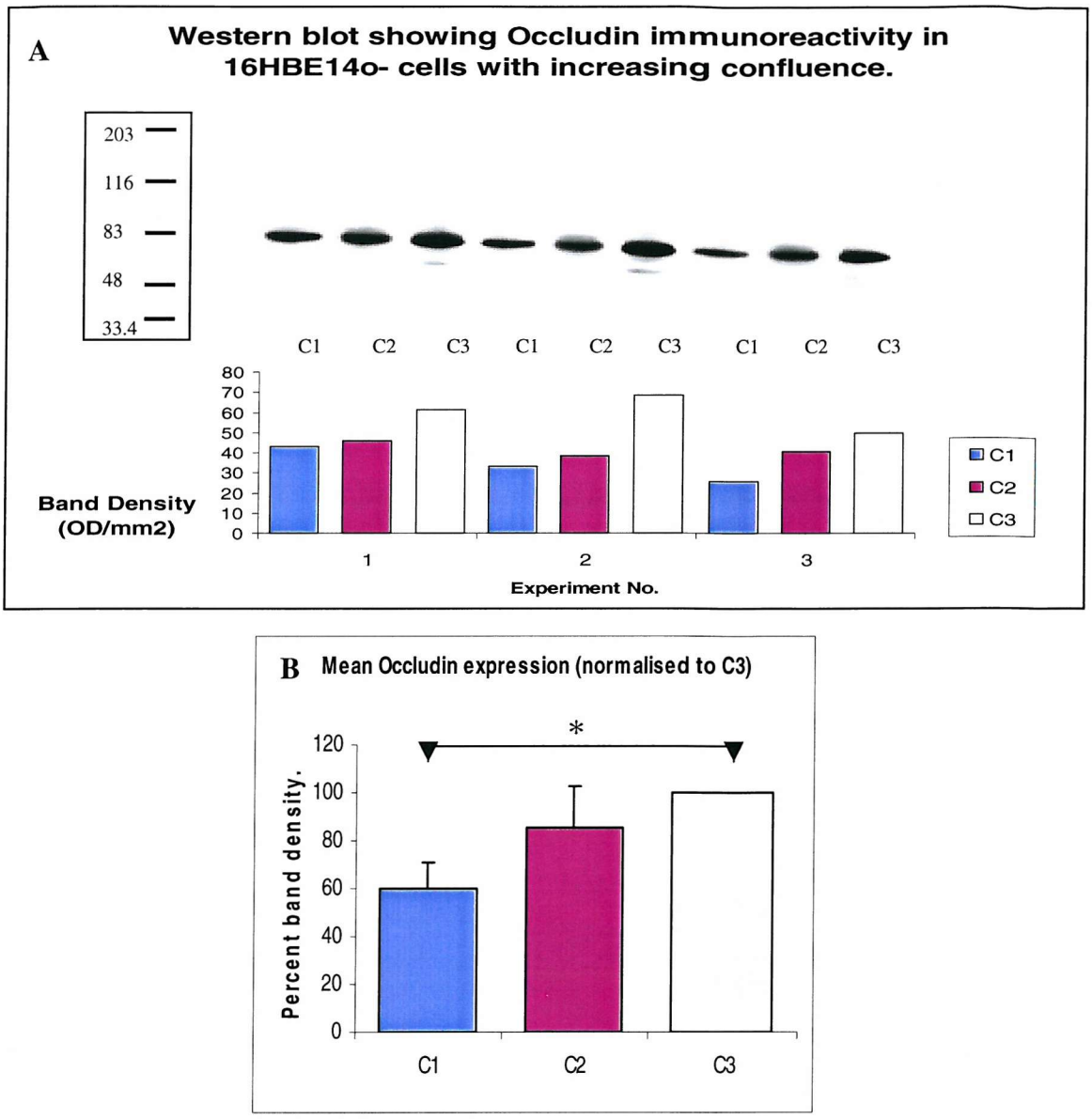

Fig 4.9 Occludin expression with increasing confluence.

16HBE14- cells were extracted from 6 well plates at time-point C3. Extracts were run on SDS-Page and western blot then probed with anti-occludin antibodies (A). Mean band density was augmented with increased confluence (B). '*' represents a significant increase in band density between C1 and C3 (P=0.002).

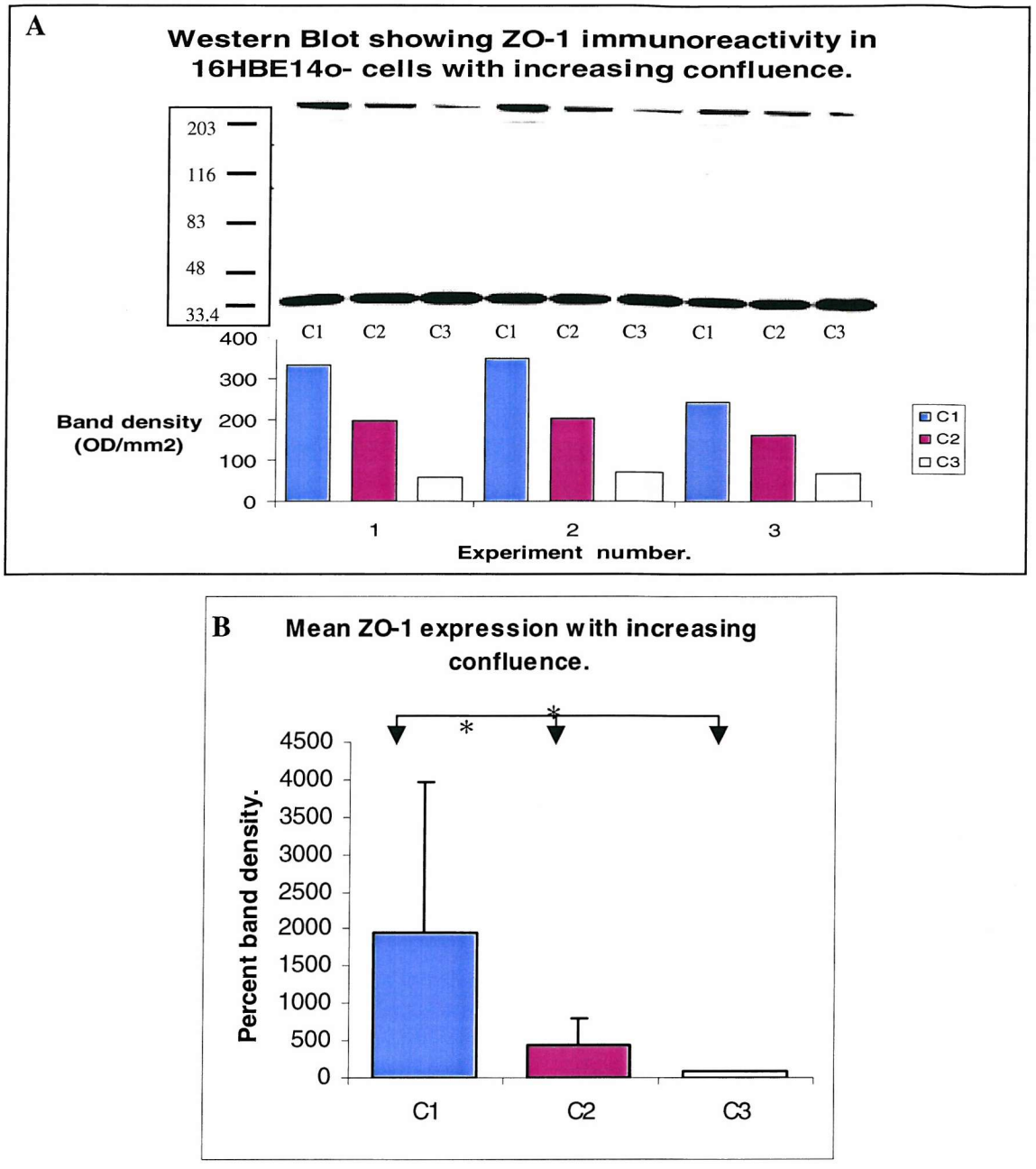

Fig 4.10 ZO-1 expression with increasing confluence.

16HBE14o- cells were extracted from 6 well plates at time-points C1, C2 and C3. Extracts were run on SDS-Page and western blot then probed with anti-ZO-1 antibodies (A). Mean band density was highest at C1 and progressively decreased with increased confluence through C2 and C3. Mean value at C3 is ~2000 times that at C1. '*' represent significant changes in band density between, C1/C3, C1/C3 ($p=0.04$ and $p=0.000$ respectively).

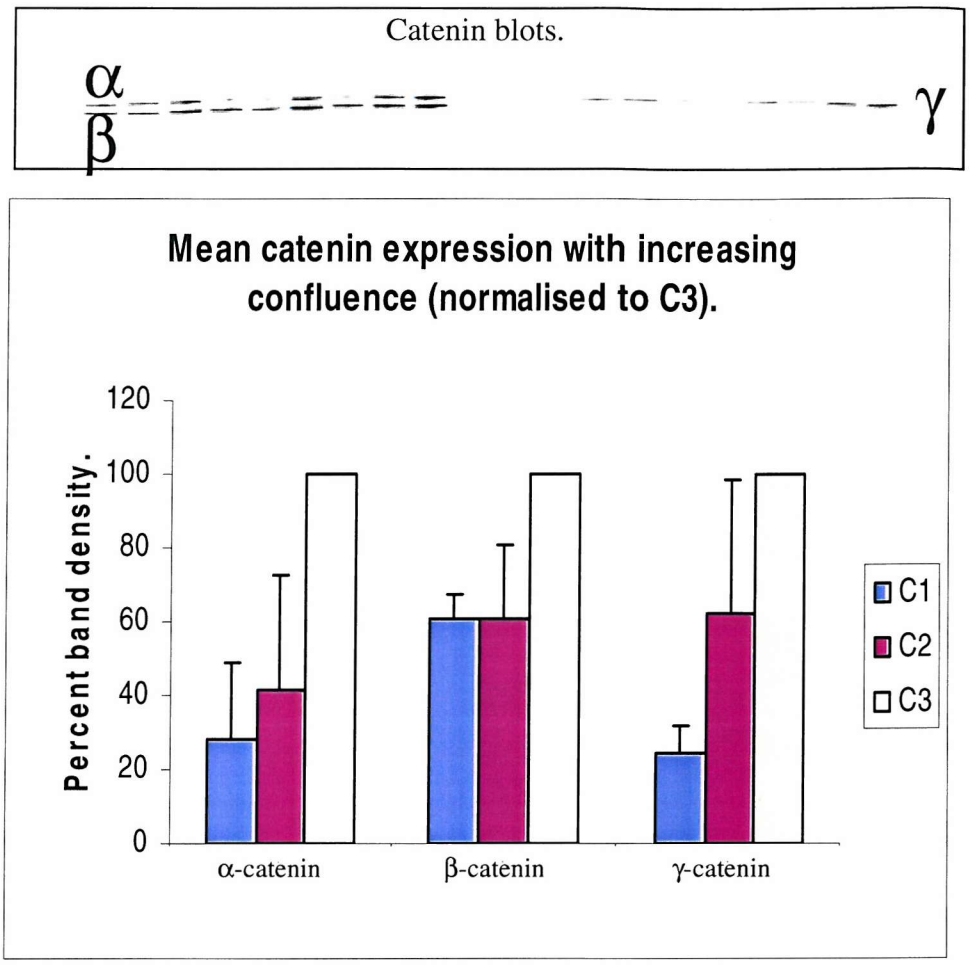

Fig 4.11 Catenin expression with increasing confluence.

3 experiments were analysed for α, β and γ-catenin expression. 16HBE14o- cells were extracted from 6 well plates at time-points C1, C2 and C3. Extracts were run on SDS-page and western blot then probed for catenin expression. In each case highest expression was seen at C3. α and γ–catenin mean band densities were lowest at C1 but β–catenin band density was at similar levels for both the earlier time-points.

4.2.2 Models of a Repairing Epithelium.

An *in-vitro* model of repair using 16HBE14o- cells was developed in order to assess cell adhesion molecule expression following epithelial injury. The first model assessed involved mechanical damage of the epithelial cell sheet and monitoring its repair using time-lapsed video-microscopy and image analysis.

4.2.2.1 Time-Lapse Model.

16HBE14o- cells were plated onto a circular coverslip (13mm diameter) at a density of 10^5 cells/well and grown to a confluent sheet comparable to C3 (post-confluence). The cell layer was then mechanically damaged using a medium sized pipette tip, the point of which is scored once across the diameter of the glass disk. The disk was rinsed thoroughly with PBS to remove cell debris then placed on a 'tripod' made from three eppendorff lids serving to elevate the coverslip from the base of a 25mm diameter petri dish (figure 4.12). Growth media supplemented with Hepes buffer (to maintain pH levels) was added to a level submerging the coverslip. The entire dish was sealed with parafilm in which a cross was cut using a scalpel directly above the region of interest. The scored cross was opened up and the microscope objective positioned directly on and through this hole so that the cells were visible but the dish remains airtight. The stage was kept at ~37 °C by positioning a fan heater adapted to blow air of 37 °C adjacent to the microscope stage (heater controlled by an external temperature sensor placed as close as possible to the petri dish).

To monitor epithelial repair, cells were wounded at T(time)=0 hours. A cooled CCD camera captures digital images at set intervals through the microscope. In this study one image every 15 minutes was adequate to give a series of pictures portraying wound repair, forming a short film. The images can then be played back and analysed for the speed and patterns of wound closure looking at individual cells and the overall leading edge (figure 4.12).

Preliminary work using this system found total wound closure to occur between 8 hours and 14 hours (figure 4.13), but this depended on wound size.

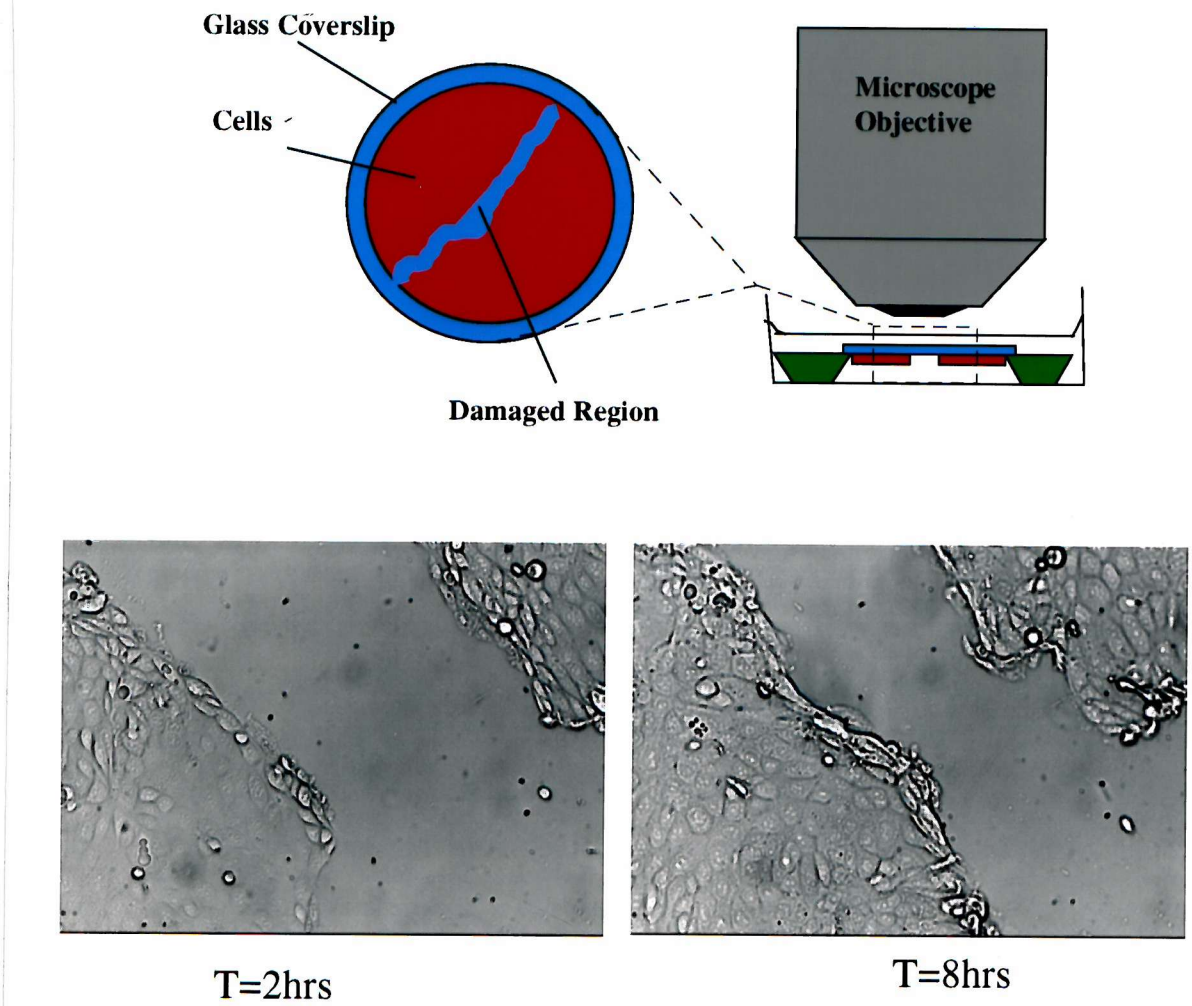

Fig 4.12 Time-lapsed video microscopy in an *in vitro* model of repair.

Diagram showing set up of apparatus for wound repair experiment. Cells are plated on glass
cover-slips and mechanically wounded. Cover-slips are mounted on a 'stage' as shown and submerged in media. Migration and wound repair is observed under a microscope attached to a digital camera which records at set intervals.

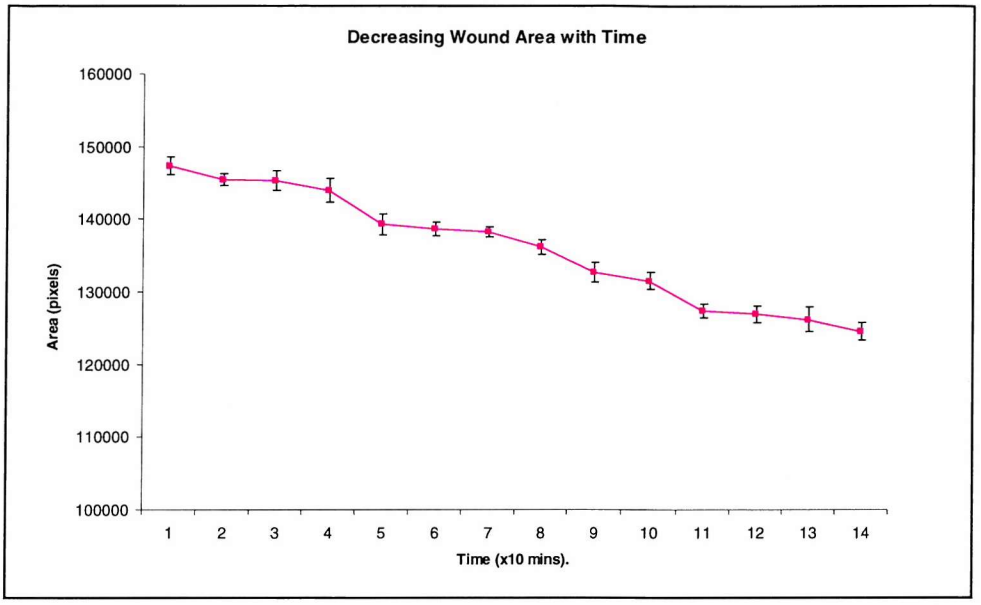

Figure 4.13 Time Lapse Wound Repair Image Analysis.

Post-wounding, the area of damage was measured in pixels by image analysis and plotted against 'time'. Standard error bars refer to duplicate measurements made on the same images.

Although in each case an identical wounding instrument was used, wounding was not repeatable giving a 'ragged' wound edge and variable position of the wound. Using this system, the majority of cells on the coverslip were not in close proximity to the damaged area and so were not in a state of 'repair'.

There also appeared to be a lag phase in repair with the cells in this model. Post wounding, cultures on the microscope stage under the described conditions appeared to have a slower repair rate to those returned to the incubator although temperature logging showed that the microscope stage temperature remained between 35-38°C. Two of the cultures had very little repair or cell movement post damage.

Due to the variability of this model, a second model was developed with the aim of establishing a more repeatable wound with increased uniformity of cell phenotype within the cell sheet.

4.2.2.2 Concentric Wound Model.

A device developed by Dr. Mike West, (GlaxoSmithKline) was used that created concentric wounding within the cell sheet. This pattern of wounding means that each cell analysed is within 1.5mm of a leading edge. When examining cell adhesion molecule expression using immunoblotting or ELISA, this is particularly important as the entire dish was examined for properties of a particular phase of repair. Cells not affected by wounding would 'dilute' changes in adhesion expression associated with the repair response.

The wounding device consists of a platform on which to site a 6 well plate and a rod with protruding steel pins (diameter ~1.12mm) positioned at such locations to create concentric wounding on rotation (figure 4.14).

16HBE14o$^-$ cells were plated out at 10^5 cells/well (6 well plate). Cultures were grown in triplicate to C3 (1 week post confluence as defined in chapter 4) and damaged using the wounding device. SDS extractions were taken at time-points of 0 (T0), 6 (T6), 16 (T16) and 24 (T24) hours post wounding in order to investigate the patterns of cell adhesion molecule expression as the cells go through a repair process re-establishing the confluent cell sheet.

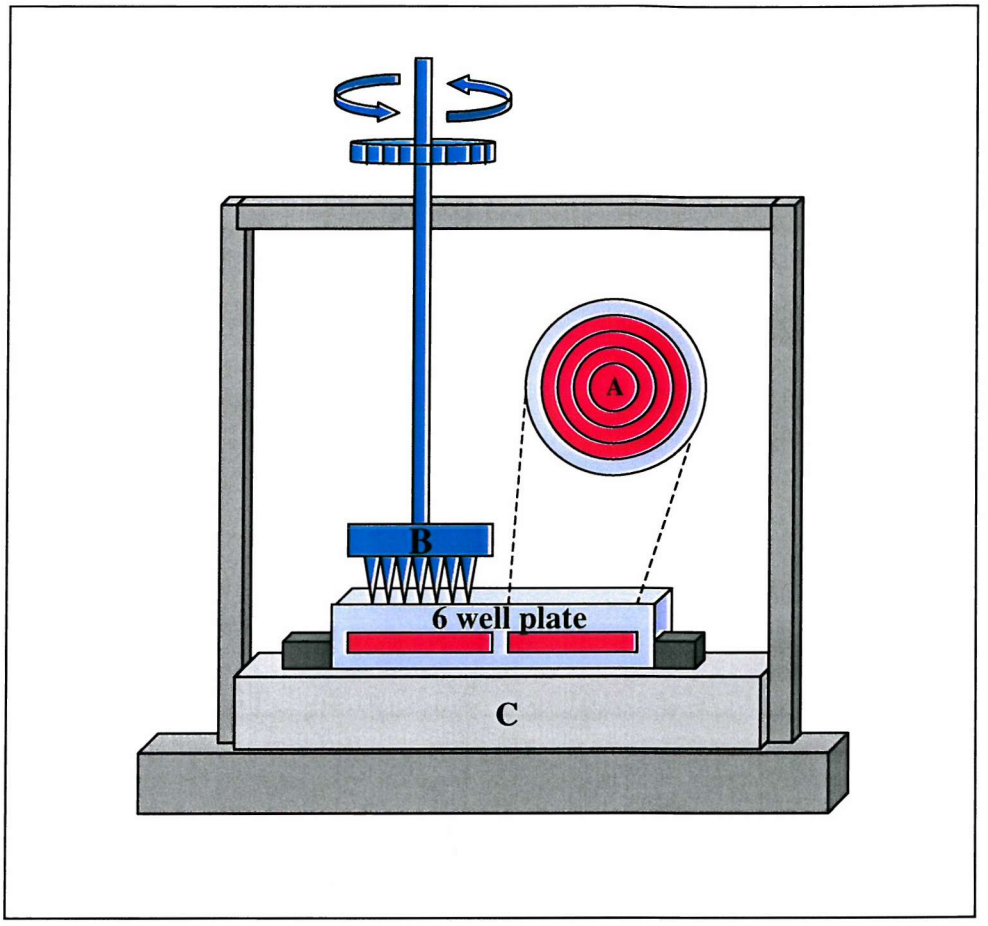

Fig 4.14 Mechanical wounding device as an *in vitro* model of repair.

Apparatus used to achieve repeatable wounding of the cell sheet (A). Cells are grown to time-point C3 in a 6 well plate which is positioned on 'B' for wounding. A rod with protruding weighted steel pins (C) is lowered onto the cells and rapidly rotated to create concentric wounding of the cell sheet. To ensure clean wounding, wells are washed several times with PBS both pre and post wounding.

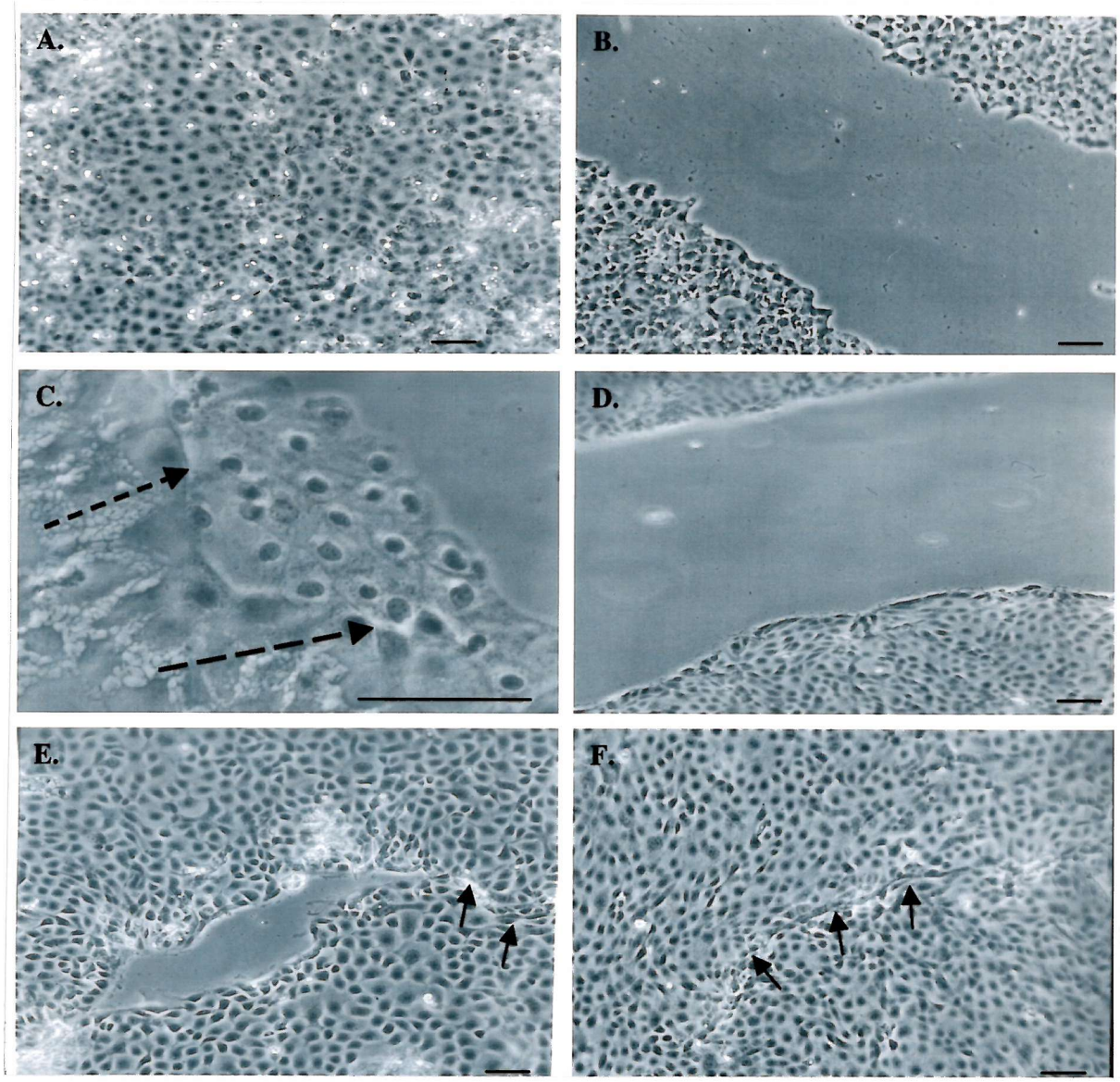

Fig 4.15 16HBE 14o- cells post wounding.

Cells were plated at 10^5 cells/well in 6 well plates. Cultures were grown to C3 (A), and mechanically wounded. 1 hour post-wounding (B and C) the wound remains clean. The culture plate is exposed at the region of damage with the undamaged cell sheet on either side. At the edge of the wound cells have a different phenotype to those further back. Cells appear to be flattening and migrating outwards beyond the original wound edge (dashed arrows). At 6 hours post-wounding (D) the wound edge has visibly migrated across the wound whereas at 16 hours post-wounding (E), opposite wound edges have met across the denuded area. The cell sheet is predominantly repaired but sporadic small gaps remain. 24hours post wounding (F) the wound has repaired but 'scarring' remains visible at the wound site (see arrows).Scale bars represent 100μm.

T0 was immediately prior to extraction and therefore the cells were in the C3 state with a densely packed continuous sheet of cells (figure 4.15A).

At T1 i.e. 1 hour post wounding (not included as an extraction point), a wound edge was seen with the border cells beginning to flatten and spread beyond the main body of cells (figure 4.15B&C).

By T6 the leading edge cells had 'spread' beginning to fill the gap in the confluent sheet. Leading edge cells had begun to migrate across the wounded area toward the opposing wounding edge with the main cell sheet remaining intact (figure 4.15D).

Several regions of the wound had re-joined and healed by T16 giving an overall impression that the cell layers had 'zipped' together. Regions of 'bridged' wounds were separated by areas still with gaps (figure 4.15E).

At 24 hours post-wounding the entire well was predominantly confluent with ~90% of the damaged areas repaired. The original concentric wounding was still visible as 'scarring' however. It was seen as raised areas of densely packed shrunken cells at the point where the leading edges either side of the wound had closed in and merged (figure 4.15F).

4.2.2.3 Cadherin Expression in Repairing Epithelium.

SDS-Page was used to analyse cell adhesion expression at time-points T0, T6, T16 and T24 as defined above. Cultures were damaged in 6 well plates and grown for each time-point. Cells were extracted in 250µl boiling 2% SDS added directly to the cell surface. Extracts were collected using a cell scraper and a positive displacement pipette, then boiled for 4 mins.

SDS-Page and western blotting were carried out and the resulting nitrocellulose membranes probed for E-cadherin and P-cadherin expression (primary and secondary antibodies as listed previously).

4.2.2.3.1 E-Cadherin

Antibodies to E-Cadherin showed clear immunoreactive bands at ~120kD (figure 4.16A). Mean band density decreases between T0 and T6 then increased in density at T16 with band densities at T24 being similar (figure 4.16B). Figure 4.16C is a dot plot of band densities showing the tendency for band density to drop at T6 then rise again at the later time-points.

Values were normalised to T0 values (the equivalent cell state to C3), regarding this as 100% expression for each experiment. Each sample was calculated as a percentage of the relevant T0 value (figure 4.17A). These normalised show that in each case E-cadherin levels decrease at T6 then increased at T16. In 8 out of 9 cases this level had increased further by T24. E-cadherin levels at T24 in most cases (7 out of 9) did not reach the initial levels seen at T0. Mean normalised values show the same trend with an 80% drop in band density between T0 and T6.

4.2.2.3.2 P-Cadherin.

P-cadherin expression in repair was examined in the same way using 13 sets of samples. Antibodies to P-cadherin showed immunoreactive bands at ~120kD (figure 4.18A). Mean band densities increase at T6, fall at T16 then rise again at T24 (figure 4.18B). Figure 4.18C is a dot plot showing the density profile for each experiment.

Values were normalised to T0 (in the same way as the E-cadherin data). Here T6 band expression was less consistent than those seen from E-cadherin immunoreactivity. This time just over half (8 out of 13) of the experiments P-cadherin levels were greater at T6 than at T0. In all but one case, levels of T16 were lower than at T6 which then returned at T24 to a similar or increased P-cadherin level to that seen at T0 (figure 4.19A). At time T16 mean normalised band densities were the lowest, with T24 showing the highest values (fig 4.19B).

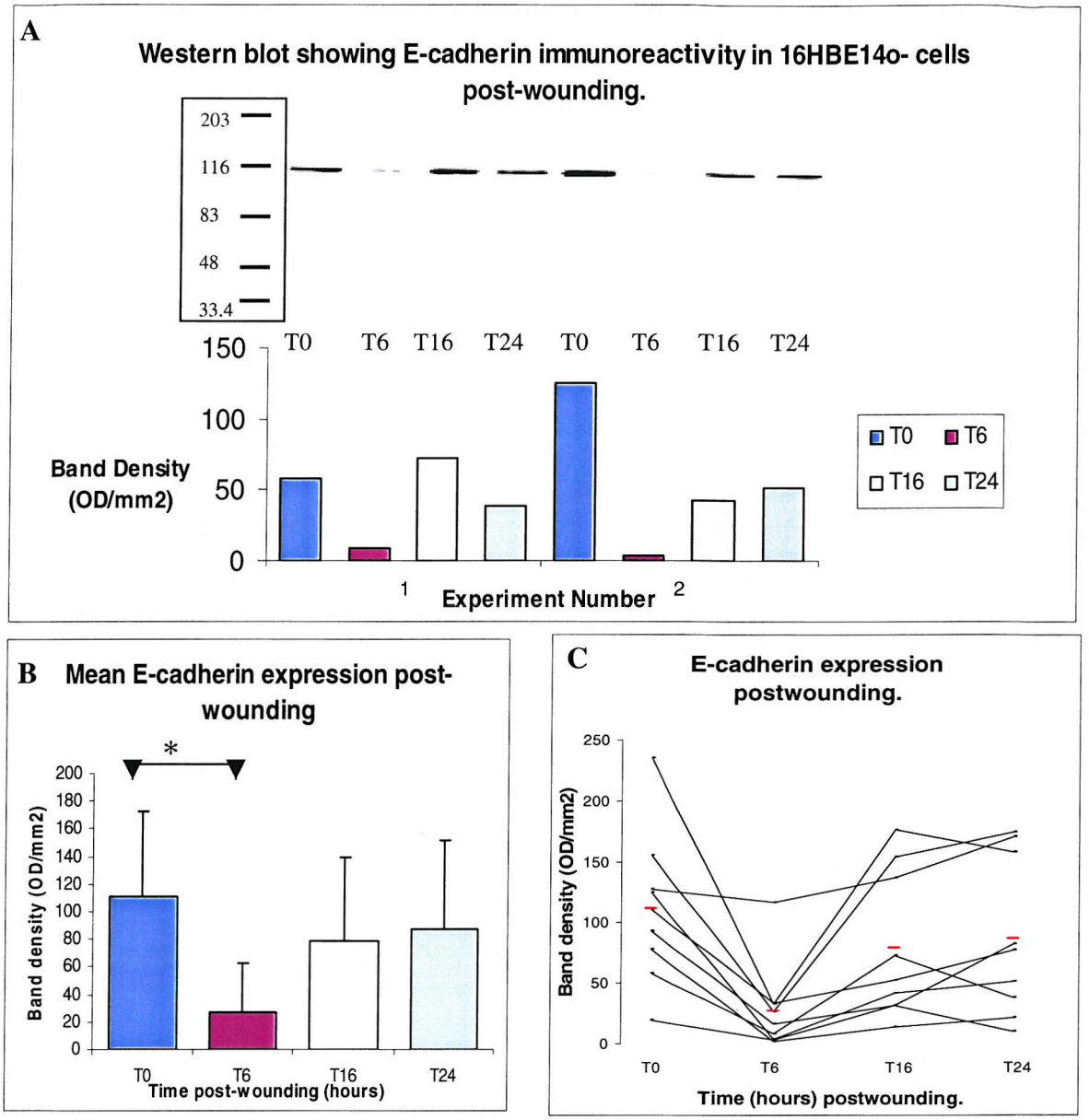

Fig 4.16 E-cadherin expression post-wounding.

16HBE14o- cells were plated in 6 well plates at 10^5 cells/dish, grown to C3 and damaged using the wounding device (fig 4.14). SDS extractions were taken at T0, T6,T16 and T24 hours post wounding. 9 extraction sets were run on SDS-Page and western blot then probed with anti-E-cadherin antibodies. Immunoreactivity was seen as bands running at ~120kD (A).

Mean band density was lowest at T6 (B). in all cases there was a drop in E-cadherin expression from T0 to T6 (C) then a rise from T6 to T16 although the level of this increase was inconsistent. Band intensities both increased and decreased at T24. '*' represents a significant decrease in band density between T0 and T6 (p=0.002).

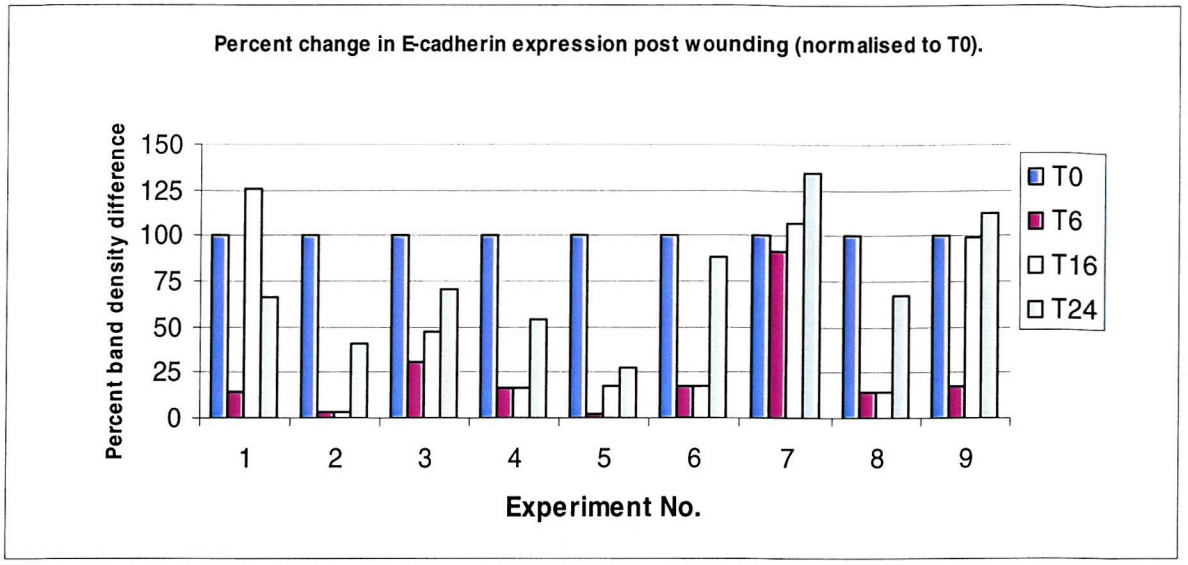

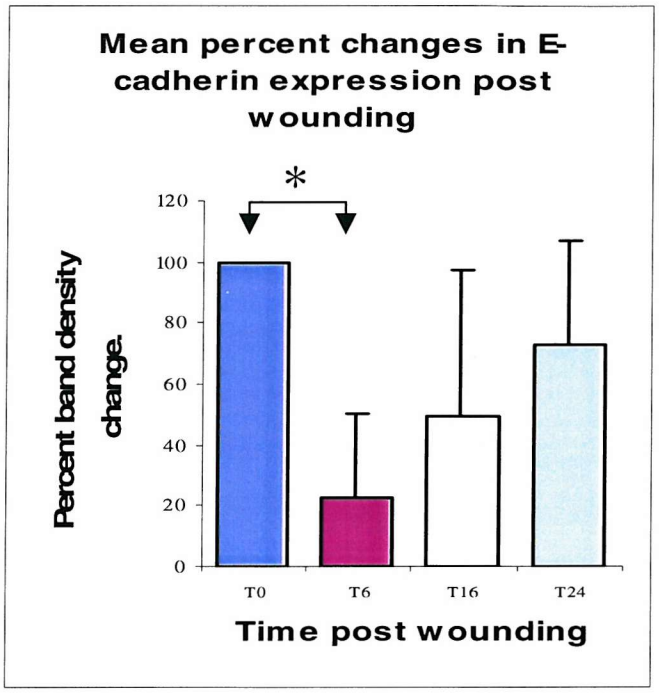

Fig 4.17 Variation in E-cadherin expression post-wounding.

Values were normalised to T0. In all but 1 case E-cadherin expression at T6 falls to below 30% of the level seen at T0. The increase in immunoreactivity that follows is very variable in that there is no apparent consistency in band density or trend except that it rises from T6. Mean normalised values (B), show this inconsistency where T16 and T24 expression levels tend to be below that of T0 with high SDs.

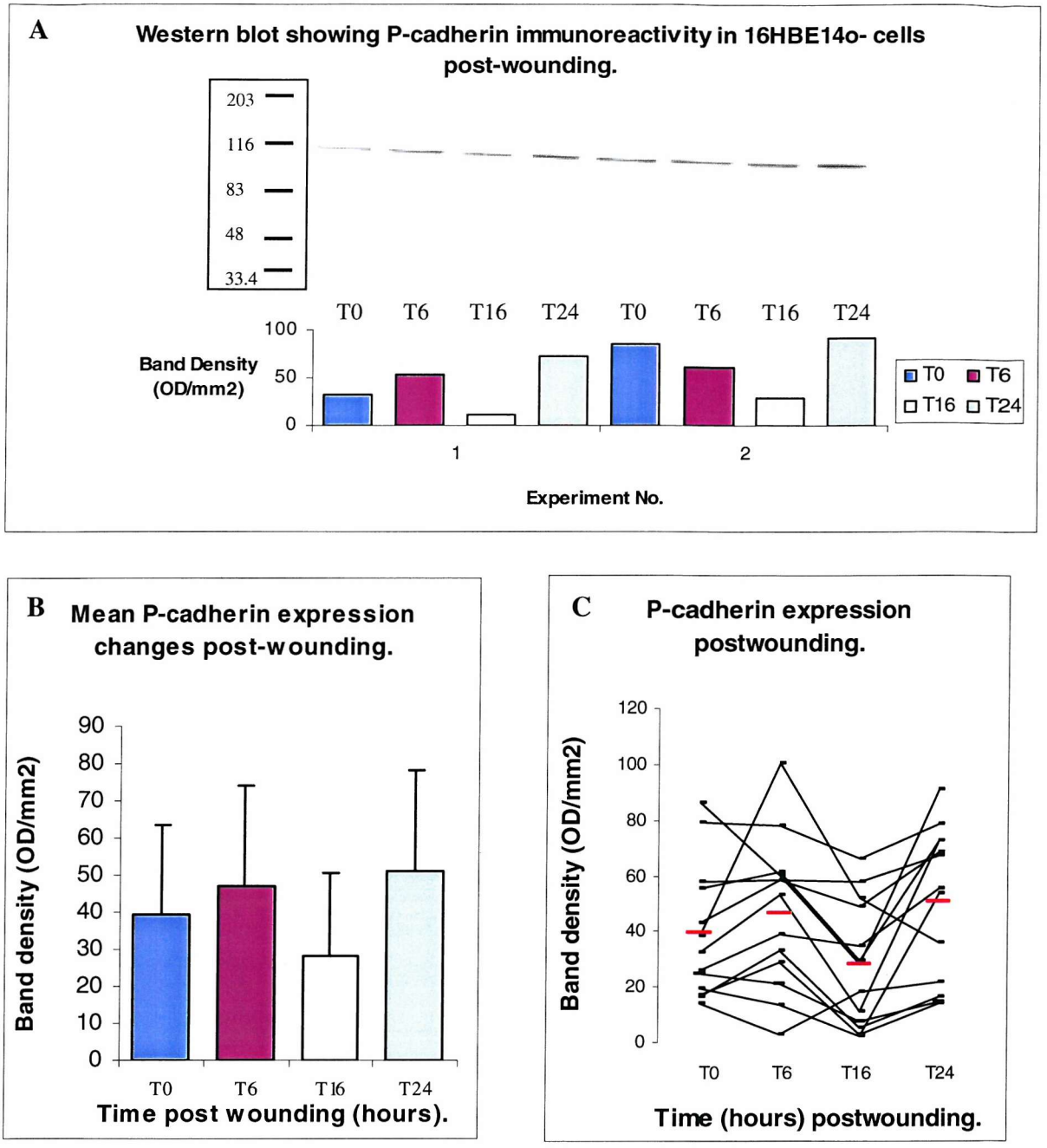

Fig 4.18 P-cadherin expression post-wounding.

16HBE14o- cells were plated at 10^5 cells/well in 6 well plates. SDS extracts were taken at T0, T6, T16 and T24 hours post-wounding. 13 sets of extracts were run on SDS-Page and western blot then probed with anti-P-cadherin antibodies (A). Immunoreactivity was seen as bands running at ~120kD. Mean real values show an increase in P-cadherin expression at T6 and a fall at T16. Highest band density was seen at T24 (B). Real values depicted as a dot plot (C) also indicates a rise in P-cadherin at T6 and drop at T16.

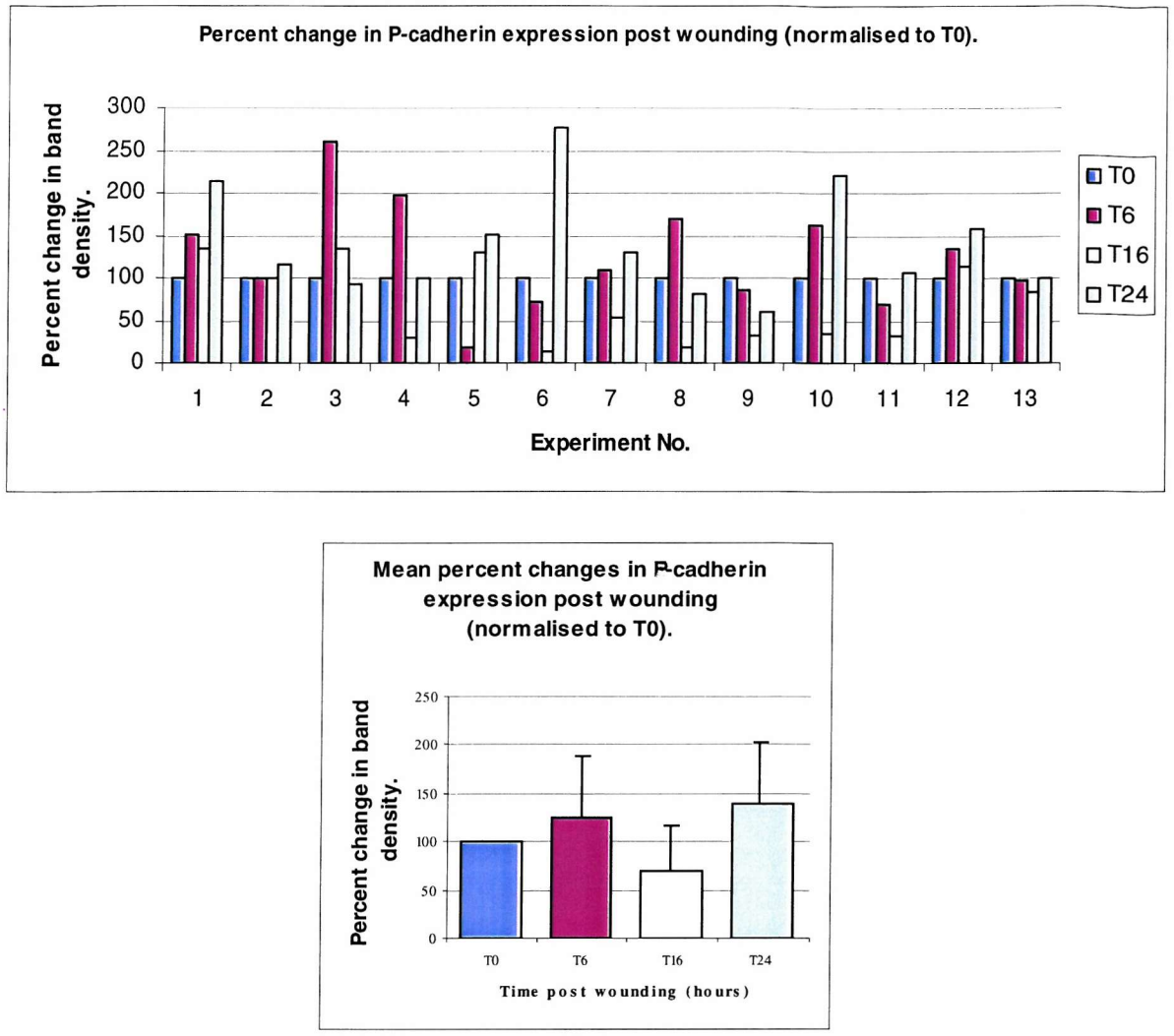

Fig 4.19 Variation in P-cadherin expression post-wounding.

Values were normalised to T0 to allow comparison of changes in band density regardless of blot exposure time(A). In all but 1 case (5), P-cadherin band density decreases from T6 to T6 and in almost all cases this value rises once again at T24. Half of the experiments have an increase in P-cadherin at T6 but in all cases T24 is similar if not higher than the original T0 value.

Mean normalised values (B) show similar standard deviations for each time-point.

4.2.2.3.3 Inhibition of protein synthesis in epithelial repair.

16HBE14o- cells were incubated with the protein synthesis inhibitor cyclohexamide (0.1M) for 30mins prior to wounding, to determine whether changes in cell adhesion molecule expression where due to an increased/decreased level of protein synthesis or a result of a greater level of molecule availability for or affinity for immunoreactivity.

At post-confluence, cells were mechanically wounded. A cell based ELISA for E- and P-cadherin was carried out. Baseline data obtained from this data is very inconsistent (fig 4.20). No significant difference in E-caderin expression was seen between intact and wounded epithelial sheets, neither in the presence nor the absence of cyclohexamide. However the reduced level of E-cadherin immunoreactivity in the absence of cyclohexamide indicates constitutive occurrence of E-cadherin synthesis.

In contrast the mean levels of P-cadherin expression increase in wounded epithelia both in the presence and absence of cyclohexamide., but immunoreactivity levels between the two conditions are similar, indicating that the immunoreactivity increase is not due to a greater level of P-cadherin expression.

However, in both these experiments the data is preliminary, the error bars are large and the wounding as yet inconsistent in the 96 well plates, therefore further work should be carried out before any conclusions are drawn.

4.3 Discussion.

In this chapter, a model of developing epithelial confluence was established in 16HBE14o- cells. Distinct stages of confluence were selected according to morphological and quantitative differences in cell density. These stages of confluence represent epithelial layer pre-confluence, confluence and post-confluence.

Cell adhesion molecule expression was examined at each time point by western blotting. All timepoints for a single experiment were run on a single blot and were therefore directly comparable. Because the visualisation method meant that different blots could not be directly compared (since differing lengths of photographic exposure were needed), data was normalised to the post-confluent time-point (C3), which was considered to be the most representative of the normal epithelial status *in* vivo and was the least variable. This allows a comparison of the relative expression difference at different confluence stages in different experiments. This model was used to determine 'trends' in expression of cell adhesion molecules.

E-cadherin immunoreactivity increased from pre- to post-confluence, although immunoreactivity did not rise with increased confluence in all cultures. Epithelial layers at early stages of confluence (C2), had both increased and decreased immunoreactivity from that seen at initial plating. This may be due to fluctuating E-cadherin levels throughout development of confluence or due to variation in cellular growth rates which may result in different cultures being at different growth stages at the designated 'confluent' extraction time-point. The seemingly equal likelihood of an increase or decrease in immunoreactivity at confluence suggests a 'see-saw' adjustment of E-cadherin expression, which ultimately results in an increased level to that seen at pre-confluence.

P-cadherin immunoreactivity was at a lower level than E-cadherin, but changes were more consistent between experiments showing a progressive decrease in P-cadherin with increasing confluence.

These apparently contrasting expression patterns between the cadherins indicate upregulation on initial response to cell contact. It has already been reported that P-cadherin seems to form less permanent cell interactions, indicated in experiments where P-cadherin is more easily extracted from MDCK cells by detergents than E-cadherin (Wu et al, 1993). P-cadherin may therefore be required to rapidly make weak initial contact with neighbouring cells in early stages of growth. This is supported by previous reports of P-cadherin's association with actively proliferating cells (Shirahama et al, 1996).

The Tight Junctional proteins occludin and ZO-1, also show a contrasting pattern of immunoreactivity. Occludin immunoreactivity increased from pre-confluence to post-confluence whereas ZO-1 immunoreactivity decreased. Given that ZO-1 binds directly to occludin it might be expected that their expression patterns would be parallel and increase with confluence due to a higher level of barrier function than at pre-confluence. However, greater ZO-1 immunoreactivity at pre-confluence indicates a surplus of ZO-1 or another role aside from it anchoring occludin to actin filaments. It may act to recruit or harbour molecules in early cell adhesion, or it may perhaps act as a signalling molecule given that ZO-1 has already been identified as a signalling molecule that can localise to the nucleus (Balda et al, 2000). Alternatively it may function in a process independent of cell adhesion.

α-, β- and γ-catenin expression were also examined briefly. In all cases immunoreactivity was highest at post-confluence, which is what might be expected given its role in cadherin adhesion. However further investigation of these molecules is required before any conclusions can be drawn from this.

Both E- and P-cadherin have been shown to be present in cadherin/catenin complexes (Johnson et al, 1993). Endogenous P-cadherin levels however, seem small compared with E-cadherin. Requirement for catenin for cadherin complexes at pre-confluence would therefore still be low compared with post-confluence despite upregulated P-cadherin levels.

Several studies have proposed a signalling role for β-catenin and possibly also γ-catenin influencing cell-cell interactions. Both have multiple binding partners other than E-cadherin and so further analysis of expression levels of this molecule in epithelial development and repair is needed to elucidate its role and the relevance of its expression levels.

An *in vitro* model of repair was established in order to assess CAM expression relating to epithelial trauma. Immediately prior to wounding, cells form a post-confluent cell layer expressing both E- and P-cadherin.

Time-points of extraction were established which had clear morphological differences reflecting stages of repair. As with the cell confluence study, immunoreactivity between experiments was not directly comparable, therefore data was normalised to the pre-wounding time-point (T0). This time-point taken before damage, is actually identical to post-confluence (C3) allowing comparison between the two studies.

E-cadherin expression was lowest at 6 hours post-wounding (>30% of immunoreactivity seen prior to wounding), but after this point E-cadherin levels increased once more toward original levels. Given that at 6 hours the cell sheet is already beginning to rearrange itself to cover the wounded area, it would appear that cell-cell E-cadherin interaction is not initially a major contributor in this process. Its dramatic reduction at such an early time-point may be indicative of the loss of many intercellular contacts in favour of a more dynamic sheet, with these contacts then reforming further into the repair process, correlating with the increased E-cadherin immunoreactivity at 16 and 24 hours.

P-cadherin expression was less consistent with no obvious trend. There was no dramatic reduction in band density as with E-cadherin, levels fluctuated over the time course but in all cases immunoreactivity was highest at 24 hours post-wounding. Given that scarring was still visible at 24 hours the cell sheet was seemingly still in a state of repair. Neither E- nor P-cadherin levels had returned to pre-wounding levels but they may be restored over a longer time.

Conclusion.

Taking together my work and that in the literature, P and E-cadherin both appear to play vital but separate roles in the establishment and maintenance of the bronchial epithelial barrier. The relationship between expression levels of these molecules may be crucial to these processes.

In a developing epithelium P-cadherin seemingly has an initial major cell adhesive role then is down-regulated at confluence. However E-cadherin appears to be up-regulated in later confluence stages.

P-cadherin possibly functions to create 'dynamic' early interactions necessary to allow migration, proliferation and epithelial reorganisation. When this is complete E-cadherin may be up-regulated and function to establish the permanent more rigid intercellular interactions required for epithelial differentiation and barrier function.

In a repairing phenotype, cells again need to be able to migrate, undergo re-organisation and change shape rapidly, this time to close the wounded area. The apparent lesser role of E-cadherin at pre-confluence is also seen in repair as rapid down-regulation of E-cadherin at just 6 hours post-wounding, then up-regulation when contacts are restored. P-cadherin in repairing cells does not experience the same down-regulation as E-cadherin, in some cases it is upregulated although it does not show the consistent expression patterns of developing cells.

Other molecular changes on wounding have been reported in other studies. White and colleagues (2001) examined the function of dystroglycan (DG) in modulating wound repair over the laminin matrix. DG forms part of a complex which anchors the sarcolemma over skeletal muscle to laminin. White showed that DG was not expressed in epithelial cells immediately after damage but was localised to the cell membrane of these cells within 12 hours of injury. This was found for both embyonic and adult lung although the function of this molecule in these tissues is not clear.

Wallis et al (2000), reported a rapid change in the adhesive state of desmosomes upon epithelial wounding. Mechanical wounding of the cell sheet resulted in a switch from calcium independent desmosomal adhesion to calcium independent desmosomal adhesion within 1 hour. Further, this switch was rapidly

propagated throughout the cell layer so that cells >100μm from the wound edge displayed calcium dependent desmosomal adhesion.

Wallis and co-workers also demonstrated that αPKC is involved in the signalling pathway that results in this altered adhesion. TPA, an activator of PKC, caused the calcium dependency switch within 15 minutes. This involvement of PKC suggests changes in protein phosphorylation may be essential for the modulation process. Wallis suggests that calcium dependent desmosomes may be more readily broken and reassembled than calcium independent desmosomes, therefore the dependency switch may be a means of facilitating re-epithelialisation.

An altered epithelial phenotype postwounding is also what is hypothesised for the role of P-cadherin. It may be that the signals that modulate calcium-dependency in desmosomes also influence the level of adhesion at the adherens junction.

PKC has been previously implicated in relation to cell adhesion, wounding and the initiation of desmosomal junction assembly (Woods et al 1992, Dustin et al. 1989 and Balda et al. 1991). Given this molecule is thought to play such an active role in optimising wound repair it is a good candidate for involvement in the signalling for cadherin switching observed following epithelial wounding.

While the results from these studies help speculation about the function of E- and P-cadherin in epithelial confluence and repair, further functional studies required the ability to manipulate cadherin levels experimentally. This was the approach taken in the next chapter.

Chapter Five

Examination of Cadherin Function by Manipulation of Cadherin Levels in Bronchial Epithelial Cells.

5 Examination of Cadherin Function by Manipulation of Cadherin Levels in Bronchial Epithelial Cells.

5.1 Introduction.

Cadherin function is required for calcium-dependent intercellular junction organisation and stratification of human keratinocytes *in vitro*. The formation of adherens junctions and desmosomes is inhibited in the presence of a combination of anti-E-cadherin and anti-P-cadherin antibodies (Lewis et al. 1994, Gumbiner et al. 1988 and Wheelock et al. 1992). This indicates a significant involvement for the cadherins in the maintenance of epithelial architecture, cadherins are also probably involved in epithelial wound repair where the intercellular contacts are thought to be more dynamic.

E- and P-cadherin are co-expressed in the development of many epithelia. Several studies have investigated the role of the cadherins in keratinocytes. P-cadherin is reported to be the predominant cadherin expressed in the basal layer of the epidermis, whereas E-cadherin is the major cadherin when the cells have divided and moved into the upper layers (Hirai et al 1989a, Wheelock et al. 1992, Lewis et al, 1994). Fully stratified epithelium is not attainable in the absence of E-cadherin although either E- or P-cadherin is sufficient for the early stages and initiation of this process (Wheelock 1992).

In mouse lip skin, Hirai et al (1989a) found that inhibition of P-cadherin resulted in stronger alteration of skin morphogenesis than similar inhibition of E-cadherin suggesting that P-cadherin plays a substantial role here with regards to the organisation of basal keratinocytes and development of hair follicles. Generally E-

cadherin was expressed at a lower level in the proliferating cell layers than in the non-proliferating layers.

The loss of P-cadherin from the upper layers of the epidermis seems to be a *response to* rather than a *signal for* detachment from the basement membrane and further differentiation as it is still expressed in the early stages of stratification (Wheelock1992).

In mouse mammary gland, E- and P-cadherin expression does not overlap. Instead discrete layers of cadherin expression are formed (Daniel et al 1995.). This study found highly localised disruptive effects on E- or P-cadherin blocking and concluded that the spatially selective expression of these cadherins is essential for mammary tissue integrity.

It is not known if the contrasting expression levels and functions of E- and P-cadherin in the bronchial epithelium are co-dependent.

Hirai et al (1989b) looked at E- and P-cadherin expression in mouse lung morphology (in parallel with the mouse lip skin study discussed above). This study found that in contrast with the epidermis data, in lung epithelia, E-cadherin mediated morphological effects dominate. This data was collected using the E- and P-cadherin blocking antibodies ECCD-1 and PCD-1. Interestingly a synergistic effect was reported in combined application of these antibodies. This would indicate a reciprocal substitution role of these cadherins and therefore potentially similar functions.

E-cadherin is the predominant adhesion molecule involved in the anchoring intermediate junction, upregulation may produce stronger intercellular attachments and increase barrier function. P-cadherin on the other hand may in many cases complement E-cadherin function or may have an unrelated role.

This chapter aims to establish whether E- and P-cadherin expression is co-incident or co-dependant, and to characterise changes that accompany different levels of E-cadherin expression and the significance of elevated or reduced levels. In the previous chapter there were variations seen in cadherin expression corresponding to

different stages of epithelial confluence and repair. This investigation endeavours to recreate those cell changes by manipulating cadherin expression in order to assess the consequences relating to cell function.

After initial characterisation, the E-cadherin transfected clones were planned to be used to examine the influence of E-cadherin expression elevation and reduction on P-cadherin levels, and epithelial barrier function.

There is still much unknown about P-cadherin, its role in the bronchial epithelium and its actions in repair are yet to be elucidated. Localisation (Hirano et al 198, Johnson et al 1993) and blocking studies (Hirai et al 1989) have led to assumptions of an adhesive role similar to that of E-cadherin. Both molecules have also been shown to have a cellular presence in the form of a cadherin/catenin complex (Johnson et al. 1993).

To complement the E-cadherin clones, work was carried out to establish a set of P-cadherin transfected clones with which to examine the consequences of P-cadherin manipulation. Full length mouse P-cadherin was transfected into 16HBE14o- cells, in order to construct a set of clones directly comparable with the E-cadherin clones.

These transfected cells would be potent tools to study epithelial cell development and repair processes.

5.2 Results.

5.2.1 Production of E-Cadherin Transfected Bronchial Epithelial Cell Clones.

5.2.1.1 Previous History of Clones.

A range of 16HBE 14o- clones produced by Dr. Mike West and Dr. Steve Evans (GlaxoSmithKline) in a previous study were used to investigate the relevance of expression levels in epithelial growth and repair. A total of 30 clones were available, consisting of 14 clones transfected with a full length sense E-cadherin sequence (kindly provided by Dr. Karl Becker) and 15 transfected with a full-length antisense E-cadherin sequence. The sense clones were intended to over-express E-Cadherin and the antisense clones were intended to under-express E-Cadherin. The parent clone was also used, which was the cell line used for transfection.

At the time of cloning (by Dr. Mike West), a doxacyclin sensitive vector was also transfected into the clones with the intention of creating an on/off switch for E-cadherin expression.

Originally Dr. Steve Evans received X65332 vector containing the human E-cadherin gene. The fragment was excised from this and inserted into the final vector. This system was a two plasmid set-up, one of which was a commercial Doxacyclin regulated plasmid that functions to switch off the expression of the final sense/antisense plasmids in the presence of doxacyclin (figure 5.1).

After successful transfection, each clone was stored frozen as aliquots. No previous characterisation or experimentation had been performed on these cells.
Sense clones were numbered 1 to 15 and suffixed by '+' and culture passage number e.g. clone 6.5+ is the 6^{th} sense clone at passage 5. Antisense clones were numbered 1

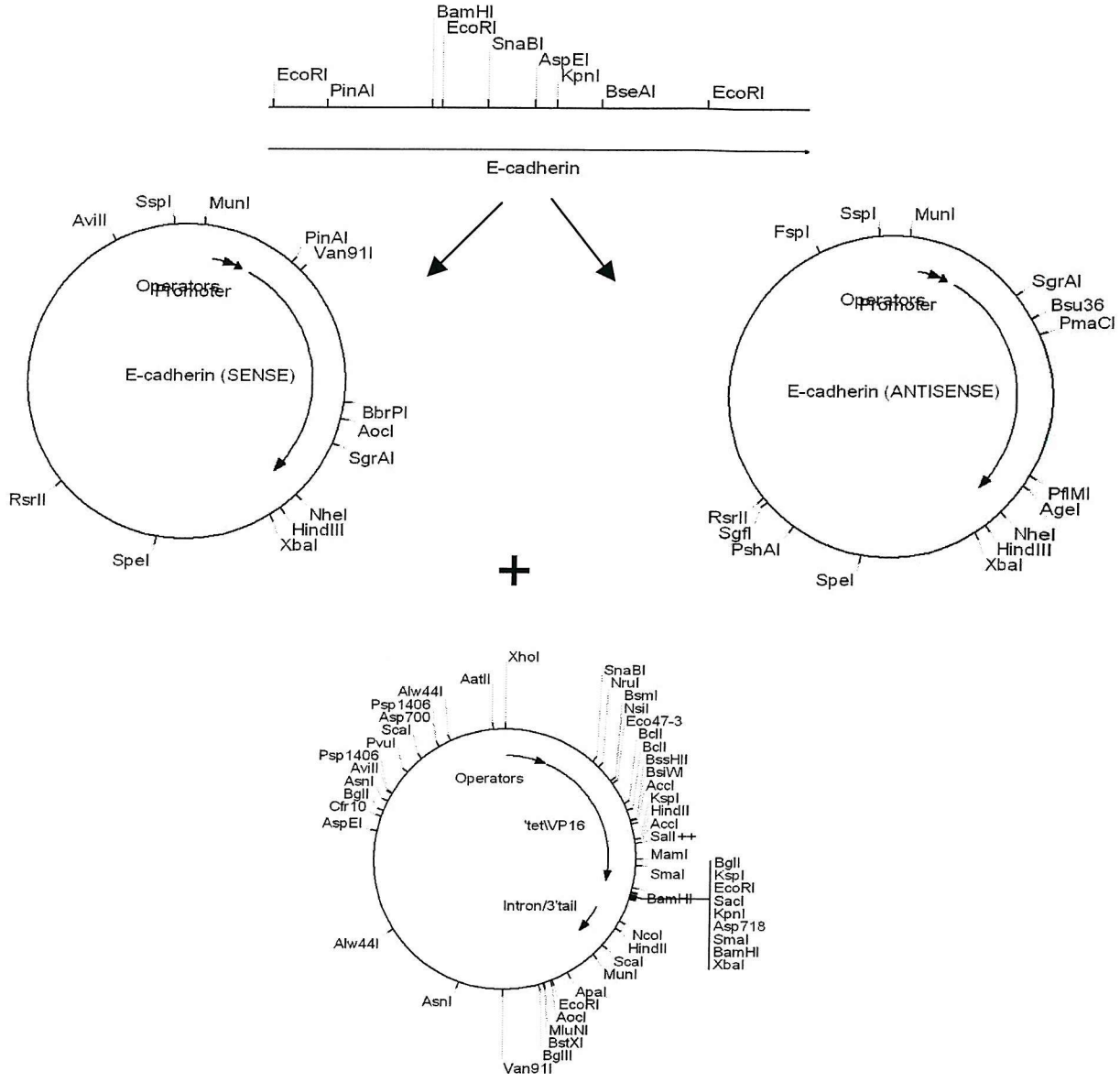

Figure 5.1 Plasmid maps of E-cadherin clones.

The full length sense and antisense E-cadherin genes were inserted into the expression vector for transfection into 16HBE14o- cells.
A second vector, a commercial doxacyclin regulated plasmid 'tet\VP16, was co-transfected with the aim of creating an on/off switch for E-cadherin expression.

to 20 and suffixed by '-' and culture passages number e.g. clone 4.6- refers to the 4th antisense clone at passage 6. The parent clone contained the doxacyclin sensitive transactivator plasmid and was named 'vp 21'. For simplicity in this study I will refer to this clone as clone 0. Clone numbers 6-, 9-, 11-, 16-, 19- and 12+ were omitted from the clone set at this stage.

5.2.1.2 Characterisation of Clones.

Individual clones were grown in the presence or absence of doxacyclin (0.1μg/ml) in order to test E-cadherin regulation. The usual FCS media supplementation was substituted by FCS (Clonetics) guaranteed to be low in tetracycline. Each clone was plated out from a frozen cell suspensions (all at passage 5) of equal cell numbers. However, variation was seen in both the recovery rate from frozen and the rate of growth between the cultures (figure 5.2).

All clones followed an epithelial like growth pattern as described in chapter 4, however, the clones varied in the speed that they formed colonies and confluent cell sheets (figure 5.2). Clones 10-, 8-, 20-, 8+ and 15+ for example all required passaging at 8 days or less, whereas clones 1-, 18-, 2+ and 9+ took over 20 days to reach the same cell density. There was also variation in recovery on thawing with some clones e.g. clone 18- having just ~20% viability and others as much as 60% e.g. clone 14-.

All of the clones had general cell morphology similar to that seen in 16HBE14o- cells with rounded adherent cells that formed discrete colonies which eventually merged to create a confluent cobblestone-like cell sheet.

	Clone	Viability on Thawing	Day of First Harvest	Growth Rate
E-Cadherin Antisense Clones (-).	1	50%	20	Low
	2	40%	18	low
	3	40%	14	Medium
	4	60%	14	Medium
	5	50%	18	Low
	6	-	-	-
	7	30%	16	Medium
	8	50%	12	Medium
	9	-	-	-
	10	60%	6	High
	11	-	-	-
	12	60%	8	High
	13	50%	16	Medium
	14	60%	16	Medium
	15	40%	12	Medium
	16	-	-	-
	17	30%	16	Medium
	18	20%	20	Low
	19	-	-	-
	20	60%	8	High

	Clone	Viability on Thawing	Day of First Harvest	Growth Rate
E-Cadherin Sense Clones (+).	1	40%	16	Medium
	2	30%	22	Low
	3	30%	14	Medium
	4	50%	14	Medium
	5	30%	10	Medium
	6	20%	18	Low
	7	50%	14	Medium
	8	50%	6	High
	9	30%	22	Low
	10	60%	14	Medium
	11	40%	16	Medium
	12	-	-	-
	13	40%	14	Medium
	14	30%	10	Medium
	15	50%	6	High

Fig 5.2 E-Cadherin Expressing Bronchial Epithelial Cell Clones.

Variation was seen in the recovery from frozen viability) and the rate of growth between cultures. Many of the slower growing clones e.g. clones 18- and 6+ had low recovery on thawing and therefore the reduced growth rate might be the consequence of a lag phase. The fastest growing clones were 8+ and 10+ and the slowest were 9+ and 2+.

5.2.2 Selection of clones for use in further studies.

5.2.2.1 Transepithelial Electrical Resistance (TER).

TERs were measured every 24 hours starting from day 1 on cells grown on membranes (see section 2.1.1.2) and monitored to a point where resistance levels had peaked and settled to a relatively constant level, (different in each case but all clones were followed for a minimum of 25 days). Each clone had a unique resistance profile although they all followed approximately the same development pattern as untransfected 16HBE140- cells (section 4.2.1.1). A lag phase of low resistance (100-400 Ωcm^2) is seen for 2-4 days post plating before resistances increased to a peak level then remained there for a few days before dropping off again.

Although clone resistance profiles all followed the same basic pattern, several of the clones did not develop resistance levels seen at peaks of the 16HBE14o- cell profile. Figure 5.3A shows clone 2.5- as an example, this clone has an initial resistance of 100-200 Ωcm^2 which increases to levels around the 500 Ωcm^2 mark, this level is maintained but not improved upon for the rest of the experiment.

Three of the clones (6+, 7+ and 10+) developed resistances much higher than those seen in 16HBE14o- cells. Clone 7.5+ (figure 5.3B) reached levels of 6000 Ωcm^2 at times, however, the resistance profile of this clone was increasingly erratic with time, some days having a 1500 Ωcm^2 increase followed the next day by a similar decrease.

Other resistance profiles such as clone 5.5- (figure 5.3C) followed a similar trend to the 16HBE14o- cells in that the resistance steadily increased to a peak then tapered off again, however, further peaks were then reached giving a very different overall profile.

Variations between readings for a particular clone on a particular day are shown by standard deviation. In most cases the degree of variation on a particular day was low with tight standard deviations. Clone 7.5+ (see figure 5.3B) with its fluctuating resistance profile has predominantly low variation for a given set of

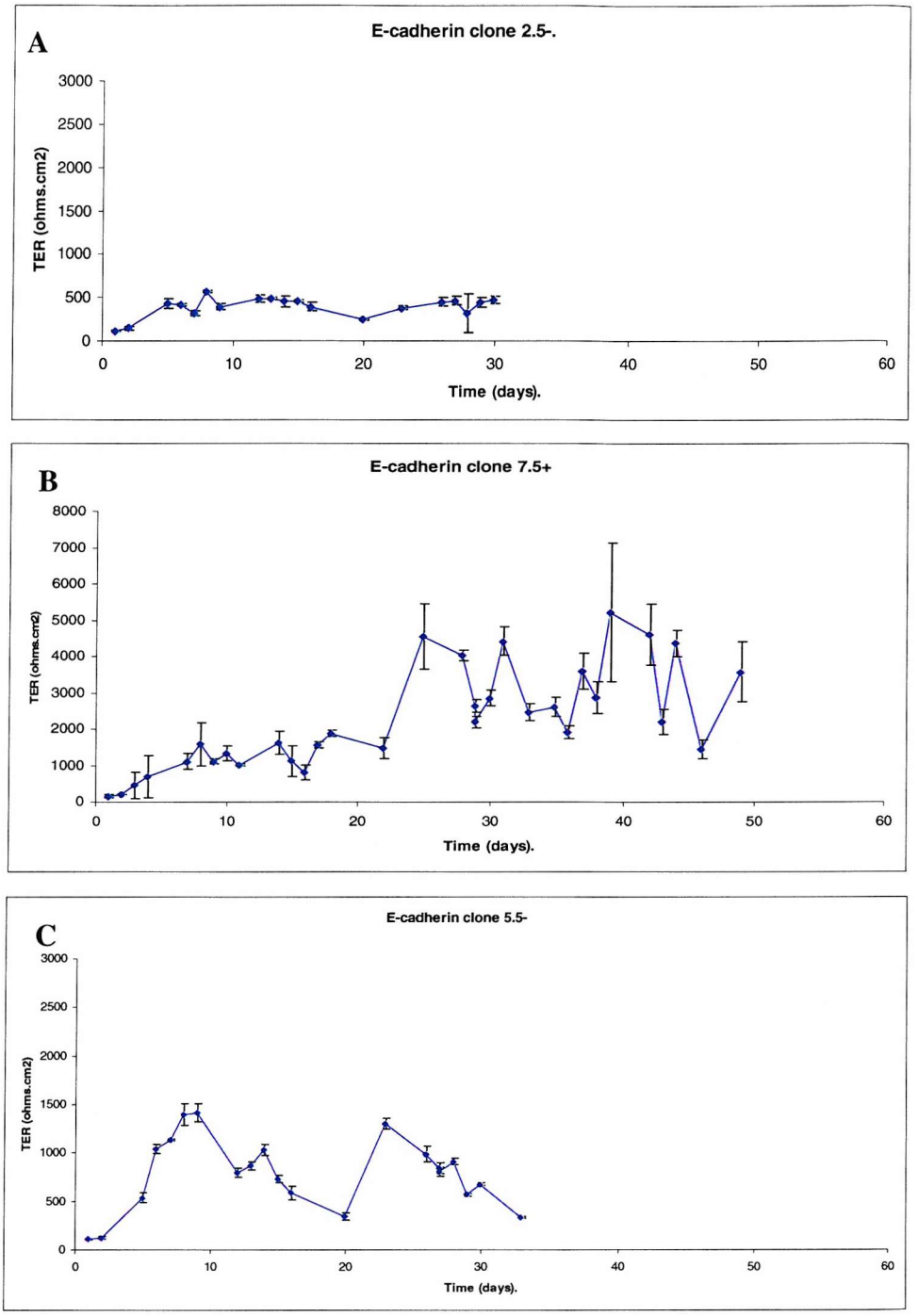

Figure 5.3 Variation in Resistance Profiles Between Clones.

Variation in resistance pattern was seen between the 30 clones. Some clones remained below 500Ωcm^2 (A clone 2-)and others reached levels beyond 5000Ωcm^2 (B clone 7+). Some clones maintained consistent resistance levels over the duration of the experiment whereas others formed peaks (C clone 5-). Other clones showed an erratic seemingly random profile of resistance (B clone 7+).

readings. However, there were instances of greater variation in this clone for example day 40 with a standard deviation that is almost 40% of the mean resistance reading indicating variation between different replicates.

5.2.2.2 Cadherin ELISA.

All of the original 30 clones were assayed by cell-based ELISA for E-Cadherin immunoreactivity levels (see section 2.2.2.1). In order to quantify the cadherin data, a crystal violet assay for total protein levels was also carried out giving a measure of E-cadherin levels expressed relative to total protein concentration.

Initially there were problems achieving uniform cell plating densities between wells, but preliminary results gave an indication of E-cadherin levels (figures 5.4 and 5.5).

These results show the sense clones to have on average a higher level of E-cadherin immunoreactivity than the antisense clones. Clones 4+, 5+, 6+, 7+, 8+, 9+ and 14+ in particular had higher levels (5-17 OD units/μg total protein) and the remaining sense clones had levels similar to those antisense clones with the highest levels (~5 OD units/μg total protein). Several antisense clones (2-, 4-, 10- and 17-) had particularly low E-cadherin immunoreactivity levels (<4 OD units/μg total protein).

For each clone, the E-cadherin ELISA was also carried out on cells grown in the presence of doxacyclin in order to test potential doxacyclin regulation. Several clones had E-cadherin expression standard deviations that did not overlap for cells grown in the presence and absence of doxacyclin (for example clones 2+, 6+ and 8+ figure 5.4). Many of the clones (in particular the antisense clones, figure 5.5) however, had similar E-cadherin expression values with and without doxacyclin.

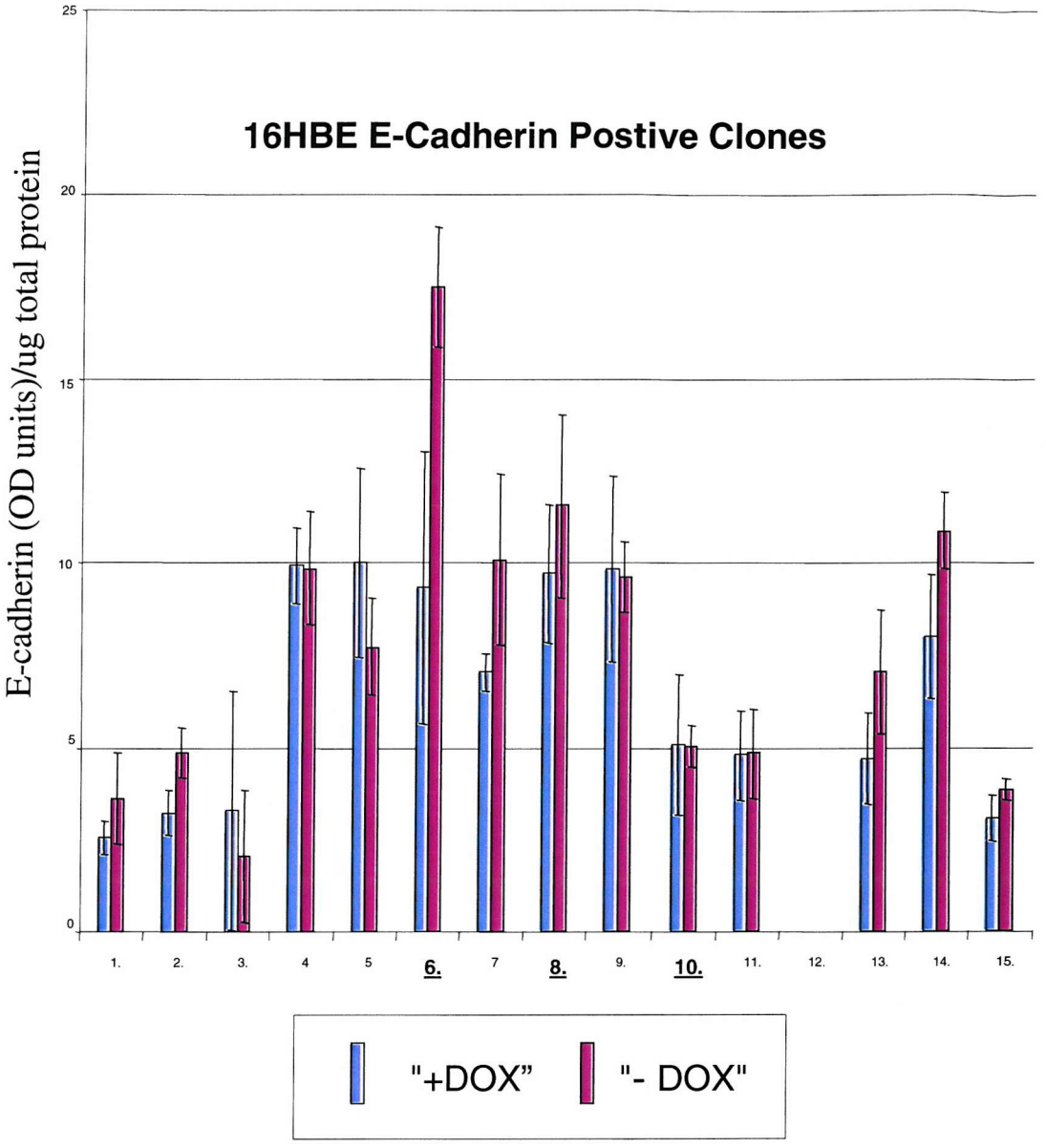

Fig 5.4 E-Cadherin ELISA of Positive E-Cadherin Expressing 16HBE 14o- Clones.

Cells with the 'sense' version of the E-Cadherin gene. Bars refer to individual clones each of which was grown in the presence and absence of 0.1µg/ml doxacyclin. Error Bars refer to standard deviation. Clone 12+ wasn't included in this study.

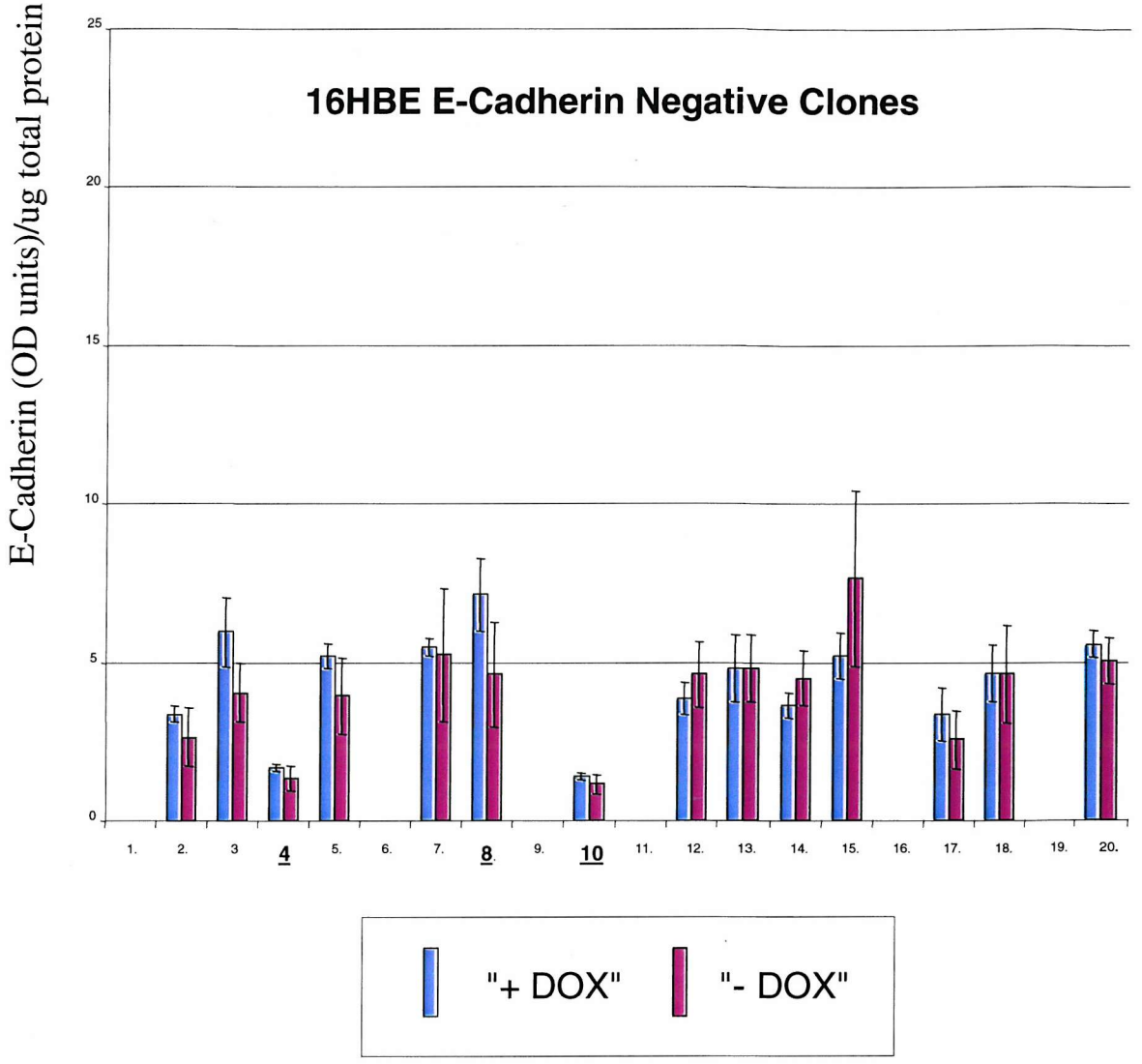

Figure 5.5 E-Cadherin ELISA of Negative E-Cadherin Expressing 16HBE 14o- Clones.

Cells with the 'anti-sense' version of the E-cadherin gene. Bars refer to individual clones, each of which were grown in the presence and absence of 0.1 μg/ml doxacyclin. Error bars refer to standard deviation. Clones 1-, 6-, 9-, 11-, 16- and 19- were not included in this study.

5.2.2.3 Selection of Clones for Further Study.

The TER analysis and ELISA results were used to select a series of clones for further characterisation. Clones were omitted from the selection procedure if they had an erratic TER profile (clones 12-, 3+, 7+ and 12+).

In order to look at the relevance of the level of E-cadherin expression, a range of expression levels was required.

Expression levels in the absence of doxacyclin were examined from which clones 6+ and 8+ were chosen as two particularly highly expressing clones (17.3 and 11.8 OD units/μg total protein) and clone 4- and 10- as two particularly low expressing clones (1.8 and 1.1 OD units/μg total protein). Two average expression clones were also selected, one sense 'clone 10+' (5.2 OD units/μg total protein), and one anti-sense 'clone 8-' (4.7 OD units/μg total protein).

An additional selection factor for these clones was that all of these had data that preliminarily indicated doxacyclin regulation, i.e. the selected positive clone cells had a lower level of E-cadherin OD units/μg total protein when grown in the presence of doxacyclin and vice versa for the negative clones.

5.2.3 Further Characterisation of selected clones.

5.2.3.1 Morphology of Selected Clones.

All selected clones displayed predominantly an epithelial-like morphology as seen in 16HBE14o- cells (figure 5.7) in that cells form discrete colonies with a 'cobblestone' appearance. Cells were adherent both to each other and the underlying surface and eventually formed a continuous cell sheet. However, the cell sheet

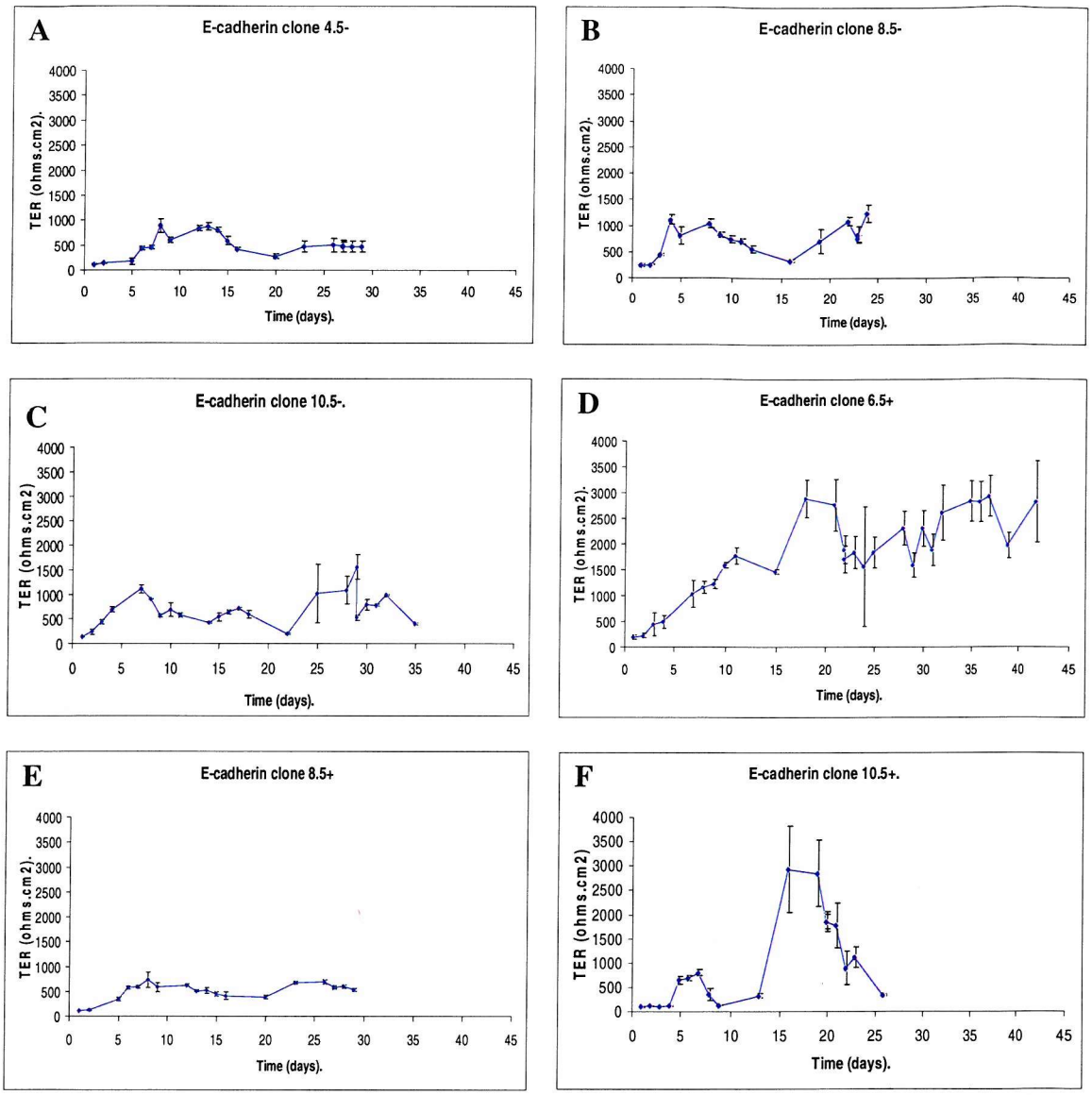

Fig 5.6 Transepithelial Electrical Resistance (TER) Profiles of selected clones.

Each selected clone has a relatively stable TER profile. Clone 6.5+ and 10.5+ have the highest resistance levels (reaching levels >3000), whereas the other selected clones have TER levels <1500Ωcm^2.

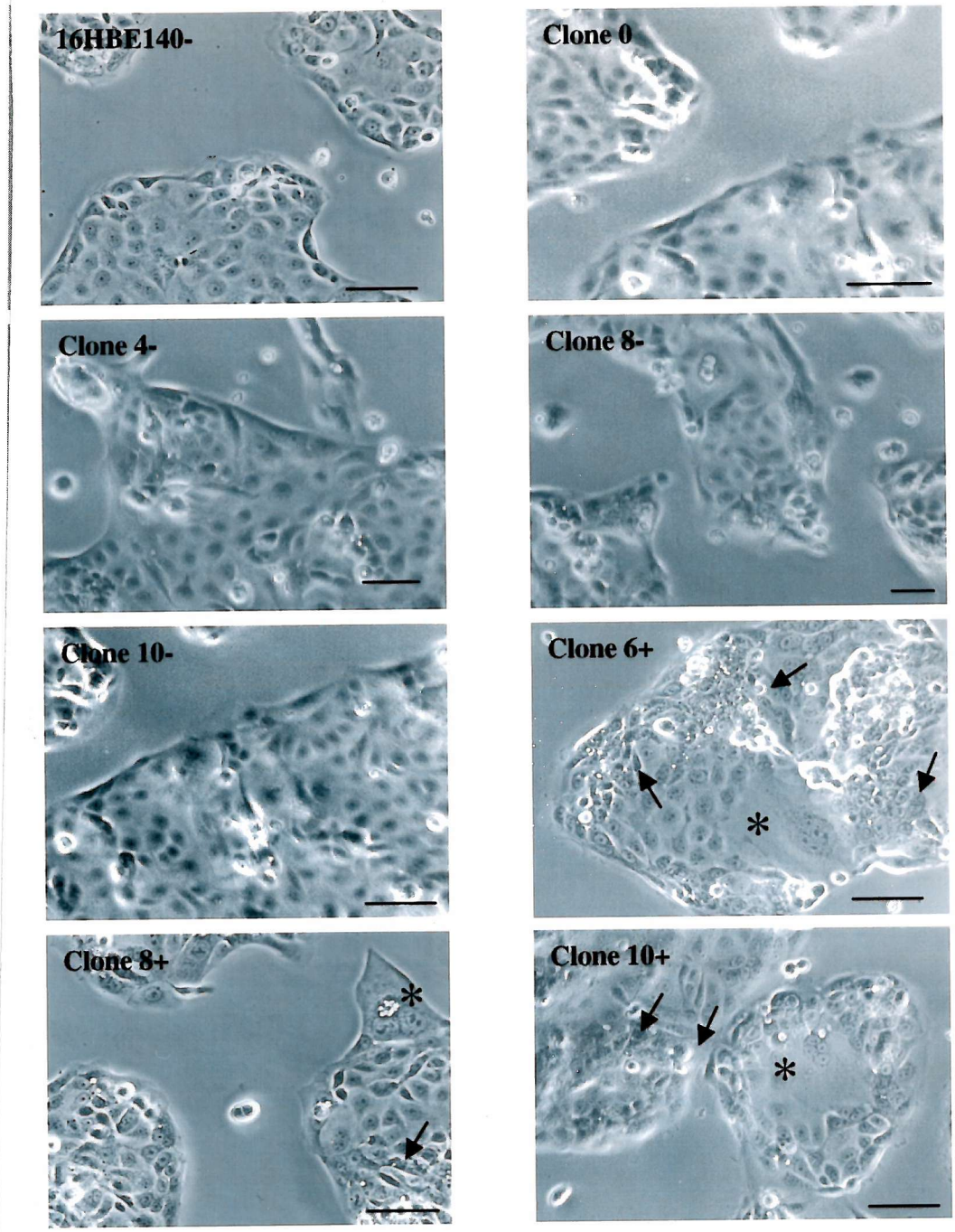

Figure 5.7 Morphology of Selected Clones.

All clones had a predominantly epithelial-like morphology as seen in 16HBE14o- cells. Clone 0,4-, 8- and 10- displayed uniform flat cell sheets whereas the sense clones, I.e. 6+, 8+ and 10+ displayed areas of raised ridges (see arrows) and 'giant' cells (see '*'). Scale bars represent 100μm.

seemed less flat in the clones than in untransfected 16HBE14o- cells making it more difficult to focus on the cell sheet as a whole.

Clone 0 had a similar morphology to 16HBE14o- cells as did the antisense clones 4-, 8- and 10-. The sense clones on the other hand displayed marked differences from the uniform cell arrangements of the 16HBE14o- cells. Predominantly the morphology was the same, with the majority of the cells (figure 5.7) displaying a rounded appearance of uniform shape and size. Other cells however formed raised 'ridges' of cells (see arrows). Ridges such as these were seen within the untransfected 16HBE14o- cell layer at post confluence when the cells were at high density (section 4.2.1.2), but never at pre-confluence as is the case here.

Most interestingly however, there were occasional cells within the layer with enlarged or perhaps more flattened cytoplasmic regions (see arrows). In some areas several of such cells seemed to have merged at the nucleus and then appeared as an 'island' from the other cells due to the surrounding cytoplasm (see '*', figure 5.7 clone 6+), breaking up the usual uniformity of the epithelial cell sheet. These areas appeared at sub-confluence and remained through cell confluence and beyond. This effect was seen most frequently in clone 6+ but also occasionally in clone 10+. Clone 8+ formed ridges of cells but predominantly displayed a normal 16HBE14o- like morphology.

5.2.3.2 TER and Permeability Analysis.

TER analysis was repeated for each of the selected clones (all at passage 13), in parallel with the clone 0 (passage 21) and untransfected 16HBE14o- cells (passage 15).

This time in each case 6 wells were examined, 3 of which had media supplemented with 0.1μg/ml doxacyclin.

TER was measured for a minimum of 15 days. Resistances were similar to those seen in the original experiment with the exception of clone 10-. The others reach similar peaks as in the original experiment over the same time frame. Clone 10-

however did not reach a 1500Ωcm^2 peak as before, this time its resistance was lower at <500Ωcm^2.

Clone 0, monitored here as a control, was not investigated in the original TER experiments. In this experiment this clone had a similar resistance profile to the 16HBE140- cells (section 4.2.1.1). Overall the sense clones had resistances reaching higher levels (>2000 Ωcm^2 in clone 6+ and 10+) than those seen in 16HBE14o- cells and clone 0 (~1000 Ωcm^2), whereas the antisense clones in contrast have resistances that peak at lower levels (~500 Ωcm^2).

Resistance profiles between the doxacyclin negative and positive wells were similar for all clones, even in the case of clones 6+ and 10+ where high resistances were reached and a less consistent profile is seen (figure 5.8).

Permeability assays were carried out on each of these wells at day 10. Permeability was assessed by the volume (ρmol/hr) of FITC dextran (4.4kD) that crosses the epithelial barrier. Highest permeability was seen in clone 0 and 16HBE14o- cells, both of which had permeabilities of approximately 200pmol/h (figure 5.9). Both sense and antisense clones had less than half this level of permeability. Clones 4-, 8-, 10- and 10+ had permeability readings of 60-80 pmol/h whereas clone 6+ was ~ 25pmol/hr, displaying approximately an eighth of the permeability seen in the control clone 0.

Each clone was also assayed for permeability in the presence of doxacyclin (continuing from TER experiments). Similar permeabilities were seen to those in the absence of doxacyclin for each clone.

5.2.3.3 Cadherin analysis of selected clones.

E- and P-cadherin immunoreactivity analysis was carried out on all 6 selected clones alongside the parent clone and untransfected 16HBE14o- cells (both in the presence and absence of doxacyclin). As in the selection process (section 5.2.1.2) E-

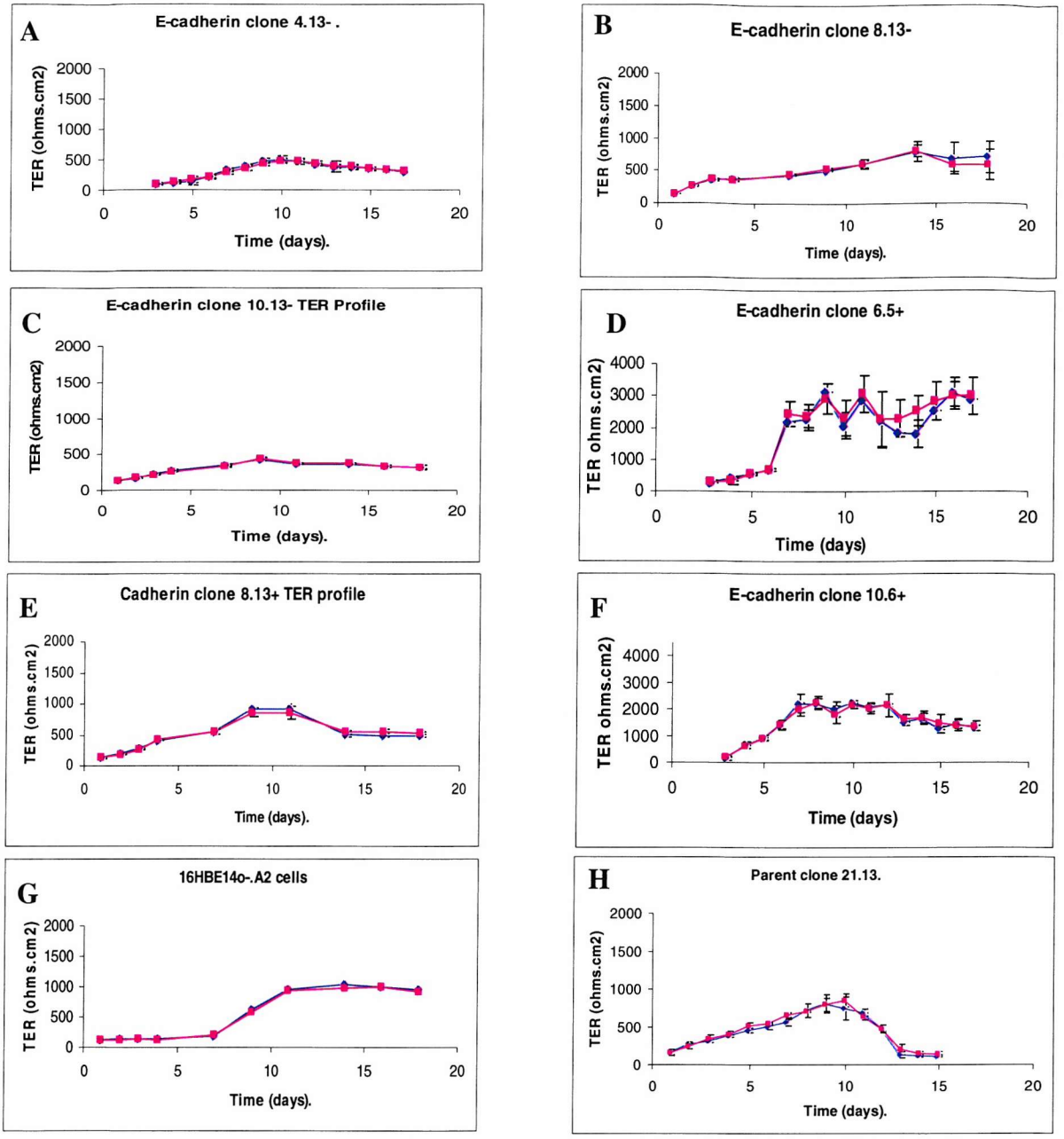

Fig 5.8 Doxacyclin Effect on TER in Selected Clones.

Clones were grown both in the presence and absence of doxacyclin supplemented media. TER was measured for both conditions over a period of 15 days. Individual clones resistances
consistantly displayed similar resistance profiles to those attained in the original TER charcterisation. Doxacyclin supplementation did not affect observed TER profiles.

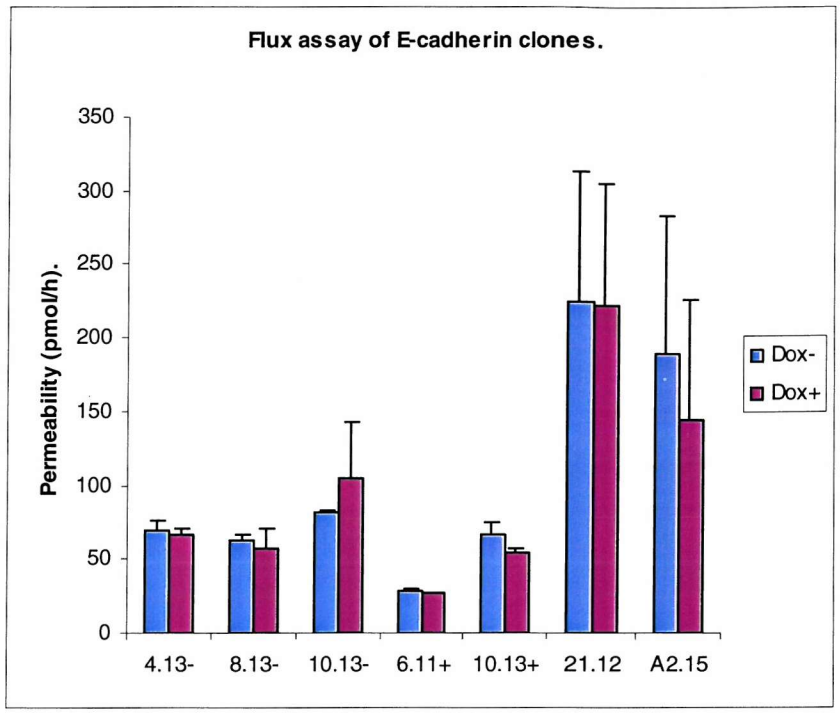

Fig 5.9 Permeability Assay.

Permeability assays were carried out on each of the selected clones (except clone 8+), alongside the parent clone (clone 0) and untransfected 16HBE14o- cells. Similar levels were seen for all clones both in the presence and absence of doxacyclin. Clone 6+ had a lower permeability whereas the parent clone and untransfected cells (A2.15) had higher permeability.

cadherin immunoreactivity levels were assessed by cell-based ELISA and then expressed relative to total protein (OD units/μg total protein). This time however, instead of the crystal violet assay for total protein, individual wells of cells were solubilised and analysed using Bio Rad protein assay kit (see section 2.1.2.1.2). A comparable P-cadherin ELISA was developed and optimised with regards to antibody dilutions and substrate incubations.

For both E- and P-cadherin, lower immunoreactivity levels (<0.04 and <0.005 OD units/μg total protein respectively) were seen in the negative clones and higher (0.04-0.12 and 0.015-0.03 OD units/μg total protein) in the positive clones.

The range of mean E-cadherin immunoreactivity was from 0.012 to 0.132 OD units/μg total protein giving an 11-fold difference (figure 5.10 A). Clone 0 and 16HBE14o- cells as the controls displayed E-cadherin immunoreactivity levels of 0.021 and 0.038 OD units/μg total protein respectively. Clone 8- had a similar expression level to clone 0 at 0.042 whereas the other antisense clones had lower E-cadherin immunoreactivity levels at 0.012 (clone 4-) and 0.017 OD units/μg total protein (clone 10-).

The range of mean P-cadherin immunoreactivity was from 0.0028 to 0.0344 OD units/μg total protein (figure 5.10 B). Here the lowest level was in clone 0 at 0.0028 OD units/μg total protein. The 16HBE140- cells had a i.r. value of 0.0108 OD units/μg total protein, which was higher than all three antisense clones.

The sense clones had E- and P-cadherin expression levels substantially above the corresponding 16HBE14o- and clone 0 levels. Highest levels were seen in clone 6+ with E-cadherin at 0.132 OD units/μg total protein and P-cadherin at 0.0344 OD units/μg total protein.

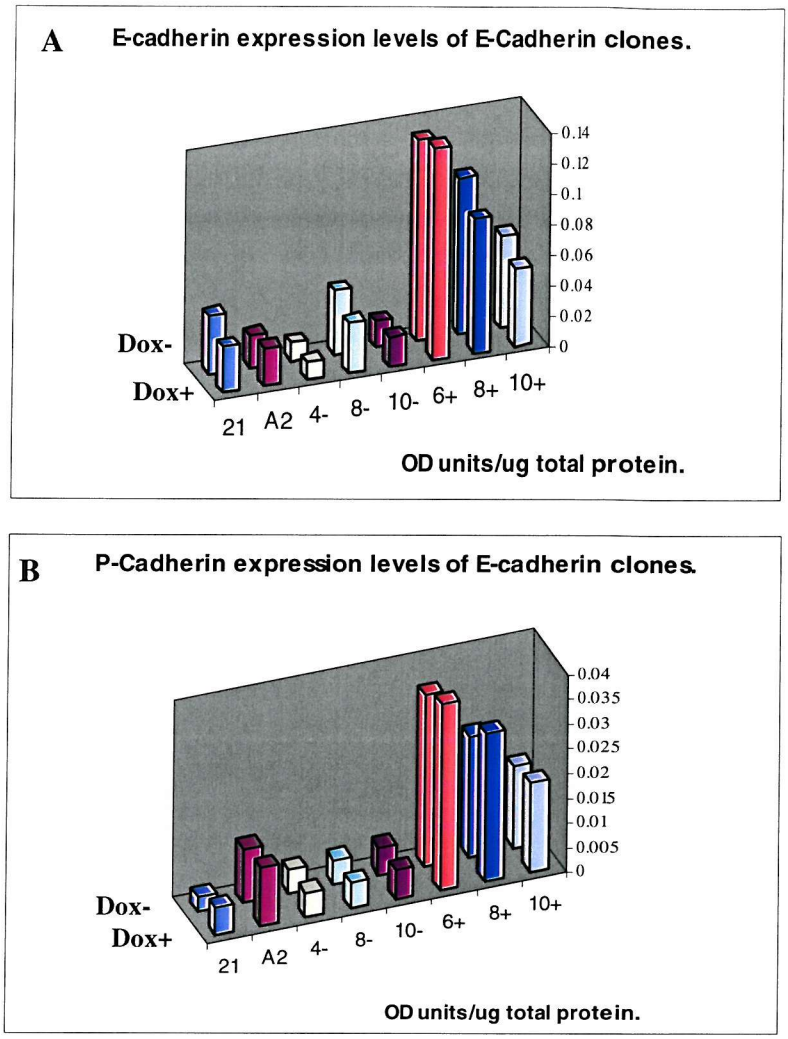

Fig. 5.10 E- and P-Cadherin Expression Levels of E-cadherin Clones.

Cell based ELISAs for both E- and P-cadherin were carried out on all 6 selected clones alongside the parent clone and untransfected 16HBE14o- cells both in the presence and absence of doxacyclin. In both cases higher cadherin levels are seen in the 3 sense clones particularly clone 6+. Lowest levels are seen in clone 0.

5.2.3.3.1 Correlations.

The correlation coefficient (R) was calculated for each comparison between E- and P-cadherin expression and then between cells grown in the presence and absence of doxacyclin.

Correlation coefficients summarise the strength of the association between two variables. A 'positive' correlation is one where both variables increase together. A 'negative' correlation is where one variable increases as the other decreases. When variables are exactly linearly related the correlation coefficient is either =+1 or –1. R=0 indicates that there is no linear relationship between the two variables. The 'R^2' value gives the proportion of the variation of one variable that can be 'explained' by the other.

In order to determine whether the observed correlation/non-correlation could have arisen by chance, p values were calculated using the student's t-distribution, values of p=<0.05 are regarded as significantly different from a value of zero.

5.2.3.3.1.1 Doxacyclin Correlation.

E-cadherin expression correlation was calculated between values in the presence and absence of doxacyclin for each clone.

As explained above, R^2 calculations give the proportion of variation attributable to variation in the other variable, therefore if doxacyclin regulation was taking place there would be a distinct difference in expression patterns in the presence of doxacyclin i.e. R^2 tending to 0.

Each clone has a positive correlation for E-cadherin immunoreactivity (IR) (figure 5.11A). Clones 8- and 8+ (figure 5.11B) have low R^2 values for E-cadherin expression at 0.192 (p=<0.03) and 0.066 (p=>0.2) respectively indicating some doxacyclin mediated regulation taking place in clone 8- only, however in other cases immunoreactivity has R^2 values tending to 1. Clones 4- and 6+ (figure 5.11C) have particularly high values at 0.64 and 0.91 respectively, (p=<0.001 in both cases),

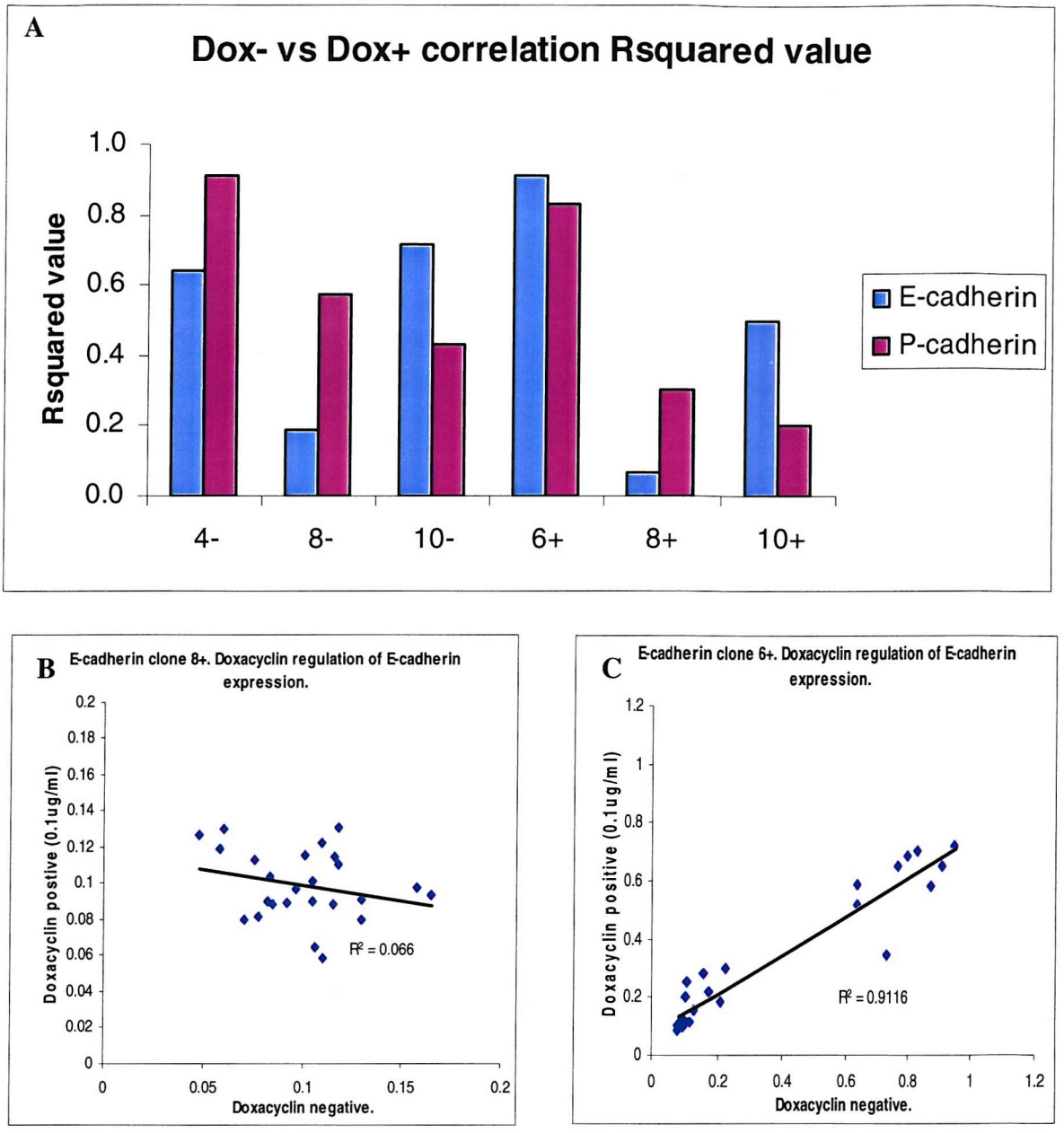

Fig 5.11 **Correlation Values (R^2) of E- and P-Cadherin Expression in Presence/Absence of Doxacyclin..**

R^2 values were calculated for Dox- versus Dox+ E- and P-cadherin expression values for each clone (see A). B and C are correlation charts for each clones 8+ and 6+ respectively.

indicating a linear relationship, i.e. the expression correlation between samples was as expected showing no influence of doxacyclin.

5.2.3.3.1.2Correlations between E- and P-Cadherin Expression.

Looking at E- and P-cadherin immunoreactivity for the entire set of clones, there is an R^2 value of 0.75 (figure 5.12) (p=<0.001). This was a positive correlation indicating that 75% of total variation of the one variable (P-cadherin immunoreactivity) was accountable by the variation of the other variable (E-cadherin immunoreactivity).

Variation within individual clones was also analysed. All 6 clones have positive correlation (figure 5.13A), although clone 8- (figure 5.13B), 8+ and 10+ have such low values they are very close to r=0 i.e. no linear relationship (p=>0.2 in all three cases). Clone 6+ (figure 5.13C) however has an R^2 value of 0.858 (p=<0.001), therefore for this clone, 86% of the variation in P-cadherin immunoreactivity is accountable by the variation in E-cadherin IR. Clones 4- and 10- have R^2 values of 0.42 and 0.37 respectively (both p=<0.001).

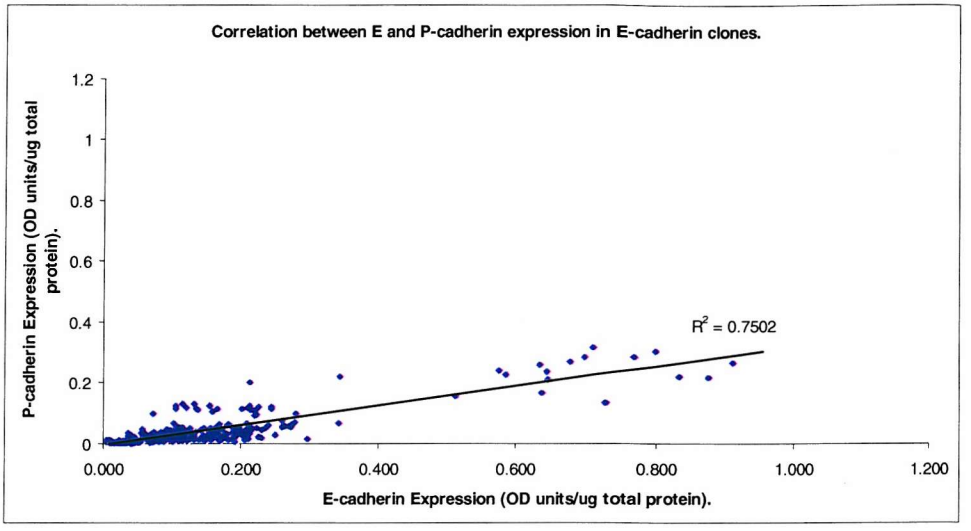

Figure 5.12 Correlation Values (R2) of E- versus P-cadherin Expression.

The R^2 value was calculated for E- and P-cadherin expression values over the entire set of clones. 75% of P-cadherin immunoreactivity was associated with that of E-cadherin.

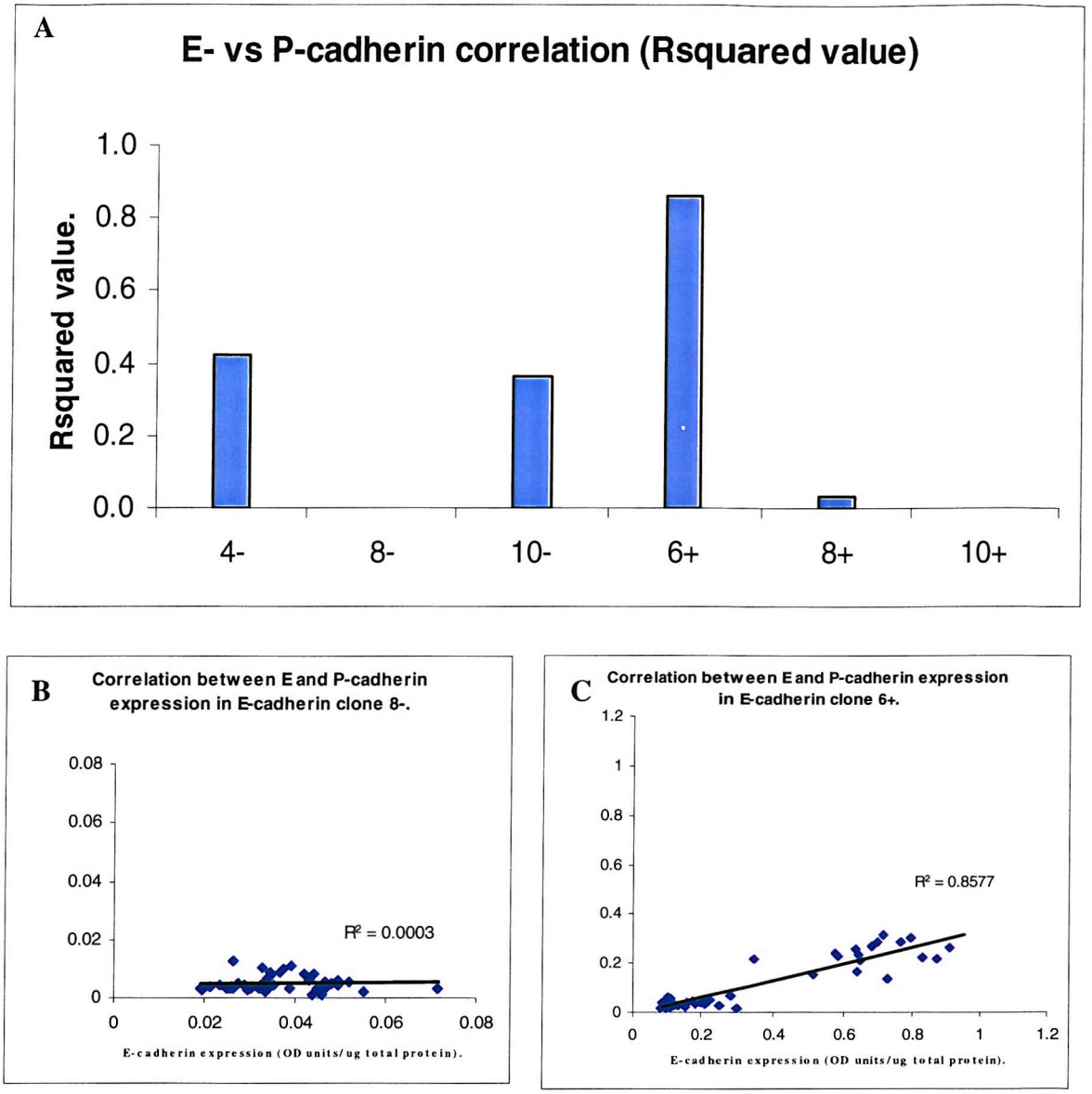

5.13 Correlation Values (R^2) of E- versus P-Cadherin Expression.

R^2 values were calculated for E- and P-cadherin expression values for each clone (see A). B and C are correlation charts for clones 8- and 6+ respectively.

5.2.4 Development of P-Cadherin Transfected Clones.

It was intended to establish a range of P-cadherin expressing 16HBE14o- clones to complement experimentation using the E-cadherin clones, and to investigate the relevance of P-cadherin expression levels in epithelial growth and repair. In order to achieve this full length mouse P-cadherin was inserted into a mammalian expression vector ready for transfection into 16HBE140- cells.

5.2.4.1 Transformation of P-Cadherin.

The P-cadherin cDNA (a kind gift from M. Tacheichi), was already cloned into pBluescript II KS^+ (fig 5.14) at the EcoR1 site within the vector's multiple cloning site (position 701bp) forming a 6138 kb plasmid.

The P-cadherin/pBluescript II KS^+ plasmid DNA was transformed into competent bacteria which were then plated and subsequently colonies selected on the basis of ampicillin resistance (section 2.1.3.2-3). DNA was purified by mini-prep (section 2.1.3.2.1) and then restriction digested with enzymes EcoR1 and Nde1 to confirm the identity of the plasmid (figure 5.15) (section 2.1.3.3). EcoR1 digestion of the plasmid produces the 3.1kb P-cadherin insert and its 2.9kb backbone. Nde1 cuts once in the P-cadherin encoding sequence alone and therefore linearises the plasmid to a 6.1kb band.

Twenty 5ml broths were grown, all of which underwent miniprep and subsequent restriction enzyme analysis to ascertain the presence of the P-cadherin/pBluescript II KS^+ plasmid. Successful transformants were re-plated and grown as a large broth (400ml) for maxi-prep (section 2.1.3.2.2) and further restriction analysis. The resulting purified DNA had a concentration of 600µg/ml and 82% purity.

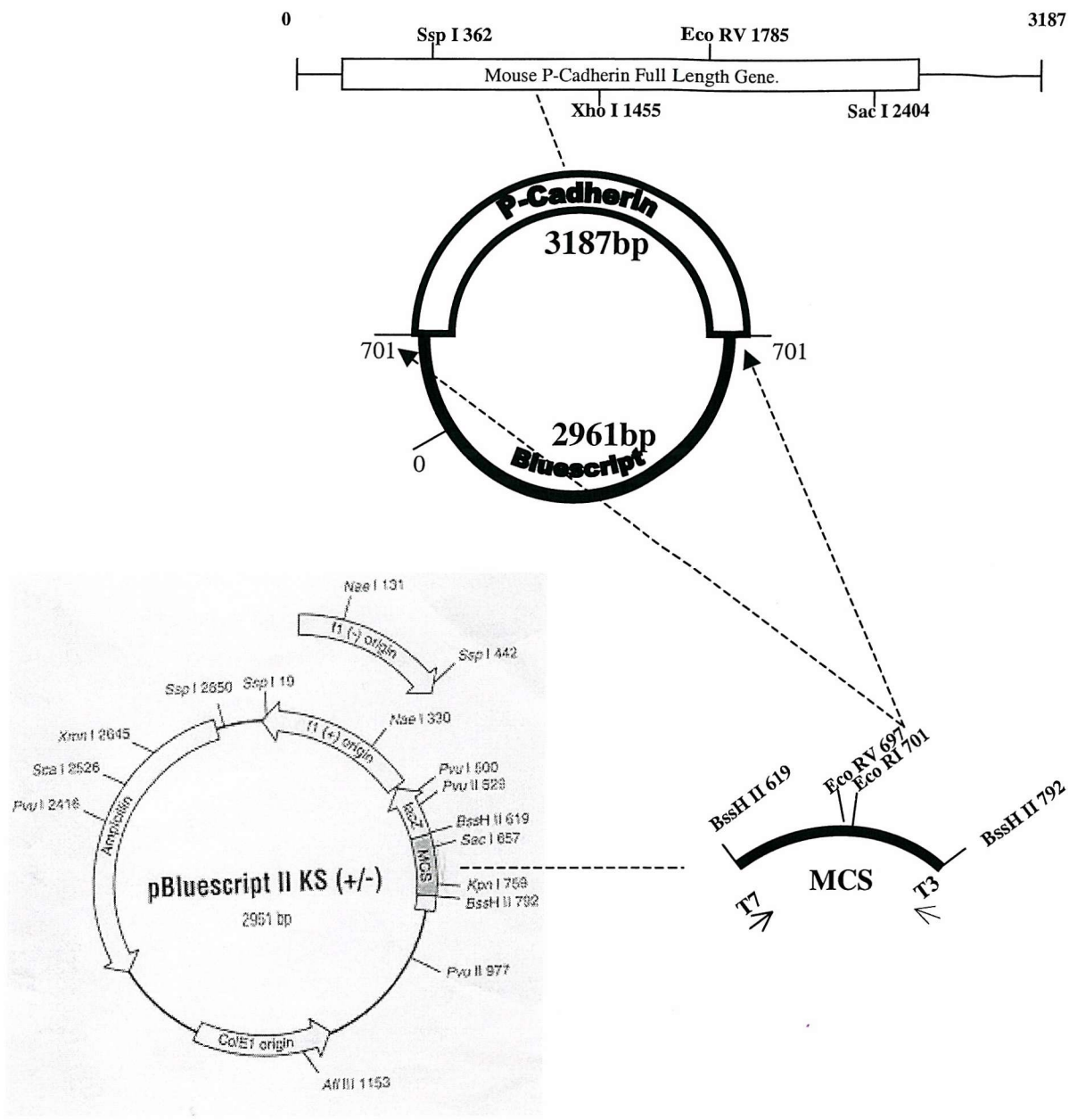

Fig. 5.14 P-Cadherin Gene in Bluescript Vector.

The full length mouse P-Cadherin gene (3187 bp) is inserted into the Eco RI restriction digest site of pBluescript. The Eco RI site is at position 701 bp in the multiple cloning site (MCS) of pbluescript, therefore we can easily 'slice' out the P-cadherin gene insert, as the flanking regions retain the Eco RI cleavage sites.

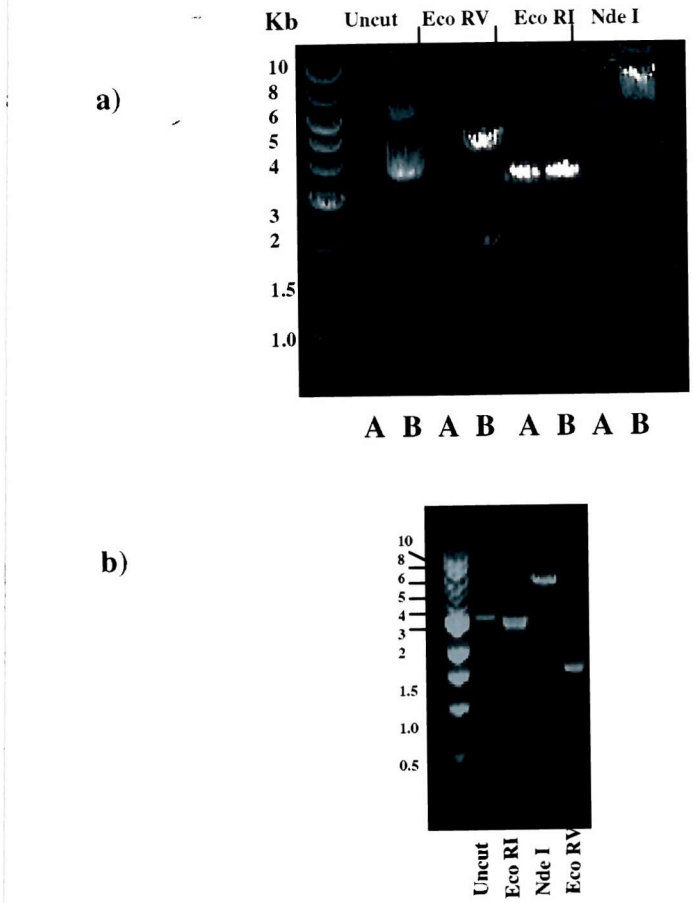

Fig 5.15 P-Cadherin/Bluescript Restriction Digests.

To ensure the P-Cadherin had not been lost during transformation restriction digests were carried out on minipreps of 2 sets of DNA, 'A' and 'B'. The uncut plasmid would give a band at ~6kD, an Eco RV digest resulting in bands at 1.8 and 4.4 kb or 1.4 and 4.7 kb depending on the orientation of the inserted P-Cadherin, regardless of orientation however, an Eco RI digest would result in bands of 2.9 and 3.1kb. Nde I cuts in P-Cadherin alone and would therefore linearise the fragment to a fragment that would run at ~6kb.
The first set of digests (a) shows that DNA 'A' is without the P-Cadherin plasmid whereas 'B' appears to have retained it. (b) is a repeat of the digests, this time on DNA 'B' alone. Here we can clearly see the double band of the similar sized fragments from the Eco RI digest, and the expected fragments from both Nde I and Eco RV digestion. From this data we can conclude that we have P-Cadherin inserted into pBluescript vector.

Before separation and purification of the P-cadherin insert (by electrophoresis and band purification respectively, see section 2.1.3.4), the plasmid was double digested with Eco R1 and Apa L1. Eco R1 slices out the P-cadherin cDNA, whereas Apa L1 further fragments the similarly sized pBluescript allowing clear access to excise the P-cadherin cDNA from the gel (figure 5.16).

Prior to gel visualisation, a block of gel was removed ensuring that one sample lane and the marker lane remained intact. The residual block was then viewed and 'nicks' cut into the gel at the point where the P-cadherin 3.1kb band is seen. Again away from the UV light, the removed block was replaced into the gel and the region that lined up with the P-cadherin nicks excised and purified using a DNA extraction kit (Qiagen). This procedure ensures that UV induced mutagenesis does not occur on the P-cadherin cDNA. A 716μg/ml (92% purity) stock was successfully attained.

5.2.4.2 Ligation of P-Cadherin cDNA into Mammalian Expression Vector.

pcDNA3 (fig 5.17) was amplified in the same way as the P-cadherin/pBluescript II KS^+ plasmid. Restrictive digestion using Ava 1 confirmed its identity and a subsequent maxiprep resulted in a pcDNA3 stock of 323μg/ml (90% purity).

Prior to ligation, pcDNA3 was cut with Eco R1, creating an insertion point for the P-cadherin cDNA and its EcoR1 induced sticky ends. The Eco R1 digestion of the vector was carried out for 4hrs to ensure complete digestion. Alkaline phosphatase (AP) was then added to the digested DNA to dephosphorylate the fragments and inhibit vector self re-ligation.

Purified DNA inserts were cloned into the linearised vector overnight at 16 C as a mixture of 100ng cut plasmid, excess insert DNA, 1μl ligase and 10μl of 10x buffer (T4 DNA ligase and buffer, Boehringer Mannheim).

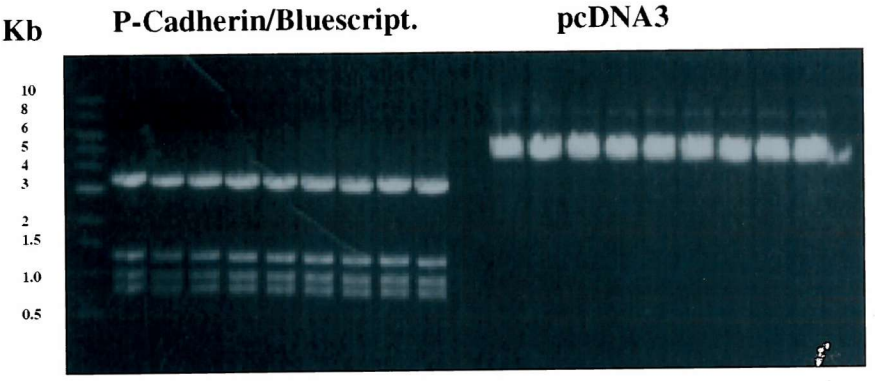

Fig. 5.16 Restriction Digests of P-Cadherin/Bluescript and pcDNA3.

P-Cadherin/pBluescript plasmid was cut with Eco RI and Apa LI. Cutting with Eco RI yields 2.9 and 3.1 kb fragments, too close together for band purification. Therefore by doing a 'double-digest' with ApaLI we can fragment the 2.9kb band further. Apa LI cuts twice in pBluescript but not at all in P-Cadherin, leaving a clear 3.1kb P-Cadherin band accessible for band excision and purification.
pcDNA3 is digested with Eco RI alone to linearise the plasmid, then incubated with an alkaline phosphatase to dephosphorylate the fragment and inhibit self religation.

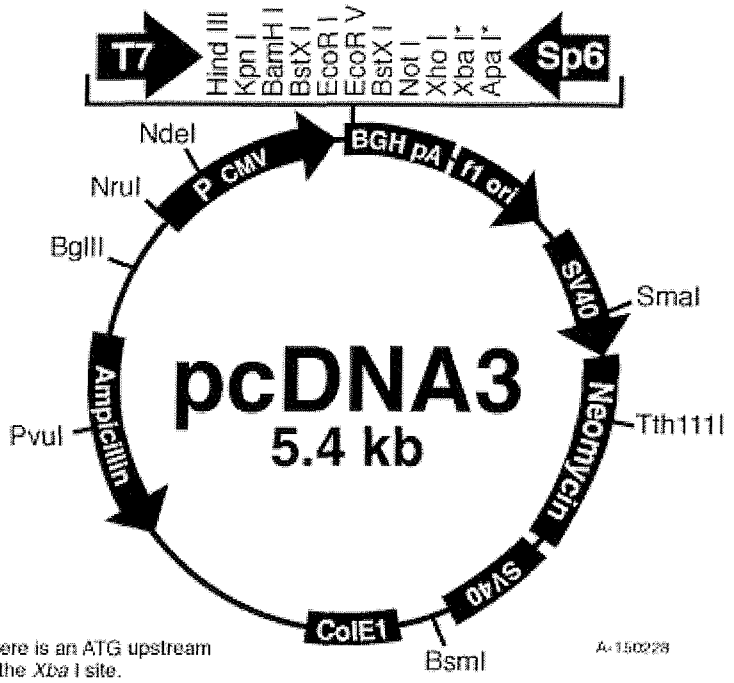

Fig. 5.17 Restriction Map of Expression Vector pcDNA3.

pcDNA3 is a 5.4kb vector, it has a single Eco RI site and therefore we can cleave here and insert the P-Cadherin gene sliced from bluescript.The ampicillin resistance is used as a selection tool for successfully transformed cells.

Restriction Map: http://www.invitrogen.com/vecgif/pcdna3.gif

Post-ligation there is rarely enough DNA to visualise on a gel, due to the small quantities added in the first instance, therefore DNA is transformed directly and the resulting preps analysed. Resulting ligates were hence transformed and miniprepped. Restriction digests with Eco R1 were carried out on all preps to establish which ones had the successfully ligated P-cadherin/pcDNA3 (fig 5.18).

Successful ligation and transformation results in 3.1kb and 5.2kb fragments after digestion with Eco R1. Several lanes had vector only, seen as a 5.4kb band alone, other lanes showed a pBluescript II KS^+ contamination. However, several lanes showing the desired fragment sizes were present, although the initial few turned out to be plasmids with P-cadherin inserted in the wrong orientation (antisense). Eventually, 4 DNA samples were shown to have the insert in the correct orientation (sense), this was confirmed by sequencing of the regions either side of and bridging the ligated Eco R1 site within the plasmid. These samples were then transformed and maxiprepped to establish a stock of P-cadherin in the pcDNA3 expression vector. The DNA in this state was ready to be transfected (section 2.1.4.5) into 16HBE14o- cells.

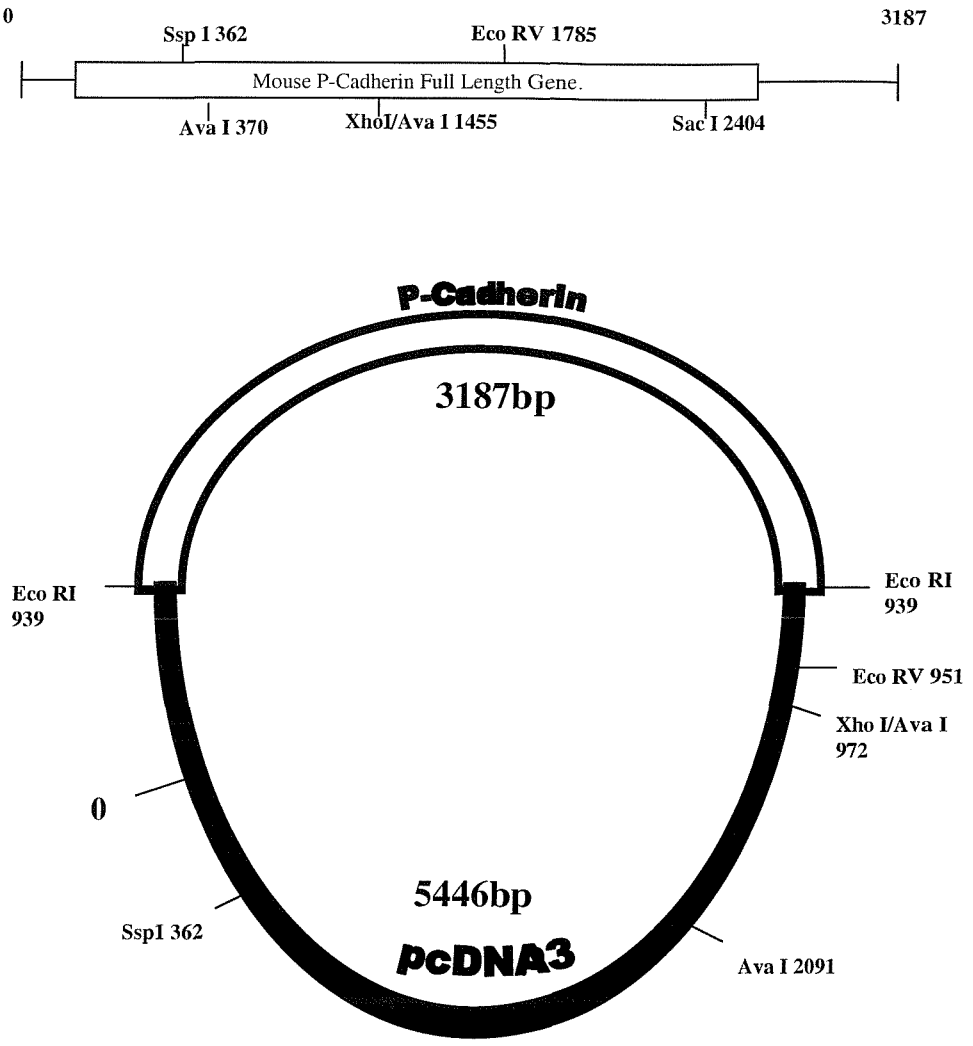

Fig 5.18 P-Cadherin and pcDNA3 Plasmid map.

Purified P-Cadherin is ligated with Eco RI digested pcDNA3 forming a 8.6 kb combined plasmid. This plasmid is transfected into cultured human bronchial epithelial cells to create P-cadherin clones.

5.3 Discussion.

This chapter looked at the possibilities and consequences of manipulating cadherin expression.

5.3.1 E-cadherin Transfected Bronchial Epithelial Cell Clones.

E-cadherin manipulated clones show different growth rates when plated out from frozen. However this observation can be explained in several cases by their recovery on thawing. Many of the vials of cells had just 30% viability. In most cases the growth rate correlated with the viability of cells recovered.

5.3.2 Selection of Clones For Use in Further Studies.

Clones were characterised with respect to TER and Cadherin expression in order to establish variations and identify desirable qualities for the range of clones. Manipulation of E-cadherin levels appears to affect the tight junction. TER analysis showed varied TER profiles between clones over a period of 15 days. Untransfected 16HBE14o- cells follow a more consistent TER profile of levels under 2000Ωcm^2 with little deviation. The clones however follow a varied pattern with several clones having resistances remaining below 500Ωcm^2, and other clones having an irregular profile at levels above 3000Ωcm^2.

Higher resistances are in general seen in the positive clones, this supports suggestions that increased E-cadherin expression increases junctional tightness and subsequently resistance (Lewis et al. 1994 and Wheelock et al. 1992).

Preliminary E-cadherin expression analysis show variation of immunoreactivity between clones with the range stretching from ~1.5 – 15 OD units/μg total protein. In general, as might have been expected, sense clones had

higher expression than the antisense, with a range of sense expression of 5 - 15 OD units/μg total protein. E-cadherin expression in the antisense clones ranged from 1.5 - 6 OD units/μg total protein.

Clones were selected on the basis of TER stability and E-cadherin expression to establish a range of 6 with low to high E-cadherin expression and a relatively stable TER profiles. These characteristics allowed analysis of the consequences of E-cadherin level to be carried out in a repeatable manner i.e. no erratic fluctuation of barrier resistance.

Clones 4-, 8-, 10-, 6+, 8+, and 10+ were the clones chosen to represent the range of E-cadherin expression.

5.3.3 TER/Permeability

Further characterisation was carried out on the selected clones. Again TER was monitored but this time in comparison with the parent clone (clone 0) and untransfected 16HBE14o- cells.

Peak TER levels were similar here to the original TER results used in selection with the exception of Clone 10- which had lower levels this time. In this study, the upregulation of E-cadherin resulted in high resistances and E-cadherin downregulation resulted in low resistances. This reinforces the suggestion that E-cadherin manipulation effects junctional tightness and therefore transepithelial electrical resistance.

Permeability assays were carried out in parallel on the same membranes. Here the clones were all less permeable than both clone 0 and 16HBE14o- cells suggesting that E-cadherin manipulation decreases permeability in all cases regardless of whether the E-cadherin levels are elevated or depressed.

Looking at the TER and Permeability data together it seems that the decreased permeability seen in antisense clones is not accompanied by increased electrical resistance. These methods of barrier function analysis both involve the passage of

substances across the epithelial barrier. All the clones showed decreased permeability to the FITC dextran molecules of 4.4kD compared to permabilities measured in clone 0 and 16HBE14o- cells. When looking at the passage of the much smaller ions as transepithelial electrical resistance, the antisense clones were more 'leaky' than clone 0 and 16HBE14o- cells, and vice versa for the sense clones. These results may indicate differential permeability properties of the epithelial layer in the clones on the basis of size and/or possibly ionic charge. This may be due to altered organisation of the junction or perhaps ion interaction with surface molecules or ion channels within the plasma membrane. In resistance and permeability assays, each clone showed similar results whether in the presence or absence of doxacyclin indicating doxacyclin independence.

5.3.4 Cadherin analysis.

E-cadherin expression analysis was repeated on the selected clones, this time in parallel with P-cadherin expression analysis.

Elevated E-cadherin tended to coincide with elevated P-cadherin as did depressed E- and P-cadherin levels. Comparing the results on the whole there is a positive correlation between E- and P-cadherin expression. However, when looking at individual clones only 6+ shows a strong correlation.

Therefore, despite there being little correlation between E- and P-cadherin expression on a small scale within individual clone data, over the whole group different levels of E-cadherin expression have an associated characteristic range of P-cadherin expression indicating some level of codependence between the two cadherins.

Similar cadherin levels were seen in doxacyclin negative and positive cultures. Cross correlation shows only clones 8- and 8+ to show any form of

regulation, and in both cases, this was seen for E-cadherin to a greater extent than P-Cadherin.

Further analysis of Clone 6+ showed very little evidence of doxacyclin regulation, although initial characterisation showed this clone to have the greatest difference between doxacyclin negative and positive cultures. This may be evidence of a loss of doxacyclin regulation with increased passaging or inconsistency in vector expression.

This work has therefore provided us with a range of E-cadherin over- and under- expressing clones. These clones are variable with regard to E-cadherin expression and also growth rate, resistance and permeability. The selected clones together represent E-cadherin expression over an eleven-fold range. The P-cadherin expression covering a twelve-fold range with clones representing low, intermediate and high expression compared with the controls.

Interestingly, manipulation of E-cadherin appears to have resulted in similar trends in P-cadherin expression. Given that only E-cadherin coding sequences were transfected, it was not expected that there would be any correlation between E- and P-cadherin expression. This response may be due to signaling as a result of the presence of the cell adhesion molecule as opposed to the gene, i.e. greater expression results in greater correlation and vice versa. However, in chapter 4 it was shown that using the confluence and wounding models that E- and P-cadherin have differing immunorectivity patterns in epithelial development and repair. In fact when E-cadherin was at its lowest levels at pre-confluence, P-cadherin immunoreactivity was at its highest. Therefore from this, it might be expected that a 'negative' correlation would exist between E- and P-cadherin expression.

It may be that the observed increase in P-cadherin immunoractivities is related to levels of endogenous E-cadherin as opposed to the exogenous. Increased levels of transfected E-cadherin may result in a reduction of endogenous E-cadherin as an attempt to maintain normal levels. This reduction may then cause the expected negative correlation of P-cadherin immunoreactivity which is in turn proportional to the observed rise in exogenous E-cadherin expression.

E-cadherin manipulation affects morphology and characteristics of cells, for example resistance and permeability. The sense clones have an altered morphology in that the cells have lost the usual uniformity associated with 16HBE14o- cells, although and the cells are still visually identifiable as epithelia.

E-cadherin expression did not appear to be regulatable by doxacyclin in any of the clones. In all experiments, expression analysis, resistance and permeability, the same conclusion was drawn in that doxacyclin regulation was not taking place. The system simply may not work in this case or it may be working at a very low level.

Cadherin and TER analysis however show obvious differences between clones and therefore we can conclude that these cells contain the E-cadherin expressing vector but are not substantially doxacyclin sensitive.

5.3.5 Development of P-Cadherin Expressing Clones.

It was intended to artificially elevate P-cadherin expression levels in 16HBE14o- cells. P-cadherin manipulation was to be achieved by construction of a set of differentially expressing P-cadherin clones as a means of analysing the significance and role of this molecule. P-cadherin cDNA was successfully transferred into a mammalian expression vector ready for transfection into 16HBE14o- cells. It was not possible unfortunately to complete the transfection during the timescale involved. However if this work is taken up in future, the resulting clones could be characterised with regards to P- and E-cadherin levels, establishing any reciprocal influence over each other's expression. Functional experiments could then proceed on the clones in parallel with the E-cadherin clones in order to discover the effect different cadherin levels inflict onto epithelial barrier function and wound repair.

Previous studies that involved E- and P-cadherin gene knockouts have showed contrasting consequences for absence of each cadherin. Unlike E-cadherin deficient mice (Larue 1994), loss of P-cadherin is compatible with normal embryonic development (Radice 1997). Mice were viable and fertile with no apparent cell adhesion defect, although the P-cadherin deficient virgin females had precocious differentiation of the mammary epithelium resembling a pregnant female (Radice 1997). A combined knockout of P-cadherin and desmoglein 3 (a desmosomal cadherin also localised to the basal layer of the epidermis), resulted in mutants that died prior to weaning. These fatalities were not seen in the knockout of desmoglein 3 alone, indicating a synergistic response between the classical and desmosomal cadherin (Lenox et al 2000). Knockout of Desmoglein 3 alone resulted in mucous membrane lesions and skin blisters, Lenox et al therefore hypothesised that a combined P-cadherin deficiency may impair a variety of cellular processes including wound healing. This may explain why the desmoglein 3 mutants overcome the lesions and develop to weaning age whereas the combined knockout mutants do not.

Sanders et al (2000) investigated P-cadherin expression in the gastrointestinal tract. This study showed upregulated membranous and/or cytoplasmic P-cadherin expression to be associated with ulceration and neoplastic transformation of this tissue, suggesting a putative involvement of P-cadherin in cell proliferation, survival and dedifferentiation.

Both of these studies strengthen suggestions in this investigation for an involvement of P-cadherin in epithelial wound repair.

P-cadherin clones together with the E-cadherin clones could be used to continue the investigation of the cadherins with regards to wound repair. Elevated E-cadherin in transfected cells showed increased barrier function by both electrical resistance and permeability. This may mean that intercellular junctions are formed more quickly with these cells or that the tight junctions are functioning more efficiently, and therefore they may have an enhanced repair phenotype.

On the other hand, it may mean that the greater barrier function means a less dynamic mobile epithelium hindering the repair process. Given the slow growth rate of the clone with highest E-cadherin expression and TER clone 6+, this may be feasible. However an improved growth rate is not be necessarily indicative of optimal repair.

Clone 8+ with the second highest level of E-cadherin expression had one of the highest viabilities and high growth rates on thawing. This may indicate that the impaired growth rate of clone 6+ is independent of the E-cadherin regulation and more a consequence of the transfection process.

Given that an increase in E-cadherin expression consistently gives the highest electrical resistance and the lowest permeability, it is most feasible that this kind of manipulation would *enhance* the repair process, in that strong barrier forming junctions would be rapidly established. Also the corresponding increase in P-cadherin expression seen in these cells may also contribute to an enhanced repair process given that previous chapters have indicated P-cadherin to be associated with highly proliferating cells and the epithelial restitution. It is not known whether E-cadherin expression is the direct trigger for this response or whether this response would be reciprocated.

The results of this study contrast the findings of Navarro et al (1993) where E-cadherin transfection into rat 3YI cells resulted in suppression of endogenous P-cadherin.

It is not clear whether the relationship between E- and P-cadherin expression in the context of epithelial development and repair is co-dependent or coincident. Results here indicate a co-dependency in epithelial development. P-cadherin was elevated in response to an artificial elevation of E-cadherin, although it is not clear whether this is a response to the endogenous or exogenous E-cadherin levels, or alternatively a different trigger.

In order to ascertain the independent/codependent roles of E- and P-cadherin, we need to understand the relationships between them. Construction of the P-cadherin

clones and subsequent migration and wound repair analysis alongside the E-cadherin clones would help to establish any synergistic or complementary roles between these molecules in bronchial epithelial cells.

Chapter Six

General Discussion.

6 General Discussion.

The bronchial epithelial lining is often impaired in asthma with observed epithelial denudation. Cells in normal epithelium are linked by various adhesion molecules which interact and co-exist in such a fashion that together with the cytoskeleton they provide a scaffolding to support an epithelium that functions to line the airway lumen forming a selectively permeable barrier and protect the underlying tissue from harmful noxious agents of the exterior environment.

Epithelial damage is a prominent feature of asthma, with the sputum of patients containing shed seemingly viable cells (Naylor et al, 1962). The epithelial shedding is thought to result in increased airway permeability, loss of tissue protection, exposure of sensory nerves and the release of mediators (Montefort et al, 1993, Jacoby et al, 1997).

The process of epithelial shedding is not fully understood. Putative restitution stages have been observed where the epithelia undergo flattening, migratory, proliferative and differentiation stages in parallel with inflammation, to restore an intact epithelial barrier (Erjefält et al, 1995, 96 & 97, Persson et al 1996, Legrande et al, 1999, Danjo et al, 1998, Abercrombie et al, 1953, Zahm et al, 1992 & 97, Barrow et al, 1993).

The detailed examination of bronchial epithelial morphology of non-asthmatics, asthmatics and chronic asthmatic patients in this study revealed characteristic cell phenotypes for each.

Non-asthmatics in general had an intact uniform epithelium with rounded basal cells covered by tall columnar epithelia with visible cilia.

Asthmatics tended to have supra-basal denudation leaving flattened basal cells with a 'squat' appearance, cells appeared to flatten out laterally but maintained a predominantly continuous coverage over the basement membrane.

Chronic asthmatics on the other hand, with a largely denuded basement membrane, had almost the reverse situation in the few cells remaining. Instead of flattening and spreading to counteract cell loss, any surviving cells appeared to shrink

closer together laterally and increase in height, resulting in 'islands' of tightly packed clusters of tall cells.

These observed differences between the profiles of asthmatic and chronic asthmatic epithelium are surprising and in itself may be an underlying cause of severity of the disease. It may be that in asthma, the epithelium undergoes cycles of restitution to maintain optimal barrier function. Cell shedding has been previously suggested to be a preventative precaution where epithelia sacrifice columnar cells and flatten out giving less junctions per unit length (Erjefält et al, 1997).

The epithelium in the chronic-asthmatic however, appears to have either lost this ability to undergo self-repair as a direct consequence of the severity of cell shedding, or was otherwise dysfunctional in the first instance, for example, abnormal adhesion molecule expression or interaction which may be a cause of cell shedding. It appears that in these epithelia, the remaining cells pack inward and upward to heighten resilience. Since chronic asthmatics were all undergoing steroid treatment while other groups were not, this may also have influenced their response to injury.

Several studies of epithelial denudation have drawn the conclusion that the adhesive structures are targeted in this process (Montefort et al, 1993, Motojima et al, 1989). Supra-basal denudation seems to be a result of basal-columnar cell interaction breakdown possibly at the desmosomes.

The active processes of restitution that are so apparent in the non-asthmatics and particularly the asthmatics involve a dynamic epithelium, able to selectively disrupt the rigid adhesive scaffolding structures and to de-differentiate, flatten, migrate, proliferate and re-differentiate all the while maintaining the highest possible level of barrier function. Characteristic adhesion molecule expression changes are likely to accompany the restitution associated phenotypic changes.

It is not fully understood how the epithelial junctional structures accommodate cell loss and subsequent repair. It must first be understood how the junctions and their component adhesive molecules interact and influence each other.

The model of confluence and epithelial development established in chapter 4 was designed to examine the interactions of adhesion molecules of adherens and tight

junctions. Adherens junctions have been shown to be a pre-requisite for the formation of all the other epithelial cell junctions (Ozawa et al, 1990). As the major components of adherens junctions, cadherins were the obvious choice when examining the events accompanying epithelial changes.

The confluence model was set up to mimic and examine the establishment and maintenance of a confluent cell layer, comparable with that of the non-asthmatic epithelial profiles of chapter 3 where the cells had a putative 'normal' functioning. The adhesion molecules of the adherens junction and the tight junction were found to have differing and contrasting expression levels accompanying increasing confluence. Total E- and P-cadherin immunoreactivity both altered with increasing confluence. P-cadherin as the cadherin with lesser immunoreactivity of the two, appeared to have its greater role in the early stages of adhesion. E-cadherin expression, on the other hand appeared to become more crucial in already established cell adhesion.

These E-cadherin data are not altogether surprising as this molecule has had a long recognised role in cell adhesion (Shapiro et al, 1995, Larue et al, 1994, Takeichi et al, 1993). As a result of studies in various tissue types, P-cadherin is rapidly emerging as being associated with actively proliferating cells such as those assumed to be required for early stages of epithelial confluence (Hirai et al, 1989, Fujita et al, 1992, Shirahama et al, 1996).

Expression of the cadherin anchoring molecules, catenins α, β and γ, were also briefly examined in the same model. This preliminary work indicated an expression pattern for each which corresponded to that of E-cadherin expression. Again this would be expected given their role as the key cadherin binding molecules (Hirano et al, 1992, Rimm et al, 1995, Nagafuchi et al, 1994). Although P-cadherin was shown to be upregulated at sub-confluence, the different scales of expression thought to be involved between the two cadherins (Takeichi et al, 1993) would always mean that an increase in the catenin pool would be required in parallel with elevation of E-cadherin levels.

A similar contrasting adhesion molecule expression pattern was seen at the tight junction between occludin and ZO-1. This is more surprising however, unlike the contrast of expression between E- and P-cadherin, which fundamentally seem to fulfill a similar intermembrane adhesive role, occludin and ZO-1 appear to function by interacting in a codependent manner. ZO-1 is part of the anchor to Occludin's intermembrane scaffold (Itoh et al, 1999, Balda et al, 1996) and therefore the expression patterns of these two proteins might be expected to be comparable to that of E-cadherin and the catenins. However, the preliminary data from this study show that where occludin immunoreactivity increased with confluence, ZO-1 immunoreactivity decreased. A conceivable explanation for this may be that ZO-1, although vital in the structural side of cell adhesion, may have an additional role at early cell confluence, hence its upregulation.

ZO-1 has previously been identified as a versatile molecule being found linked at the adherens junction in times of low calcium concentration (Itoh et al, 1997) and within the cell nucleus at times of low cell polarity (Gottardi et al, 1996). It has also been implicated as playing an active role in signal transduction in collaboration with the transcription factor ZONAB, together modulating paracellular permeability and cell cycle progression (Balda et al,, 2000).

Although the higher levels of ZO-1 at pre-confluence may simply reflect a surplus of ZO-1 at this time which is adjusted in the established differentiated epithelium, it is more likely, given the diversity of ZO-1 reported in the literature, that ZO-1 is required for some purpose other than a structural role, such as signalling at initial cell contact.

This study concentrated on the investigation of the changes associated with the cadherins ,however as recognised major mediators of adhesion in the airway epithelium and their putative role as initiators of intercellular interactions (Takeichi et al, 1993).

In order to compare the model of 'normal' *developing* epithelium with a *repairing* epithelium representing the asthmatic epithelium with apparent cycling

stages of restitution of chapter 3, a wounding model was established examining adhesion molecule interactions in parallel with the confluence study.

In this model, cadherin levels prior to wounding were comparable to those seen at the post-confluence stage of development model. However, 6 hours after mechanical wounding, a dramatic reduction of E-cadherin levels was seen. This was followed by subsequent increase in P-cadherin over the next 18 hours of the experiment. Given the previous conclusions from the confluence model regarding the differing adhesive roles of these two cadherins, this would suggest a coordinated downregulation of E-cadherin contacts adhesion allowing incremental migration and dynamic adhesion, supplemented by elevated P-cadherin promoting requisite proliferation and differentiation to occur.

Given that several studies have found P-cadherin to be proliferation associated (Obara et al, 1999, Hirai et al, 1989), and that repairing epithelium in other models has involved a characteristic proliferative phenotype behind the leading edge (Zahm et al, 1997), and it is possible that P- and E- cadherin exist in coordinated parallel roles with regard to cell adhesion. Each fulfilling similar superficial adhesive roles, indicated by localisation experiments (Hirano et al, 1987, Johnson et al, 1993) and various immunohistochemical (Lin et al, 1996, Wu et al, 1993) and blocking studies (Hirai et al, 1989). However despite the demonstrated similarities of homophilic binding and catenin association (Takeichi et al, 1983, Johnson et al, 1993) significant functional differences regards to level of adhesion and rigidity of the epithelial sheet have been reported (Hirai et al, 1989, Obara et al, 1999 and Daniel et al, 1995).

It may be that the hypothetical repair impairment of the chronic asthmatic epithelium in chapter 3, stems from an inability to co-ordinate a switch from a rigid epithelial phenotype with predominantly E-cadherin expression, to a dynamic epithelium, more able to flatten and migrate to counteract the denudation of the basement mnembrane. As a result, such an epithelium would maintain putative unyielding E-cadherin contacts and perhaps be unable to undergo the usual processes of restitution.

When cell loss occurs, the residual cells may attempt to counteract denudation by increasing the adhesive structures in remaining epithelium resulting in the observed narrowed and heightened epithelium.

Whether this is the case or not, the cadherin switching phenomena is interesting with regards to the treatment of epithelial wounding in that it may be possible to strengthen epithelial organisation and barrier structure by increasing E-cadherin or alternatively encourage and accelerate a repair phenotype by increasing P-cadherin levels. In order to address these possibilities and examine the functional requirement for E- or P-cadherin, experimental manipulation of cadherins was examined in chapter 5. Both antisense and sense E-cadherin coding sequences transfected into 16HBE14o- cells resulted in altered epithelial morphology and barrier function.

An increased level of permeability to the passage of ions in the sense clones was observed with a permeability decrease in the antisense clones, agreeing with the suggestion that elevated E-cadherin expression is associated with a higher level of epithelial barrier function.

The antisense and sense clones revealed a positive correlation between the expression of E- and P-cadherin. This however, contrasted with the findings of the previous chapter where putative cadherin switching was reported (sections 4.2.2 and 4.2.5). Taking into account this observed change in cadherin expression emphasis in developing and repairing epithelia, it may be feasible that while the enhanced E-cadherin expression levels of the sense clones may directly suppress endogenous E-cadherin (and vice versa in the antisense clones), it is perhaps this reduced level of endogenous E-cadherin expression that influences the level of P-cadherin expression. This would result in an artificial E- and P-cadherin expression correlation with an *indirect* influence of E-cadherin manipulation toward P-cadherin expression.

In order to examine the reverse effect, i.e. whether manipulation of P-cadherin expression levels could directly or indirectly influence E-cadherin expression, work was commenced with the aim of establishing a range of P-cadherin expressing clones comparable with those of E-cadherin.

Despite isolation and amplification of the P-cadherin gene and insertion into mammalian expression vector, it was not possible to complete this work in the time available. However, if this work is continued at a later date, the E- and P-cadherin clones in parallel with the development and wounding models established for this thesis, would prove essential experimental tools in the investigation of cadherin involvement in epithelial cell adhesion and wound repair.

6.1. Conclusion.

This thesis has addressed the morphological and molecular differences between the epithelium of non-asthmatics and asthmatics. It has confirmed a significant difference in morphology between these patient groups and identified a further epithelial condition in chronic asthmatics.

Using *in vitro* models of epithelial development and repair, this study has demonstrated molecular modifications that are characteristic of these epithelial phenotypes, confirming separate adhesive roles and changing expression levels for E- and P-cadherin determined by cell cycle requirement.

Future therapeutic approaches in airway inflammation and disease will benefit from investigating the potential and consequences of cadherin manipulation.

References
&
Appendices.

Appendices.

Appendix 1: Suppliers of Reagents..

General lab chemicals were obtained from Sigma Aldrich Company Ltd., Poole, Dorset and from B.D.H. Ltd., Poole, Dorset, UK.

All cell culture media and reagents were obtained from GibcoBRL, Life Technologies Ltd., Paisley, Scotland, UK.

Restriction Enzymes, T4 DNA Ligase and molecular biology buffers supplied by Boehringer Mannheim, Lewes, East Sussex, UK.

Suppliers referred to in-text:-

-Amersham Pharmacia Biotech UK, Little Chalfont, Buckinghamshire, UK.
-BIO-Rad Laboratories Ltd., Hemel Hempstead, Hertfordshire, UK.
-Corning and Costar Science Prods UK, High Wycombe Buckinghamshire, UK.
-New England Biolabs, Beverly Massachusetts USA.
-Novex Experimental, San Diego, California, USA.
-Pierce Chemicals, Rockford, Illinois, USA.
-Promega Corp, Madison, Wisconsin USA.
-Qiagen Inc., Chatsworth , California, USA
-Stratagene Co. La Jolla, California. USA.
-Transduction Laboratories, Lexington, Kentucky, USA.
-Zymed Laboratories, San Fransico, California, USA

Appendix 2: General Solutions

16HBE 14o- Growth Media

Eagles MEM + salts.

5% FCS

1% L-Glutamine

1% Penicillin Streptomycin.

16HBE14o- Clone Media

500ml 16HBE14o- growth media.

40μg/ml Hygromycin B.

300μg/ml G418.

N.B. Parent clone media –as 16HBE14o- clone media but minus Hygromycin B.

Coating Media

Eagles MEM + salts

1% L-Glutamine

1% Penicillin Streptomycin

1mg/ml Fatty acid free BSA

1% Vitronectin

1% Fibronectin

10x TBST (5L)

1L Tris HCL 1M pH 7.6

400g NaCl

50ml Tween-20

Appendix 3: Antibody concentrations.

Dilutions based on a 1μg/μl working concentration.

All made up in blocking solution (5% milk powder with 1% TWEEN)

Primary Abs

Mouse Anti-E-cadherin (SHE 78.7)	1:4,000
Mouse Anti-P-cadherin	1: 100
Rat Anti- α-catenin	1:3,000
Mouse Anti β-catenin	1:2,000
Mouse Anti γ-catenin	1:2,000
Rat Anti-Occludin	1:6,000
Rat Anti-ZO-1	1: 500

Secondary Abs

Anti-mouse Ig horseradish linked Ab	1:20,000
Anti-rat Ig horseradish linked Ab	1:15,000

Appendix 4: Patient characteristics

Biopsy	Classification	Age	Gender	FEV1 % predicted	Atopy
N1	Normal	24	M	109.8	-
N2	Normal	20	F	118.3	-
N3	Normal	19	F	100	-
N4	Normal	21	F	106.9	-
N5	Normal	24	F	91.8	-
N6	Normal	21	M	98.1	-
N7	Normal	26	F	114.6	-
N8	Normal	33	M	91.1	-
N9	Normal	21	F	-	-
N10	Normal	21	F	-	-
N11	Normal	21	F	-	-
N12	Normal	35	F	105.7	-
N13	Normal	22	F	105.6	-
N14	Normal	27	M	123	-
M1	Asthma	20	M	75.1	+
M2	Asthma	28	F	86.6	+
M3	Asthma	23	M	64.8	+
M4	Asthma	45	M	94.2	+
M5	Asthma	38	M	61.4	+
M6	Asthma	44	M	70.9	+
M7	Asthma	37	M	87.5	+
M8	Asthma	31	M	84.6	+
M9	Asthma	31	F	76.3	+
S1	Chronic Asthma	56	F	77.5	+
S2	Chronic Asthma	60	F	40.3	+
S3	Chronic Asthma	64	F	41.8	-
S4	Chronic Asthma	36	M	50.4	+
S5	Chronic Asthma	55	F	39	+
S6	Chronic Asthma	33	M	23	-
S7	Chronic Asthma	56	M	46	+
S8	Chronic Asthma	30	F	88.1	+
S9	Chronic Asthma	48	M	79.7	+
S10	Chronic Asthma	18	F	52.9	+
S11	Chronic Asthma	42	F	42.9	+
S12	Chronic Asthma	37	M	58.1	+
S13	Chronic Asthma	36	F	49.5	-
S14	Chronic Asthma	29	M	39.3	+

References.

Altraja A., Laitinen A., Virtanen I., Kampe M., Simonsson BG., Karlsson SE., Hakansson L., Venge P., and Laitinen LA. 1996.Expression of laminins in the airways in various types of asthmatic patients: a morphometric study. *American Journal of Respiratory Cell & Molecular Biology.* **15**.[4], 482-488.

Amin K., Ludviksdottir D, Janson C., Nettelbladt O., Bjornsson E., Roomans GM., Boman G., Seveus L., and Venge P. 2001.Inflammation and structural changes in the airways of patients with atopic and nonatopic asthma. BHR Group. *American Journal of Respiratory & Critical Care Medicine.* **162**.[6], 2295-2301.

Anastasiadis PZ. and Reynolds AB. 2000.The p120 catenin family: complex roles in adhesion, signaling and cancer. *Journal of Cell Science.* **113**.[8], 1319-1334.

Anderson JM and van Itallie CM. 1995.Tight junctions and the molecular basis for regulation of paracellular permeability. *American Journal of Physiology* **269**.[32], G467-G475.

Balda MS and Anderson JM. 1993.Two classes of tight junctions are revealed by ZO-1 isoforms . *American Journal of Physiology.* **264**.[C], 918-924.

Balda MS, Whitney JA, Flores C, Gonzalez S, Cereijido M, and Matter K. 1996.Functional dissociation of paracellular permeability and transepithelial electrical resistance and disruption of the apical-basolateral intramembrane diffusion barrier by expression of a mutant tight junction membrane protein. *Journal of Cell Biology.* **134**.[4], 1031-1049.

Balda MS and Matter K. 1998.Tight junctions. *Journal of Cell Science* **111**.[5], 541-547.

Balda MS, Gonzalez-Marriscal RG, Contreras M, Marcias-Silva ME, Torres-Marquez JA, and Cereijido M. 1991. Assembly and sealing of the tight junctions: possible participation of G-proteins, phopholipase C, protein kinase C and calmodulin. *Journal of Membrane Biology.* **122**, 193-202.

Balda MS, Flores-Maldonado C, Cereijido M, and Matter K. 2000.Multiple domains of occludin are involved in the regulation of paracellular permeability. *Journal of Cellular Biochemistry* **78**, 85-96.

Balda MS and Matter K. 2000.Transmembrane proteins of tight junctions. *Cell & Developmental Biology.* **11**, 281-289.

Barrow RE, Wang CZ, Evans MJ, and Herndon DN. 1993.Growth-factors accelerate epithelial repair in sheep trachea. *Journal of Cell Biology.* **101**, 1307-1315.

Bauer H., Stelzhammer W, Fuchs R., Weiger TM., Danninger C., Probst G., and .Krizbai IA. 1999. Astrocytes and neurons express the tight junction-specific protein occludin in vitro. *Experimental Cell Research.* **250**.[2], 434-438.

Beasley R, Roche WR, Roberts JA, and Holgate ST. 1989.Cellular events in the bronchi in mild asthma and after bronchial provocation. *American Review of Respiratory Disease.* **139**, 806-817.

Bement WM., Forscher P, and Mooseker MS. 1993.A novel cytoskeletal structure involved in purse string wound closure and cell polarity maintenance. *Journal of Cell Biology.* **121**.[3], 565-578.

Ben-Ze'ev A, Shtutman M, and Zhurinsky J. 2000.The Integration of Cell Adhesion with gene expression: the Role of β-catenin. *Experimental Cell Research.* **261**, 75-82.

Bierkamp C, Mclaughlin KJ, Schwarz H, Huber O, and Kemler R. 1996.Embryonic heart and skin defects in mice lacking plakoglobin. *Developmental Biology.* **180**.[2], 780-785.

Birchmeier W and Behrens J. 1994.Cadherin expression in carcinomas: role in the formation of cell junctions and the prevention of invasiveness. *Biochimica et Biophysica Acta.* **1198**, 11-26.

Blaschuk OW, Sullivan R, David S, and Pouliot Y. 1990.Identification of a cadherin cell-adhesion recognition sequence. *Development Biology* **139**, 227-229.

Boers JE, Ambergen AW, and Thunnissen JM. 1998.Number and proliferation of basal and parabasal cells in normal human airway epithelium. *American Journal of Respiratory Critical Care Medicine* **157**, 2000-2006.

Bruzzone S., Guida L., Franco L., Zocchi E., Corte G., and De Flora A. 1998. Dimeric and tetrameric forms of catalytically active transmembrane CD38 in transfected HeLa cells. *FEBS Letters.* **433**.[3], 275-278.

Buck RC. 1979.Cell migration in repair of mouse corneal epithelium. *Investigative Ophthalmology & Visual Science.* **18**.[8], 767-784.

Cepek KL, Shaw SK, Parker CM, Russell GJ, Morrow JS, Rimm DL, and Brenner MB. 1994.Adhesion between epithelial cells and T lymphocytes mediated by E-cadherin and the $\alpha^{E}\beta_{7\ \text{integrin}}$. *Nature* **372**, 190-193.

Chanez P, Vignola AM, Vic P, Guddo F, Bonsignore G, Godard P, and Bousquet P. 1999.Comparison between nasal and bronchial inflammation in asthmatic and control subjects. *American Journal of Respiratory & Critical Care Medicine.* **159**, 588-595. ,.

Chitaev NA and Troyanovsky SM. 1998.Adhesive but not lateral E-cadherin complexes require calcium and catenins for their formation. *Journal of Cell Biology* **142.**[3], 837-846.

Citi S. 2000.introduction: opening up tight junctions. *Cell & Developmental Biology.* **11**, 277-279.

Daniel CW, Strickland P, and Friedmann Y. 1995.Expression and functional role of E- and P-cadherins in mouse mammary ductal morphogenesis and growth. *Development Biology* **169**, 511-519.

Danjo Y and Gipson IK. 1998.Actin 'purse string' filaments are anchored by E-cadherin-mediated adherens junctions at the leading edge of the epithelial wound, providing coordinated cell movement. *Journal of Cell Science* **111**, 3323-3331.

Del Maschio A., De Luigi A, Martin-Padura I, Brockhaus M., Bartfai T., Fruscella P, Adorini L., Martino G., Furlan R., De Simoni MG., and Dejana E. 1999.Leukocyte recruitment in the cerebrospinal fluid of mice with experimental meningitis is inhibited by an antibody to junctional adhesion molecule (**JAM**). *Journal of Experimental Medicine.* **190.**[9], 1351-1361.

Donnelly **GM., Haack DG., and Heird CS.** 1982. Tracheal epithelium: cell kinetics and differentiation in normal rat tissue. *Cell & Tissue Kinetics.* **15.**[2}, 119-130.

Droufakou S., Deshmane V., Roylance R., Hanby A., Tomlinson I, and Hart IR. 2001. Multiple ways of silencing E-cadherin gene expression in lobular carcinoma of the breast. *Journal of Cancer.* **92.**[3], 404-408.

Dunnill MS. 1960.The pathology of asthma with special reference to changes in the bronchial mucosa. *Journal of Clinical Pathology.* **13**, 27-33.

Dustin ML and Springer TA. 1989. T-cell receptor cross-linking transiently stimulates adhesiveness through LFA-1. *Nature.* **341**. 619-624.

Elwood RK, Kennedy S, Belzberg A, Hogg JC, and Pare PD. 1993.Respiratory mucosal permeability in asthma. *American Review of Respiratory Disease.* **128**, 523-527.

Erjefält JS, Erjefält I, Sundler F, and Persson CGA. 1995.*In-vivo* restitution of airway epithelium. *Cell and Tissue Research* **281** , 305-316.

Erjefält JS, Sundler F, and Persson CGA. 1996.Eosinophils, neutophils, and venular gaps in the airway mucosa at epithelial removal-restitution. *American Journal of Respiratory Cell and Molecular Biology.* **153**.[5], 1666-1674.

Erjefält JS, Sundler F, and Persson CGA. 1997.Epithelial barrier formation by airway basal cells. *Thorax* **52**.[3], 213-217.

Erjefält JS, Korsgren MC, Nilsson MC, Sundler F, and Persson CGA. 1997.Association between inflammation and epithelial damage -restitution processes in allergic airways *in-vivo. Clinical and Experimental Allergy.* **27**, 1344-1355.

Erjefält JS and Persson CGA. 1997.Airway epithelial repair: breathtakingly quick and multipotentially pathogenic. *Thorax* **52**, 1010-1012.

Erjefält JS, Korsgren MC, Nilsson MC, Sundler F, and Persson CGA. 1997.Prompt epithelial damage and restitution processes in allergen challenged guinea-pig trachea *in vivo. Clinical and Experimental Allergy.* **27**.[12], 1458-1470.

Evans MJ and Plopper CG. 1988.The role of basal cells in adhesion of columnar epithelium to airway basement membrane. *American Review of Respiratory Disease.* **138**, 481-483.

Evans MJ, Cox RA, Shami SG, Wilson B, and Plopper CG. 1989.The role of basal cells in attachment of columnar cells to the basal lamina of the trachea. *American Journal of Respiratory Cell and Molecular Biology.* **1**, 463-469.

Evans MJ, Cox RA, Shami SG, and Plopper CG. 1990.Junctional adhesion mechanisms in airway basal cells. *American Journal of Respiratory Cell and Molecular Biology.* **3** .[4], 341-347.

Evans MJ and Moller PC. 1991.Biology of airway basal cells. *Experimental Lung Research.* **17**.[3], 513-531.

Fahy JV., Corry DB, and Boushey HA. 2000.Airway inflammation and remodeling in asthma. *Current Opinion in Pulmonary Medicine.* **6**.[1], 15-20.

Fahy JV., Steiger DJ., Liu J., Basbaum CB., Finkbeiner WE., and Boushey HA. 2001. Markers of mucus secretion and DNA levels in induced sputum from asthmatic and from healthy subjects. *American Review of Respiratory Disease.* **147**.[5], 1132-1137.

Fanning AS., Jameson BJ., Jesaitis LA., and Anderson JM. 1998.The tight junction protein ZO-1 establishes a link between the transmembrane protein occludin and the actin cytoskeleton.. *Journal of Biological Chemistry* **273**.[45], 29745-29753.

Foty RA and Steinberg MS. 1997.Measurement of tumor cell cohesion and suppression of invasion by E- or P-cadherin. *Cancer Research* **57**.[22], 5033-5036.

Fuchs M., Muller T., Lerch MM., and Ullrich A. 1996. Association of human protein-tyrosine phosphatase kappa with members of the armadillo family. *Journal of Biological Chemistry.* **271**.[28], 16712-16719.

Fujita M, Furukawa F, Fujii K, Horiguchi Y, Takeichi M, and Imamura S. 1992.Expression of cadherin cell adhesion molecules during human skin development: morphogenesis of epidermis, hair follicles and sweat ducts. *Arch.Dermatol.Res.* **284**, 159-166.

Furuse M, Hirase T, Itoh M, Nagafuchi A, Yonemura S, and Tsukita S. 1993.Occludin -a novel integral membrane-protein localising at tight junctions. *Journal of Cell Biology.* **123**, 1777-1788.

Furuse M, Sasaki H, Fujimoto K, and Tsukita S. 1998.A single gene product, claudin-1 or -2, reconstitutes tight junction strands and recruits occludin in fibroblasts. *Journal of Cell Biology.* **143**.[2], 391-401.

Furuse M, Fujita K, Hiiragi T, Fujimoto K, and Tsukita S . 1998.Claudin-1 and -2: Novel integral membrane proteins localising at tight junctions with no sequence similarity to occludin. *Journal of Cell Biology* **141**.[7], 1539-1550.

Garrod DR. 1986.Formation of desmosomes in polarized and non-polarized epithelial cells: implications for epithelial morphogenesis. *Biochemical Society Transactions.* ***14***.*[1]*, 172-175.

Garrod DR. 1993.Cell to cell and cell to matrix adhesion. *British Medical Journal* **306**, 703-705.

Giancotti FG. 1996.Signal transduction by the alpha 6 beta 4 integrin: charting the path between laminin binding and nuclear events. *Journal of Cell Science.* **109**.[6], 1165-1172.

Gonzalez-Mariscal L, Betanzos A, and Avila-Flores A. 2000.MAGUK proteins:structure and role in the tight junction. *Cell & Developmental Biology.* **11**, 315-324.

Goto Y, Uchida Y, Nomura A, Sakamoto T, Ishii Y, Morishima Y, Masuyama K, Sekizawa K. 2000. Dislocation of E-cadherin in the airway epithelium during an antigen-induced asthmatic response. *Am. J. Respir. Cell Mol. Biol.* **23**, 712-718.

Gottardi CJ, Arpin M., Fanning AS., and Louvard D. 1996.The junction-associated protein, zonula occludens-1, localizes to the nucleus before the maturation and during the remodeling of cell-cell contacts. *Proceedings of the National Academy of Sciences of the United States of America.* **93**.[20], 10779-10784.

Gow A., Southwood CM, Li JS., Pariali M., Riordan GP., Brodie SE., Danias J., Bronstein JM., Kachar B., and Lazzarini RA. 1999.CNS myelin and sertoli cell tight junction strands are absent in Osp/claudin-11 null mice. *Cell.* **99**.[6], 649-659.

Gumbiner BM, Stevenson BR, and Grimaldi A. 1988.The role of the adhesion molecule uvomorulin in the formation and maintenance of epithelial junctional complex. *Journal of Cell Biology.* **107**, 1575-1587.

Gumbiner BM, Lowenkopf T, and Apatira D. 1991.Identification of a 160kDa polypeptide that binds to the tight junction protein ZO-1. *Proceedings of the National Academy of Science USA.* **88**, 3460-3464.

Gumbiner BM and McCrea PD. 1993.Catenins as mediators of the cytoplasmic functions of cadherins. *Journal of Cell Science* **17**, 155-158.

Gumbiner BM. 1993.Proteins associated with the cytoplasmic surface of adhesion molecules. *Neuron* **11**.[4], 551-564.

Han AC., Edelson MI., Peralta Soler A., Knudsen KA., Lifschitz-Mercer B., Czernobilsky B., Rosenblum NG., and Salazar H. 2000.Cadherin expression in glandular tumors of the cervix. *Cancer.* **89**.[10], 2053-2058.

Haskins J., Gu L., Wittchen ES., Hibbard J., and Stevenson BR. 2001.ZO-3, a novel member of the MAGUK protein family found at the tight junction, interacts with ZO-1 and occludin. *Journal of Cell Biology.* **141**.[1], 199-208.

Hatta M, Miyatani S, Copeland NG, Gilbert DJ, Jenkins NA, and Takeichi M. 1991.Genomic organisation and chromosomal mapping of the mouse P-cadherin gene . *Nucleic Acids Research* **19**, 4437-4441.

Herard AL, Pierrot D, Hinnrasky J, Kaplan H, Sheppard D, Puchelle E, and Zahm JM. 1996.Fibronectin and its alpha (5) beta (1) -integrin receptor are involved in the wound-repair process of airway epithelium. *American Journal of Physiology -Lung Cellular and Molecular Physiology.* **15**, L726-L733.

Hirai Y, Nose A, Kobayashi S, and Takeichi M. 1989.Expression and role of E- and p-cadherin adhesion molecules in embryonic histogenesis. II Skin morphogenesis. *Development* **105**, 271-277.

Hirai Y, Nose A, Kobayashi S, and Takeichi M. 1989.Expression and role of E- and P-cadherin adhesion molecules in embryonic histogenesis. I Lung epithelial morphogenesis. *Development* **105**, 263-270.

Homer RJ. and Elias JA. 2000.Consequences of long-term inflammation. Airway remodeling. *Clinics in Chest Medicine.* **21**.[2], 331-343.

Holgate, ST, Davies, DE, Lackie, PM, Wilson, SJ, Puddicombe, SM, and Lordan, JL (2000a) Epithelial-mesenchymal interactions in the pathogenesis of asthma *Journal of Allergy and Clinical Immunology* **105**:193-204

Holgate, S. T., Lackie, P., Wilson, S., Roche, W., Davies, D. (2000b) Bronchial epithelium as a key regulator of airway allergen sensitization and remodeling in asthma. *Am.J.Respir.Crit Care Med.* **162:**S113-S117.

Huber D, Balda MS, and Matter K. 2000.Occludin modulates transepithelial migration of neutrophils. *Journal of Biological Chemistry.* **275**.[8], 5773-5778.

Ikeda W., Nakanishi H., Miyoshi J., Mandai K., Ishizaki H., Tanaka M., Togawa A., Takahashi K., Nishioka H., Yoshida H., Mizoguchi A., Nishikawa S., and Takai Y. 1999.Afadin: A key molecule essential for structural organization of cell-cell junctions of polarized epithelia during embryogenesis. *Journal of Cell Biology.* **146**.[5], 1117-1132.

Inai T, Kobayashi J, and Shibata Y. 1999.Claudin-1 contributes to the epithelial barrier function in MDCK cells. *European Journal of Cell Biology.* **78**.[12], 849-855.

Itoh M., Nagafuchi A, Moroi S., and Tsukita S. 1997.Involvement of ZO-1 in cadherin-based cell adhesion through its direct binding to alpha catenin and actin filaments. *Journal of Cell Biology.* **138**.[1], 181-192.

Itoh M., Furuse M., Morita K., Kubota K., Saitou M., and Tsukita S. 1999.Direct binding of three tight junction-associated MAGUKs, ZO-1, ZO-2, and ZO-3, with the COOH termini of claudins. *Journal of Cell Biology.* **147**.[6], 1351-1363.

Izumi Y, Hirose T, Tamai Y, Hirai S, Nagashima Y, Fujimoto T, Tabuse Y, Kemphues KJ, Ohno S. 1998. An atypical PKC directly associates and colocalises at the epithelial tight junction with ASIP, a mammalian homolgue of Caenorhabditis elegans polarity protein PAR-3. *Journal of Cell Biology.* **143**, 95-106.

Jacoby DB. 1997.Role of the respiratory epithelium in asthma. *Research in Immunology.* **148**, 48-58.

Jeffery PK. 1983.Morphologic features of airway surface epithelial cells and glands. *American Review of Respiratory Disease.* **128**.[2 Pt 2], s14-s20.

Jeffery PK, Wardlaw AJ, Nelson FC, Collins JV, and Kay AB. 1989.Bronchial biopsies in asthma -an ultrastructural, quantitative study and correlation with hyperreactivity. *American Review of Respiratory Disease.* **140**, 1745-1753.

Johnson KR, Lewis JE, Li D, Soler AP, Knudsen KA, and Wheelock MJ. 1993.P- and E-cadherin are in seperate complexes in cells expressing both cadherins. *Experimental Cell Research.* **207**, 252-260.

Kanai Y., Ochiai A., Shibata T., Oyama T., Ushijima S., Akimoto S., and Hirohashi S. 1995.c-erbB-2 gene product directly associates with beta-catenin and plakoglobin. *Biochemical & Biophysical Research Communications.* **208**.[3], 1067-1072.

Kemler R, Ozawa M, and Ringwald M. 1989.Calcium-dependent cell adhesion molecules. *Current Opinion in Cell Biology* **1**, 892-897.

Keon BH., Schafer S., Kuhn C., Grund C., and Franke WW. 1996.Symplekin, a novel type of tight junction plaque protein. *Journal of Cell Biology.* **134**.[4], 1003-1018.

Korman NJ, Eyre RW, Klaus-Kovtun V, and Stanley JR. 1989.Demonstration of an adhering-junction molecule (plakoglobin) in the autoantigens of pemphigus foliaceus and pemphigus vulgaris. *New England Journal of Medicine* **321**.[10], 631-635.

Kuwano K., Bosken CH., Pare PD., Bai TR., Wiggs BR., and Hogg JC. 1993. Small airways dimensions in asthma and in chronic obstructive pulmonary disease. *American Review of Respiratory Disease.* **148**.[5], 1220-1225.

Laitinen A. 1985.Ultrastructural organisation of intraepithelial nerves in the human airway tract. *Thorax.* **40**.[7], 488-492.

Laitinen LA, Heino M, Laitinen A, Kava T, and Haahtela T . 1985.Damage of the airway epithelium and bronchial reactivity in patients with asthma. *American Review of Respiratory Disease.* **131**.[4], 599-606.

Larue L, Ohsugi M, Hirchenhain J, and Kemler R. 1994.E-cadherin null mutant embryos fail to form a trophoectoderm epithelium. *Proceedings of the National Academy of Science USA.* **91**, 8263-8267.

Legrand C, Polette M, Tournier JM, de Bentzmann S, Huet E, Monteau M, and Birembaut P. 2001.uPA/PLasmin System-Mediated MMP-9 Activation Is Implicated in Bronchial Epithelial Cell Migration. *Experimental Cell Research* **264**, 326-336.

Lenox JM, Koch PJ, Mahoney MG, Lieberman M, Stanley JR, and Radice GL. 2000.Postnatal lethality of P-cadherin/desmoglein 3 double knockout mice: demonstration of a cooperative effect of these cell adhseion molecules in tissue homeostasis of stratified squamous epithelia. *Journal of Investigative Dermatology* **114**, 948-952.

Lewis JE, Jensen PJ, and Wheelock MJ. 1994.Cadherin function is required for human keratinocytes to assemble desmosomes and stratify in response to calcium. *Journal of Investigative Dermatology* **102**.[6], 870-877.

Lin LH and DePhilip RM. 1996.Differential expression of placental (P)-cadherin in sertoli cells and peritubular myoid cells during postnatal development of the mouse testis. *Anatomical Record* .[2], 155-164.

Lin LH and DePhilip RM. 1996.Sex-dependent expression of placental (P)-cadherin during mouse gonadogenesis. *Anatomical Record.* **246**.[4], 535-544.

Liu D, Huang C., Kameyama K., Hayashi E., Yamauchi A, Kobayashi S., and Yokomise H. 2001.E-cadherin expression associated with differentiation and prognosis in patients with non-small cell lung cancer. *Annals of Thoracic Surgery.* **71**.[3], 949-955.

Martin-Padura I., Lostaglio S., Schneemann M., Williams L., Romano M., Fruscella P., Panzeri C., Stoppacciaro A., Ruco L., Villa A., Simmons D., and Dejana E. 1998.Junctional adhesion molecule, a novel member of the

immunoglobulin superfamily that distributes at intercellular junctions and modulates monocyte transmigration. *Journal of Cell Biology.* **142**.[1], 117-127.

Mattey DL. and Garrod DR. 1986. Splitting and internalization of the desmosomes of cultured kidney epithelial cells by reduction in calcium concentration. *Journal of Cell Science.* **85**, 113-124.

Mattey DL. and Garrod DR. 1986. Calcium-induced desmosome formation in cultured kidney epithelial cells. *Journal of Cell Science.* **85**, 95-111.

McDowell EM, Newkirk C., and Coleman B. 1985.Development of hamster tracheal epithelium: II. Cell proliferation in the fetus. *Anatomical Record.* **213**.[3], 448-456.

Middleton E, Atkins FM, Fanning M, and Georgitis JW. 1981.Cellular mechanisms in the pathogenesis and pathophysiology of asthma. *Medical Clinics of North America* **65** , 1013-1031.

Miyahara M., Nakanishi H., Takahashi K., Satoh-Horikawa K., Tachibana K., and Takai Y. 2000.Interaction of nectin with afadin is necessary for its clustering at cell-cell contact sites but not for its cis dimerization or trans interaction. *Journal of Biological Chemistry.* **275**.[1], 613-618.

Montefort S, Roche WR, and Holgate ST. 1993.Bronchial epithelial shedding in asthmatics and non-asthmatics. *Respiratory Medicine* **87**, 9-11.

Morita K, Sasaki H, Fujimoto K, Furuse M, and Tsukita S. 1999.Claudin-11/OSP-based tight junctions of myelin sheaths in brain and sertoli cells in testis. *Journal of Cell Biology* **145**.[3], 579-588.

Motojima S, Frigas E, Loegering DA, and Gleich GJ. 1989.Toxicity of eosinophil cationic proteins for guinea-pig tracheal epithelium *in-vitro*. *American Review of Respiratory Disease.* **139**, 801-805.

Muller-Rover S, Tokura Y, Welker P, Furukawa F, Wakita H, Takigawa M, and Paus R. 1999.E- and P-cadherin expression during murine hair follicle morphogenesis and cycling. *Experimental Dermatology* **8**.[4], 237-246.

Muresan Z., Paul DL., and Goodenough DA. 2000.Occludin 1B, a variant of the tight junction protein occludin. *Molecular Biology of the Cell.* **11**.[2], 627-634.

Nagafuchi A, Shirayoshi Y, Okazaki K, Yasuda K, and Takeichi M. 1987.Transformation of cell-adhesion properties by exogenously introduced E-cadherin cDNA. *Nature* **329**, 341-343.

Nagafuchi A, Ishihara S, and Tsukita S. 1994.The roles of catenins in the cadherin-mediated cell adhesion: functional analysis of E-cadherin-alpha catenin fusion molecules. *Journal of Cell Biology* **127**.[1], 235-245.

Navarro P, Lozano E, and Cano A. 1993.Expression of E- or P-cadherin is not sufficient to modify the morphology and the tumorigenic behaviour of murine spindle carcinoma cells. Possible involvement of plakoglobin. *Journal of CellScience* **105**.[4], 923-934.

Naylor B. 1962.the shedding of the mucosa of the bronchial tree in asthma. *American Review of Respiratory Disease.* **17**, 69-72.

Nievers MG, .Schaapveld RQ., and Sonnenberg A. 1999. Biology and function of hemidesmosomes. *Matrix Biology.* **18**.[1], 5-17.

Noren NK., Liu BP., Burridge K., and Kreft B. 2000. p120 catenin regulates the actin cytoskeleton via Rho family GTPases. *Journal of Cell Biology.* **150**.[3], 567-580.

Nose A and Takeichi M. 1986.A novel cadherin cell adhesion molecule: its expression patterns associated with implantation and organogenesis of mouse embryos. *Journal of Cell Biology.* **103**.[6 Pt 2], 2649-2658.

Nose A., Nagafuchi A, and Takeichi M. 1987.Isolation of placental cadherin cDNA: identification of a novel gene family of cell-cell adhesion molecules. *EMBO Journal.* **6**.[12], 3655-3661.

Obara N, Suzuki Y, Nagai Y, and Takeda M. 1999.Immunofluorescence detection of cadherins in mouse tooth germs during root development. *Archives of Oral Biology.* **44**.[5], 415-421.

Orford K., Crockett C., Jensen JP., Weissman AM., and Byers SW. 2001.Serine phosphorylation-regulated ubiquitination and degradation of beta-catenin. *Journal of Biological Chemistry.* **272**.[40], 24735-24738.

Ornondez C, Ferrando R, Hyde DM, Wong JV, and Fahy JV. 2000.Epithelial Desquamation in Asthma. Artifact or Pathology? *American Journal of Respiratory & Critical Care Medicine.* **162**, 2324-2329.

Pece S and Gutkind JS. 2000.Signaling from E-cadherins to the MAPK Pathway by the Recruitment and activation of Epidermal Growth factor receptors upon Cell-Cell Contact Formation. *Journal of Biological Chemistry.* **275**.[52], 41227-41233.

Peifer M, McCrea PD, Green KJ, Wieschaus E, and Gumbiner BM. 1992.The vertebrate adhesive junction proteins beta-catenin and plakoglobin and the Drosophila segment polarity gene armadillo form a multigene family with similar properties. *Journal of Cell Biology.* **118**.[3], 681-691.

Persson CGA, Gustafsson B, Erjefält JS, and Sundler F . 1993.Mucosal exudation of plasma is a noninjurious intestinal defense mechanism. *Allergy* **48**.[8], 581-586.

Persson CGA, Erjefält JS, Andersson M, Greiff L, and Svensson C. 1996.Extravasation, lamina propia flooding and lumenal entry of bulk plasma exudate in mucosal defence, inflammation and repair. *Pulmonary Pharmacology* **9**.[3], 129-139.

Pizarro A, Gamallo C, Benito N, Palacios J, Quintanilla M, Cano A, and Contreras F. 1995.Differential patterns of placental and epithelial cadherin expression in basal cell carcinoma and in the epidermis overlying tumours. *British Journal of Cancer* **72**.[2], 327-332.

Pokutta S, Herrenknecht K, Kemler R, and Engel J. 1994.Confirmational changes of the recombinant extracellular domain of E-cadherin upon calcium binding. *European Journal of Biochemistry* **223**, 1019-1026.

Polakis P. 2000.Wnt signaling and cancer. *Genes & Development.* **14**.[15], 1837-1851.

Radice GL, Ferreira-Cornwell, Robinson SD, Rayburn H, Chodosh LA, Takeichi M, and Hynes RO. 1997.Precocious mammary gland development in P-cadherin-deficient mice. *Journal of Cell Biology* **139**.[4], 1025-1032.

Raeburn D and Webber SE. 1994.Proinflammatory potential of the airway epithelium in bronchial asthma. *European Respiratory Journal.* **7**, 2226-2233.

Revel JP and Karnovsky MJ. 1967.Hexagonal array of subunits in intercellular junctions of the mouse heart and liver. *Journal of Cell Biology.* **33**.[3], c7-c12.

Rimm DL, Koslov ER., Kebriaei P., Cianci CD., and Morrow JS. 1995.Alpha 1(E)-catenin is an actin-binding and -bundling protein mediating the attachment of F-actin to the membrane adhesion complex. *Proceedings of the National Academy of Sciences of the United States of America.* **92.**[19], 8813-8817.

Rodriguez-Boulan E and Nelson WJ. 1989.Morphogenesis of the Polarised Epithelial Cell Phenotype. *Science* **245**, 718-725.

Roisman GL, Peiffer C, Lacronique JG, Lecae A, and Dusser DJ. 1995.Perception of bronchial obstruction in asthmatic-patients, relationship with bronchial eosinophilic inflammation and epithelial damage and effect of corticosteroid treatment. *Medical Clinics of North America* **96**, 12-21.

Saitou M, Ando-Akatsuka Y, Itoh M, Furuse M, Inazawa J, Fujimoto K, and Tsukita S. 1998.Mammalian occludin in epithelial cells: its expression and subcellular distribution. *European Journal of Cell Biology.* **73.**[3], 222-231.

Sakula A. 1986.Charcot-Leyden crystals and Curschmann spirals in asthmatic sputum. *Thorax* **41.**[7], 503-507.

Sanders DS, Perry I, Hardy R, and Jankowski JA. 2000.Aberrant P-cadherin expression is a feature of clonal expansion in the gastrointestinal tract associated with repair and neoplasia. *Journal of Pathology* **190**, 526-530.

Shapiro L., Fannon AM., Kwong PD., Thompson A, Lehmann MS., .Grubel G., Legrand JF., Als-Nielsen J, .Colman DR., and Hendrickson WA. 1995. Structural basis of cell-cell adhesion by cadherins. *Nature.* **374.**[6520], 327-337.

Shariat SF., Pahlavan S., Baseman AG., Brown RM, Green AE., Wheeler TM., and Lerner SP. 2001.E-cadherin expression predicts clinical outcome in carcinoma in situ of the urinary bladder. *Urology.* **57.**[1], 60-65.

Sheth B, Fesenko I, Collins JE, Moran B, Wild AE, Anderson JM, and Fleming TP. 1997.Tight junction assembly during mouse blastocyst formation is regulated by late expression of ZO-1 alpha+ isoform. *Development* **124.**[10], 2027-2037.

Shimizu T, Nishihara M, Kawaguchi S, and Sakakura Y. 1994.Expression of phenotypic markers during regeneration of rat tracheal epithelium following mechanical injury. *American Journal of Respiratory Cell & Molecular Biology.* **11.**[1], 85-94.

Shimoyama Y and Hirohashi S. 2000.Expression of E- and p-cadherin in gastric carcinomas. *Cancer Research* **51.**[8], 2185-2192.

Shirahama S, Furukawa F, Wakita H, and Takigawa M. 1996.E- and P-cadherin expression in tumor tissues and soluble E-cadherin levels in sera of patients with skin cancer. *Journal of Dermatological Science* **13.**[1], 30-36.

Sleigh MA. 1966.The co-ordination and control of cilia. *Symposia of the Society for Experimental Biology.* **20**, 11-31.

Smith DL. and Deshazo RD. 1993. Bronchoalveolar lavage in asthma. An update and perspective. *American Review of Respiratory Disease.* **148.**[2], 523-532.

Smith SJ, Leigh IM., McMillan JR., Rugg EL., Kelsell DP., Bryant SP., Spurr NK., Geddes JF., Kirtschig G., Milana G., de Bono AG., Owaribe K., Wiche G., Pulkkinen L., Uitto J., McLean WH., and Lane EB. 1996. Plectin deficiency results in muscular dystrophy with epidermolysis bullosa. *Nature Genetics.* **13.**[4], 450-457.

Soderberg M, Hellstrom S., Lundgren R., and Bergh A. 1990.Bronchial epithelium in humans recently recovering from respiratory infections caused by influenza or mycoplasma. *European Respiratory Journal.* **3.**[9], 1023-1028.

Sonnenberg A., .Linders CJ., Daams JH., and Kennel SJ. 1990.The alpha 6 beta 1 (VLA-6) and alpha 6 beta 4 protein complexes: tissue distribution and biochemical properties. *Journal of Cell Science* **96**.[2], 207-217.

Stevenson BR, Siliciano JD, Mooseker MS, and Goodenough DA. 1986.Identification of ZO-1, a high molecular weight polypeptide associated with the tight junction (zonula occludens) in a variety of epithelia. *Journal of Cell Biology.* **103**, 755-766.

Suzuki K., Tanaka T., Enoki M., and Nishida T. 2000.Coordinated reassembly of the basement membrane and junctional proteins during corneal epithelial wound healing. *Investigative Ophthalmology & Visual Science.* **41**.[9], 2495-2500.

Suzuki ST. 1996.Protocadherins and diversity of the cadherin superfamily. *Journal of Cell Science* **109**, 2609-2611.

Tachibana K., Nakanishi H, Mandai K., Ozaki K., Ikeda W., Yamamoto Y., Nagafuchi A., Tsukita S., and Takai Y. 2000.Two cell adhesion molecules, nectin and cadherin, interact through their cytoplasmic domain-associated proteins. *150(5):1161-76, 2000 . Journal of Cell Biology.* **150**.[5], 1161-1176.

Takeichi M. 1991.Cadherin cell adhesion receptors as a morphogenetic regulator. *Science* **251**, 1451-1455.

Tomee JF. Wierenga AT. Hiemstra PS. Kauffman HK. 1997. Proteases from Aspergillus fumigatus induce release of proinflammatory cytokines and cell detachment in airway epithelial cell lines. *Journal of Infectious Diseases.* **176**. [1], 300-303

Troyanovsky SM., Eshkind LG., Troyanovsky RB., Leube RE., and Franke WW. 1993.Contributions of cytoplasmic domains of desmosomal cadherins to desmosome assembly and intermediate filament anchorage. *Cell* **72**.[4], 561-574.

Unger VM., Kumar NM., Gilula NB., and Yeager M. 1999. Expression, two-dimensional crystallization, and electron cryo-crystallography of recombinant gap junction membrane channels. *Journal of Structural Biology.* **128**.[1], 98-105.

Wakita H, Shirahama S, and Furukawa F. 1998.Distinct P-cadherin expression in cultured normal human keratinocytes and squamous cell carcinoma cell lines. *Microscopy Research & Technique.* **43**.[3], 218-223.

Wallis S, Lloyd S, Wise I, Ireland G, Fleming TP and Garrod D.B 2000. The α Isoform of protein kinase C is involved in signaling the response of desmosomes to wounding in cultured epithelial cells. *Molecular Biology of the Cell.* **11**. 1077-1092.

Wan H, Winton HL, Soeller C, Tovey ER, Gruenert DC, Thompson PJ, Stewart GA, Taylor GW, Garrod DR, Cannell MB, and Robinson C. 1999. Der p 1 facilitates transepithelial allergen delivery by disruption of tight junctions. *The Journal of Clinical Investigation.* **104**. [1] 123-133.

Wardlaw AJ, Dunnette S, Gleich GJ, Collins JV, and Kay AB. 1988.Eosinophils and mast cells in bronchoalveolar lavage in subjects with mild asthma. *American Review of Respiratory Disease.* **137**, 62-69.

Weber E, Berta G, Tousson A, St. John P, Green MW, Gopalokrishnan U, Jilling T, Sorscher EJ, Elton TS, Abrahamson DR and Kirk KL. 1994 Expression and polarised targeting of a Rab3 isoform in epithelial cells. *Journal of Cell Biology.***125**. 583-594.

Wheelock MJ and Jensen PJ. 1992.Regulation of keratinocyte intercellular junction organisation and epidermal morphogenesis by E-cadherin. *Journal of Cell Biology* **117**.[2], 415-425.

White SR., Dorscheid DR., Rabe KF., Wojcik KR., and Hamann KJ. 1999.Role of very late adhesion integrins in mediating repair of human airway epithelial cell monolayers after mechanical injury. *American Journal of Respiratory Cell & Molecular Biology.* **20**.[4], 787-796.

White SR, Wojcik KR, Gruenert D, Sun S, Dorscheid DR. 2001. Airway epithelial cell wound repair mediated by α-dystroglycan. *American Journal of Respiratory Cell & Molecular Biology.***24**. 179-186.

Williams LA, Martin-Padura I, Dejana E, Hogg N, and Simmons DL. 1999.Identification and characterisation of human Junctional Adhesion Molecule (JAM). *Molecular Immunology.* **36**, 1175-1188.

Wiseman LL. and Strickler J. 1981. Desmosome frequency: Experimental alteration may correlate with differential cell adhesion. *Journal of Cell Science.* **49**, 217-223.

Wittchen ES., Haskins J., and Stevenson BR. 1999. Protein interactions at the tight junction. Actin has multiple binding partners, and ZO-1 forms independent complexes with ZO-2 and ZO-3. *Journal of Biological Chemistry.* **274**.[49], 35179-35185.

Woods A, Couchman JR. 1992. Protein kinase C involvement in focal adhesion formation. *Journal of cell science.* **101** 277-190

Wu JC, Gregory CW, and DePhilip RM. 1993.P-cadherin and E-cadherin are co-expressed in MDCK cells. *Biochemical and Biophysical Research Communications* **195**, 1329-1335.

Yoshida-Noro C, Suzuki N, and Takeichi M. 1984.Molecular nature of the calcium-dependent cell-cell adhesion system in mouse teratocarcinoma and

embryonic cells studied with a monoclonal antibody. *Development Biology* **101**, 19-27.

Yukawa T, Read RC, Kroegal C, Rutman A, Chung KF, Wilson R, Cole PJ, and Barnes PJ. 1990.The effects of activated eosinophils and neutrophils on guinea-pig airway epithelium *in-vitro*. *American Journal of Respiratory Cell and Molecular Biology*. **2**, 341-353.

Zahm JM, Chevillard M, and Puchelle E. 1991.Wound repair of human surface respiratory epithelium. *American Journal of Respiratory Epithelium*. **5**, 242-248.

Zahm JM, Kaplan H, Herard AL, Doriot F, Pierrot D, Somelette P, and Puchelle E. 1997.cell migration and proliferation during the *in vitro* wound repair of the respiratory epithelium. *Cell Motility and the Cytoskeleton*. **37**, 33-43.

Zahm JM., Pierrot D., Chevillard M., and Puchelle E. 2001. Dynamics of cell movement during the wound repair of human surface respiratory epithelium. *Biorheology*. **29**.[5-6], 459-465.

Zheng Z, Pen J, Chu B, Wong YC, Cheung ALM, and Tsao SW. 1999.downregulation and abnormal expression of E-cadherin and β-catenin in nasopharyngeal carcinoma: close association with advanced disease stage and lymph node metastasis. *Human Pathology* **30**.[4], 458-466.

Zhong Y, Saitoh T, Minase T, Sawada N, Enomoto K, and Mori M. 1993.Monoclonal antibody 7H6 reacts with a novel tight junction associated protein distinct from ZO-1, cingulin and ZO-2. *Journal of Cell Biology*. **120**, 477-483.